Aspects of Holographic Superconductivity

BARCLAY, LUKE

Aspects of Holographic Superconductivity

Luke Barclay

A Thesis presented for the degree of
Doctor of Philosophy

Centre for Particle Theory
Department of Mathematical Sciences
University of Durham
England

October 2011

Dedicated to

m, d, m, a, l & g

Aspects of Holographic Superconductivity

Luke Barclay

Submitted for the degree of Doctor of Philosophy
October 2011

Abstract

In this thesis we study two different aspects of holographic superconductivity. First we study fully backreacting Gauss-Bonnet (GB) holographic superconductors in 5 bulk spacetime dimensions. We explore the system's dependence on the scalar mass for both positive and negative GB coupling, α. We find that when the mass approaches the Breitenlohner-Freedman (BF) bound and $\alpha \to L^2/4$ the effect of backreaction is to increase the critical temperature, T_c, of the system: the opposite of its effect in the rest of parameter space. We also find that reducing α below zero increases T_c and that the effect of backreaction is diminished. We study the zero temperature limit, proving that this system does not permit regular solutions for a non-trivial, tachyonic scalar field and constrain possible solutions for fields with positive masses. We investigate singular zero temperature solutions in the Einstein limit but find them to be incompatible with the concept of GB gravity being a perturbative expansion of Einstein gravity. We study the conductivity of the system, finding that the inclusion of backreaction hinders the development of poles in the conductivity that are associated with quasi-normal modes approaching the real axis from elsewhere in the complex plane.

In the latter part of the thesis we investigate asymptotically anti de-Sitter (adS) and Lifshitz black holes in a bulk gravitational model that has a consistent embedding in string theory and that permits an arbitrary dynamical exponent, $z \geq 1$. We find numerically that for both types of asymptotic spacetime there exists a two parameter family of black hole solutions. In the adS case these numerical solutions are supported by analytic solutions in the 'probe' or non-backreacting limit. Finally, we study the dependence of the black hole's temperature on these two parameters.

Declaration

The work in this thesis is based on research carried out whilst in the Centre for Particle Theory Group in the Department of Mathematical Sciences at Durham University, England. No part of this thesis has been submitted elsewhere for any other degree or qualification and is all my own work unless referenced to the contrary in the text.

The material covered in chapters 1 and 2 is background material relevant to the research presented in the remaining chapters. The research presented in chapter 3 is largely contained in two papers, [1] and [2]. The first of which I co-authored the other is all my own work. The research in chapter 4 is based on collaborative work with my supervisor that has yet to be published.

Acknowledgements

First and foremost I would like to thank my supervisor Ruth Gregory. Ruth's guidance over the last four years has been invaluable. I would also like to thank my secondary supervisor Paul Sutcliffe for useful discussions throughout my time here. I must also thank the STFC, without whose funding I could not have achieved this. And then there are my friends, family and Layla who I would like to thank for just being quality.

Conventions

Throughout this thesis we will use *natural units*, in which Planck's constant (divided by 2π), $\hbar$, and the speed of light, c, are set to 1. In general we shall keep Newton's gravitational constant explicit. The conversion factors that allow us to change between the SI system of units, based on the metre, second and kilogram, and the natural system of units are:

$$\hbar = 1.054571596 \times 10^{-34}\text{J s}$$
$$c = 2.99792458 \times 10^{8}\text{m s}^{-1}.$$

In addition, Boltzmann's constant will be set to 1 throughout this work unless stated to the contrary in the text. For reference Boltzmann's constant is

$$k_B = 1.3806503 \times 10^{-23}\text{m}^2\text{kg s}^{-2}\text{K}^{-1}.$$

In representing the spacetime line element ds^2 we shall use the mostly minus signature, such that

$$ds^2 = dt^2 - dr^2 - dx^2 - dy^2 - ...$$

In this thesis we denote the Levi-Civita symbol by $\varepsilon_{\mu_1\mu_2...\mu_n}$ and the Levi-Civita tensor by $\epsilon_{\mu_1\mu_2...\mu_n}$, where the two are related by

$$\epsilon_{\mu_1\mu_2...\mu_n} = \sqrt{-g}\varepsilon_{\mu_1\mu_2...\mu_n},$$

where g is the determinant of the metric.

Contents

List of Figures

Chapter 1

Introduction and Background

In 1986 Karl Müller and Johannes Bednorz investigated the conductivity of a particular doped, cuprate material and found it to exhibit superconducting behaviour with a critical temperature as high as 30K, [3]. In doing this, they discovered a new class of so called "high temperature" superconductors that fell outside the theoretic understanding of superconductivity. This new class of superconductor is thought to be described by a theory with strong coupling which limits the ability to understand these systems perturbatively. In recent years however, string theory has provided science with a new avenue by which to explore strongly coupled field theories: the gauge/gravity correspondence [4]. This correspondence conjectures a duality between strongly coupled quantum field theories and weakly coupled gravity theories. This duality allows one to investigate one of the theories by studying the dynamics of the other. The gravitational system is defined in a higher number of dimensions to the quantum field theory and can be thought of as a holographic "image" of the lower dimensional theory. In recent years this powerful conjecture has been applied to problems in condensed matter physics. The systems that attempt to describe superconductivity in this way have become known as *holographic superconductors*.

The correspondence is actually a duality between a gauge theory and a string theory. For calculational feasibility Einstein's theory of gravity is often used as a low energy effective description of the string theory. Much of the work presented in this thesis is concerned with this approximation and its effect on holographic superconductivity. We investigate this by studying the key features of a simple

model of holographic superconductivity using Einstein gravity with the addition of the next leading order term in a perturbative expansion towards the full string theory. Such a theory is known as *Gauss-Bonnet gravity*. By doing this we shall be investigating the stability of these holographic models to the inclusion of higher order terms.

The latter part of this thesis is concerned with another aspect of holographic superconductivity, namely the scaling symmetries of the strongly coupled field theory. Due to a relevance to condensed matter systems there has been a great deal of recent interest in holographic models of superconductivity in which both the gravity and quantum field theory exhibit a particular scaling known as *Lifshitz scaling*. In such theories the temporal and spatial coordinates scale as $t \to \lambda^z t$, $x^i \to \lambda x^i$ and $r \to r/\lambda$ where z is referred to as the dynamical exponent. A number of models of holographic superconductivity with this scaling have been found. However, these models are all either only phenomenological or, if rooted in string theory, only apply to a fixed value of z. We investigate one particular gravitational model that has a consistent embedding in string theory and generates a Lifshitz spacetime with arbitrary z with a view to developing a holographic superconductor. Black holes are a crucial ingredient of a model of holographic superconductivity and our research is concerned with the black holes that can be found in this particular gravitational theory.

The layout of the thesis will be as follows: In the remainder of this chapter we will introduce much of the background material relevant to the later chapters by giving a brief overview of superconductivity and the gauge/gravity correspondence. In chapter 2 we review the key concepts of holographic superconductivity. In chapter 3 we study the effect that the inclusion of higher curvature corrections has on a simple model of a holographic superconductor. In chapter 4 we consider a system that exhibits Lifshitz scaling and study the black holes that can be found there. In chapter 5 we conclude and summarize future directions of research.

1.1 Superconductivity:

Superconductivity was discovered in 1911 [5] when Heike Onnes noticed that the resistivity of certain metals dropped suddenly to zero below a characteristic temperature, T_c, of the order of a few Kelvin. These infinitely conducting systems were named superconductors. Twenty two years later Walther Meissner and Robert Ochsenfeld noticed that any magnetic field present in these materials was expelled as the temperature dropped below T_c. This discovery, commonly known as the Meissner effect, distinguishes superconductivity from the idea of perfect conductivity since the latter would allow a pre-existing magnetic field to persist in the material. A phenomenological description of these two phenomena was provided only two years later by the London brothers [6], but it was not until 1957 that a more complete microscopic understanding of superconductivity was found. In that year Bardeen, Cooper and Schrieffer presented their Nobel prize winning work that has become known as BCS theory, a brief outline of which can be found below. This theory had explanatory and predictive power and was able to accommodate the key developments in superconductivity until 1986. In that year Bednorz and Müller discovered a new class of so called "high temperature" superconductors with critical temperatures above the limit posed by BCS theory of approximately 30K. This discovery reignited interest in the field of superconductivity partly due to the practical applications of having superconducting systems at higher temperatures, but also because of the desire to have a theoretical understanding of these unusual materials that fall outside the scope of BCS theory.

This thesis is concerned with the attempt to understand this new class of superconductor via the gauge/gravity correspondence. Before we go about building the model of a superconducting system it is prudent to have some understanding of the system that we wish to model.

1.1.1 BCS theory

Here we present a brief description of BCS theory, a more full discussion can be found in [7]. BCS theory was developed in 1957 by Bardeen, Cooper and Schrieffer [8],

however a key development to its discovery came a year prior to its publication when Cooper discovered that electrons very close to the Fermi surface[1] of a material are unstable to forming a bound state, now known as a Cooper pair [9]. The attractive force necessary for the binding of the electrons arises as a result of their interaction with the material's atomic lattice. As an electron propagates through a medium it polarizes the surrounding lattice, attracting positive ions. This concentration of positive charge can then attract another electron binding the two via this weak electron-lattice interaction. Cooper demonstrated that the energy of an electron in a Cooper pair is lower than the energy of the lowest free state for a single electron, referred to as the Fermi energy. This instability means these Cooper pairs will continue to form until the Fermi surface has been altered sufficiently such that the Fermi energy equals that of an electron in the bound state. The following year, Bardeen, Cooper and Schrieffer developed this idea into their microscopic theory of superconductivity. The electrons in the Cooper pair have equal and opposite spin meaning the bound state has spin 0 and is a boson. As such, in a similar way to Bose-Einstein condensation, the Cooper pairs can form a highly correlated condensate. The phenomenon of zero resistivity is a consequence of the Cooper pairs being a part of the condensate as a whole. In a normal conductor, resistance arises as a result of thermal fluctuations of the lattice scattering and impeding the flow of the conducting electrons. In a superconductor, individual Cooper pairs cannot simply be scattered by an arbitrary energy interaction due to the nature of the condensate. There exists a finite "energy gap", $E_g = 2\Delta$, equal to the disassociation energy of a pair of electrons, which is the minimum energy required to alter the flow of the condensate. If the temperature of a material is low enough the thermal fluctuations of the lattice have insufficient energy to affect the condensate allowing the current to flow unimpeded and the material will superconduct. BCS theory predicts a universal relation between the energy gap (as measured at zero temperature) and the critical

[1]Electrons, being fermions, must obey Pauli's exclusion principle forbidding two or more fermions from occupying the same quantum state simultaneously. As a result the free states of a material are filled one by one forming an abstract volume in momentum space, the surface of which is the Fermi surface.

temperature

$$E_g = 2\Delta = 3.528 k_B T_c \tag{1.1}$$

where k_B is Boltzmann's constant. The agreement of this expression with experiment provided early verification of this microscopic theory.

1.1.2 High Temperature Superconductivity

In 1986 the supremacy of BCS theory ended with the discovery of high temperature superconductors whose critical temperatures can reach well above $100K$ and cannot be fully described by the BCS model. The first type of this new class to be discovered consisted of a layered material dominated by copper-oxide planes sandwiched between a compound that serves to dope electrons or holes onto the conducting planes. These materials are now referred to as *cuprate superconductors*. Other, non-copper based examples have since been discovered.

Despite a great deal of research over the last 25 years there is still no satisfactory microscopic explanation of the mechanisms that cause these materials to superconduct. One of the complicating factors is that the underlying physics seems to involve strong coupling which prohibits a perturbative understanding.

An example of where this can be seen comes from a phenomenological model that seems the capture the physics of the cuprate superconductors at low temperature: the Hubbard model [10, 11]. This is a very simple model describing the movement of electrons between sites in a lattice of atoms in a material. In its simplest form the Hubbard Hamiltonian consists of two terms: a kinetic term that governs the likelihood of an electron to 'hop' between two sites and a potential term that accounts for the Coulomb interaction between the electrons at each lattice site. The coupling that determines the relative strength of these two terms is analogous to the degree of the 'doping' of the material and can dramatically alter the nature of the material. When the potential term dominates, the material becomes an insulator as conduction is prevented by the strong Coulomb repulsion between the electrons at each site. When the kinetic terms dominates, the free movement of electrons is

characteristic of a Fermi liquid. Superconductivity is found between the two. These characteristics are consistent with the phase diagram of a cuprate superconductor. Since superconductivity does not occur at either of the extremes perturbation theory is not possible which can make calculations very difficult.

Holographic superconductors attempt to circumvent these problems by using the gauge/gravity correspondence. In attempting to model superconductivity in this way it is sensible to begin by replicating the details of a more macroscopic theory as opposed to the microscopic detail of a theory like BCS theory. Ginzburg and Landau presented such a model of superconductivity seven years prior to the publication of BCS theory. It is now known as the Ginzburg-Landau (GL) theory of superconductivity, [12].

1.1.3 Ginzburg Landau Theory

In GL theory the total density of electrons in a material, n, is split into two types; the normal electron density, n_n, and the superconducting electron density, n_s. A complex pseudowavefunction, $\psi(x)$, is then introduced as an order parameter representing n_s

$$n_s = |\psi(x)|^2. \tag{1.2}$$

If ψ and its derivatives are small then the free energy density of the system, f_s, can be expanded in a series of the form

$$f_s = f_n + \alpha|\psi(x)|^2 + \frac{1}{2}\beta|\psi(x)|^4 + ... \tag{1.3}$$

where f_n is the free energy of the material in its normal state. Such an expansion is valid very close to the critical temperature where $|\psi|^2 \to 0$. For this approximation to remain valid we see that $\beta > 0$ but there is no such constraint on α and indeed two different cases emerge depending on the sign of α, see figure 1.1. Plotting the free energy as a function of ψ we see that for $\alpha > 0$ the free energy is minimised when $|\psi|^2 = 0$ but for $\alpha < 0$ a new minimum appears at

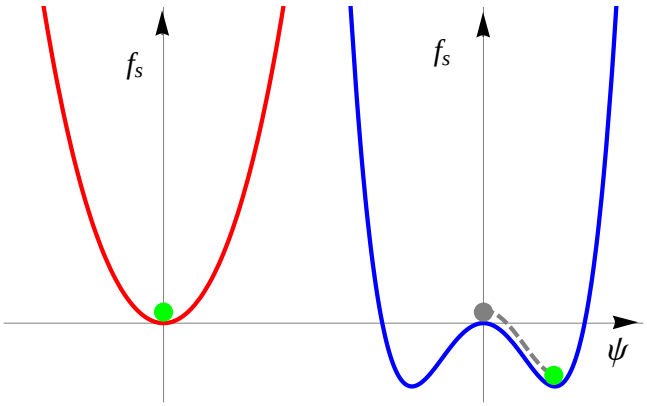

Figure 1.1: Plots depicting the free energy, f_s, as a function of ψ as described by (1.3). The left and right plots shows f_s for $\alpha > 0$ and $\alpha < 0$ respectively. One can see that as α drops below zero new minima appear at non-zero ψ.

$$|\psi|^2 = \frac{-\alpha}{\beta} \tag{1.4}$$

that is lower then the energy of the normal state. If such a picture is to describe superconductivity then α must change sign as the temperature drops below T_c. Expanding α in a Taylor's series about T_c we find

$$\alpha(T) = \alpha'(T - T_c) + ... \qquad \alpha' > 0 \tag{1.5}$$

which, using (1.4) gives

$$|\psi|^2 \propto (T - T_c). \tag{1.6}$$

Thus, in GL theory, the superconducting phase transition is associated with the breaking of the $U(1)$ symmetry of the complex phase of ψ. As we shall see in subsequent chapters a very similar mechanism appears in the holographic models of superconductivity.

1.1.4 Conductivity

The conductivity is the linear response of a system to the application of an electric field. If the energy (or frequency) of the electric field is greater than the energy gap, E_g, of the superconductor then the Cooper pairs disassociate and normal conductiv-

ity resumes. As a result the plots of the conductivity as a function of the frequency of the electric field have two distinct regions; above and below the frequency gap, ω_g.

It is possible to understand some of the key characteristics of the conductivity below the frequency gap using the very simple Drude model of electrical conduction [13]. In this model the drift velocity, $\mathbf{v}$ of the electron gas is governed by Newton's second law

$$m\frac{d\mathbf{v}}{dt} = q\mathbf{E} - m\frac{\mathbf{v}}{\tau}. \tag{1.7}$$

Here m is the electron mass, q is its charge, $\mathbf{E}$ is the electric field strength and τ is the time it takes for the electron to come effectively to rest as a result of interactions with the medium. The current density is given by $\mathbf{J} = nq\mathbf{v}$ where n is the number density of the electrons. In the steady state approximation it is straightforward to derive Ohm's law $\mathbf{J} = \sigma\mathbf{E}$ where σ is the conductivity given by

$$\sigma = \frac{nq^2\tau}{m}. \tag{1.8}$$

For an electric current given by $\mathbf{E} = Ee^{i\omega t}\mathbf{e}_x$ the complex conductivity is found to be

$$\sigma = \sigma_r + i\sigma_i = \left(\frac{nq^2\tau}{m}\right)\left(\frac{1}{1+\omega^2\tau^2} - i\frac{\omega\tau}{1+\omega^2\tau^2}\right). \tag{1.9}$$

We can use this expression to get a qualitative understanding of the conductivity of a superconductor for frequencies below the energy gap. The conductivity associated with the superconducting electrons can be modelled by letting τ increase continuously to infinity which is consistent with there being no resistance to their flow. Figure 1.2 shows plots of the real and imaginary parts of the conductivity for a number of different values of τ. The right plot shows that as τ increases the curve of σ_r forms an increasingly high and narrow peak about $\omega = 0$. An integration of σ_r over the positive frequencies shows the area under the curve remains constant despite alterations in τ. Thus as $\tau \to \infty$, σ_r shrinks to a Dirac δ-function about

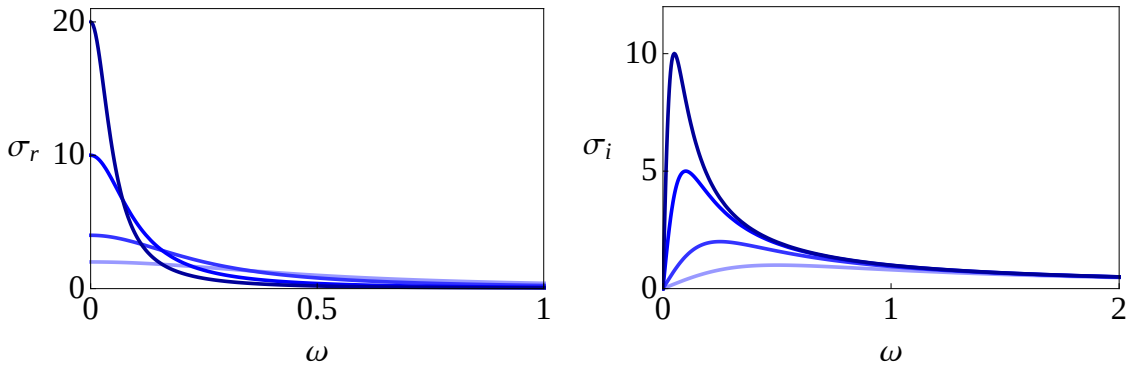

Figure 1.2: Plots showing the real, σ_r, and imaginary σ_i parts of the conductivity as a function of ω. Here ω is the frequency of any applied electric field given by $\mathbf{E} = Ee^{i\omega t}\mathbf{e}_x$. The darker lines correspond to larger relaxation time, τ.

$\omega = 0$. This δ-function profile indicates the infinite conductivity of the system. In this same limit $\sigma_i \propto 1/\omega$. This is not unexpected since by the Kramers-Kronig relations, [14],

$$\sigma_i(\omega) = -\frac{1}{2\pi}\int_{-\infty}^{\infty}\frac{\sigma_r(\omega')d\omega'}{\omega' - \omega}, \tag{1.10}$$

the delta function in σ_r is associated with a pole in σ_i [2].

These are some of the basic characteristics that we wish to reproduce in our holographic models. Before we discuss these holographic models in detail it is worth introducing the gauge/gravity correspondence upon which these models are based.

1.2 The Gauge/Gravity Correspondence

The gauge/gravity correspondence is a proposed duality between a field theory involving gravity and a quantum field theory without gravity in one dimension fewer. The correspondence is only a conjecture and has not been proven, however there is a great deal of supporting circumstantial evidence that has led many to believe it to be true.

The conjecture has arisen out of research into string theory. String theory was first developed as an attempt to describe the large number of mesons and hadrons

[2]The Kramers-Kronig relations apply to all complex functions that are analytic in the upper half plane. Causality constraints guarantee that this is true in this system, [15].

discovered in the 1960s, [16], but is now studied with a somewhat more ambitious aim: to unify all the known fundamental forces under one "theory of everything" (TOE). There are four known fundamental forces; the *strong* force, the *weak* force, the *electromagnetic* force and *gravity*. The first three forces have been unified by one highly successful quantum field theory (QFT) known as the Standard Model of particle physics and gravity is accurately described by Einstein's theory of General Relativity (GR), [17]. A key problem is that these theories appear inconsistent, and that when one attempts to include GR in a QFT infinities arise that cannot be renormalised away. Reconciling these theories to form a consistent theory of quantum gravity has been one of the core aims of theoretical physics over the last 40 years. String theory is one such attempt that has had many successes at reproducing a perturbative theory of GR and QFT similar to the standard model, but a lack of experimental testability has meant the theory still has its critics. Whether or not string theory actually does describe the world around us is in many ways irrelevant to the validity of the correspondence, which for the duration of this research we will hold to be true.

Below we provide a brief overview of the key concepts of string theory focussing on those areas that are relevant for a motivation of the gauge/gravity correspondence.

1.2.1 String Theory:

String theory is a theory of one dimensional objects that sweep out a two dimensional worldsheet in some d dimensional spacetime. The number of these d dimensions can be substantially larger than the four that we observe around us. The idea is that the strings are sufficiently small in order to appear to the low energy observer as point particles, as is consistent with current experimental observation. The strings can be open or closed and can oscillate in many different ways which would appear to the low energy observer as different particle excitations.

The action of a bosonic string is described by the Polyakov action, [18, 19]:

$$S = -\frac{T}{2}\int_{-\infty}^{\infty} d\tau \int_0^l d\sigma \sqrt{-\gamma}\gamma^{AB}\partial_A X_\mu \partial_B X^\mu, \tag{1.11}$$

where γ_{AB} is the metric on the worldsheet, X^μ are coordinates of the full spacetime and σ and τ are spacelike and timelike coordinates on the worldsheet. T is tension of the string given by

$$T = \frac{1}{2\pi l_s^2} = \frac{1}{2\pi\alpha'}. \tag{1.12}$$

where l_s is the string length and $\alpha' = l_s^2$ is the referred to as the Regge slope. We can think of α', or indeed l_s, as a parameter which sets the energy scale at which we observe the theory. The limit in which $\alpha' \to 0$ corresponds to the low energy limit where the string length goes to zero. Thus the strings become points and "stringy effects" can be ignored.

Extremising the action with respect to X^μ gives a wave equation with boundary conditions that are different for open and closed strings. The end points of open strings must obey either Dirichlet or Neumann boundary conditions, and for closed strings, the end points must connect smoothly.

The bosonic string can be quantized, leading to an infinite tower of states of different masses. Unfortunately the ground-states of both the open and closed strings are unphysical tachyonic states with $m^2 < 0$. This is one reason why this theory can never be a TOE. As well as the infinite tower of massive states there are massless states which are the only states to remain in the low energy limit, as $\alpha' \to 0$. The open and closed strings have different massless states. The open string has a massless gauge field with $U(1)$ gauge symmetry. So massless open strings correspond to a $U(1)$ gauge theory. There are three types of state in the closed string sector, the most important being a massless, traceless, symmetric spin two tensor called the graviton. This field allows the low energy oscillations of the closed string to correspond to classical gravity. There is also a scalar field called the dilaton, Φ,

which determines the string coupling constant, g_s, via

$$g_s = e^{\langle \Phi \rangle} \tag{1.13}$$

where $\langle \Phi \rangle$ is the vacuum expectation value of the dilaton. These observations allow one to begin to see how string theory can provide a unified description of both a QFT and a theory of gravity.

There are two key flaws in bosonic string theory: the existence of tachyons and the fact that there are no fermions. These problems can be resolved by the inclusion of supersymmetry.

Supersymmetry is the only known extension to the Poincaré symmetry group, [20]. This is achieved by the introduction of new, fermionic generators to the algebra. One consequence of adding these new symmetries to a theory is the introduction of additional "super-partners" to the field content that already exists in that theory. So, for example, by adding supersymmetry to the Standard Model, one would expect there to be a super-partner to every particle that already exists in that model. The fact that no such super-partners have yet been observed in the real world has not rendered this concept un-viable as it is possible that the additional supersymmetries are broken at some large energy scale and that the masses of these super-partners are too large to be detected by current experiment. The number, $\mathcal{N}$, of these additional fermionic generators determines the degree of supersymmetry in the theory. The more generators the more supersymmetric degrees of freedom.

In the 1980s it was shown that the inclusion of fermions to the worldsheet action leads to theories with spacetime supersymmetry, [21]. These supersymmetric string theories have become known as "superstring" theories. With the inclusion of supersymmetry it is possible to find string theoretic models for which the groundstate is not tachyonic. In fact there are five different consistent superstring theories known as; Type I, Type IIA, Type IIB and two types of Heterotic string theory. The inclusion of supersymmetry in the string theory means that the low energy limit is now not simply classical gravity, but gravity with local supersymmetry. This is referred to as "supergravity" (SUGRA) and will be discussed shortly. Another consequence

of quantizing the superstring is that the number of spacetime dimensions, d, is fixed to $d = 10$.

In addition to the fundamental string, string theory contains other objects called D-branes, see [22] for a review. These are $D + 1$ dimensional, solitonic objects in string theory upon which open strings can end. The boundary conditions of the open string mean that the endpoints can move freely on the brane itself but have Dirichlet boundary conditions in the transverse directions, hence the name D(irichlet)-branes. It was noted above that the massless open string spectrum contains a $U(1)$ gauge field. Such gauge fields decompose into fields that reside on, and transverse to the brane. The D-brane is itself a dynamical object whose low energy dynamics are described by the "DBI" action, [23]. Studying the low energy dynamics of these objects allows one to identify the gauge fields that reside on the branes.

As well as being thought of as the end points of open strings, D-branes can be thought of in a different way. Due to the reparameterization invariance of the metric (1.11),

$$(\tau, \sigma) \to (\tau'(\tau, \sigma), \sigma'(\tau, \sigma)), \tag{1.14}$$

an open string that moves in a closed loop on a D-brane can be thought of as a closed string being emitted from that brane, see figure 1.3. Since the massless excitations of the closed string contain the graviton, D-branes also have a gravitational description as well as the gauge field description that we discussed above. It is through these two differing views of the same objects in string theory that one can begin to see how the gauge/gravity correspondence may arise. Before we develop this further towards the full correspondence we must look briefly at the gravity theory that is described by the low energy limit of superstring theory: supergravity.

Supergravity was initially studied in its own right as a supersymmetric extension to classical gravity, [24], however it was soon realized to describe the low energy dynamics of some superstring theories. A key step towards understanding the correspondence came in 1995 when Polchinski identified the low energy dynamics of D-branes in string theory with extremal black p $(= D)$ branes in supergravity, [25].

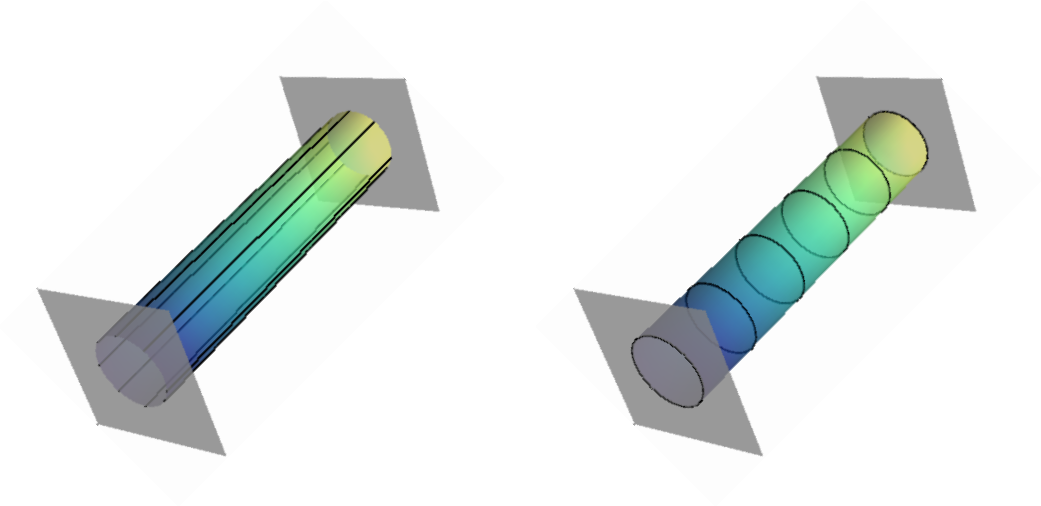

Figure 1.3: The left plot shows the world sheet of an open string moving in a closed loop between two D-branes. Reparameterization invariance of the worldsheet action allows this to viewed as the worldsheet of a closed string moving between the D-branes, shown on the right. In this way D-branes can be seen as sources of closed strings.

Black p-branes are $p+1$ dimensional solutions to supergravity and are analogous to black holes in general relativity. Via this analysis one sees that the D-branes of string theory can be viewed as gravitational objects that appear to warp the spacetime around them.

We have presented two very different views of the same objects in string theory. It was the identification of these two interpretations that led Maldacena in 1997 to propose what is now considered the canonical example of the correspondence. In [4], he suggested that there exists a duality between a Type IIB string theory in an $adS_5 \times S^5$ spacetime with an $\mathcal{N} = 4$ supersymmetric Yang Mills (SYM) $SU(N)$ gauge theory in four dimensions. This we shall now explain.

1.2.2 The Correspondence

The string theory set up, from which this correspondence arises, consists of N parallel, coincident $D3$-branes in the 10 dimensional spacetime of Type IIB string theory. In this set up there can be closed strings that can propagate in the bulk and open strings whose endpoints can end on any of the N $D3$-branes. We shall analyse this theory by considering the low energy limit as $\alpha' \to 0$, first in the open string picture

and then in the closed.

In the open string picture we have two types of theory. Far from the branes we have a Type IIB string theory of closed strings propagating in a 10 dimensional flat spacetime. At the branes we have open strings which can be described by a gauge field theory plus corrections due to the massive states. The action for such a system is given by

$$S = S_{\text{brane}} + S_{\text{interactions}} + S_{\text{bulk}}. \tag{1.15}$$

where the interactions between brane modes and bulk modes are proportional to positive powers of the gravitational constant $\kappa \approx g_s l_s^4$. In the low energy limit these two theories decouple and the massive state corrections are suppressed leaving a gauge field on the N $D3$-branes and a free, ten dimensional Type IIB supergravity theory away from the branes. The gauge theory for this set up turns out to be an $\mathcal{N} = 4$ SYM field theory with an $SU(N)$ gauge group living in $3 + 1$ dimensions. Theories of this sort have a lagrangian of the form

$$\mathcal{L} \approx -\frac{1}{g_{YM}^2}\text{Tr}(F^2) \tag{1.16}$$

where g_{YM} is the Yang Mills coupling constant and $F_{\mu\nu}$ is the field strength tensor corresponding to a non-Abelian gauge field A_μ.

We shall now consider the same set up from the purely closed string picture. Away from the branes we have the same closed string theory as before. In this picture the branes are now sources of closed strings and have a gravitational description. Even for non-zero α' the supergravity description can be used to identify the background geometry of this superstring theory set up. The $D3$-branes of the string theory correspond to the extremal black $p = 3$-branes in supergravity which have a metric of the form, [26, 27]

$$ds^2 = H(r)^{-1/2}\left(f(r)dt^2 - dx^2 - dy^2 - dz^2\right) - H^{1/2}\left(f(r)^{-1}dr^2 + r^2 d\Omega_5^2\right) \tag{1.17}$$

where

$$H(r) = 1 + \left(\frac{L}{r}\right)^4, \qquad f(r) = 1 - \left(\frac{r_0}{r}\right)^4,$$
$$L^4 = 4\pi g_s N l_s^4. \tag{1.18}$$

Here L is a lengthscale and $d\Omega_5^2$ is the metric of a 5-sphere, S^5. r_0 is related to the outer horizon, r_+, of the p-brane in supergravity by $r_0^4 = r_+^4 - L^4$. At extremality, $r_0 = 0$ and $f(r_0) = 1$ and the event horizon is replaced by the Poincaré horizon of adS space. Far from the branes, for $r \gg L$, $H(r) \to 1$ and the spacetime is asymptotically flat. Near the branes when $r \ll L$, $H(r) \to (L/r)^4$ and the metric takes the form of an $adS_5 \times S^5$ spacetime, where L is the radius of curvature. Globally we can see that a deep "throat", or gravitational well, has developed in the vicinity of the branes. As we did before we shall take the low energy limit. This differs slightly from the previous picture as in curved spacetimes energies are measured from the point of view of an observer at infinity. Due to the infinite throat in the vicinity of the branes the energy of any modes propagating out towards infinity are red-shifted and arbitrarily large excitations close to the brane can be consistent with a low energy limit. Once again the theories in the two regions decouple, [28], leaving two distinct theories; 10 d supergravity away from the branes and full Type IIB string theory on an $adS_5 \times S^5$ background in the vicinity of the branes.

The fact that these open and closed pictures are two different interpretations of the same set up, and that the asymptotic theories are the same in each description, led Maldacena to conjecture the strong form of the correspondence: That Type IIB superstring theory with $adS_5 \times S^5$ boundary conditions is equivalent to $\mathcal{N} = 4$ $SU(N)$ SYM in $3+1$ dimensions. Maldacena's conjecture allows the coupling of the gauge theory to be identified with the string coupling constant, g_s,

$$g_{YM}^2 = 2\pi g_s. \tag{1.19}$$

Whilst there is still no formal proof for this conjecture it has so far passed every test thrown at it, see [28] for a review. One of the obstacles to developing a formal

proof is the difficulty of quantizing the superstring on a curved background. This also limits the usefulness of the conjecture in this form. In order to be able to perform useful calculations we must take limits of the correspondence to regimes where calculations are possible. It is by doing this that we shall identify one of the most powerful aspects of the correspondence; namely that it is what is known as a strong/weak duality.

For a gauge theory, the way in which the coupling constant, g, changes at different energy scales, μ, is governed by the β function

$$\beta(g) = \frac{\partial g}{\partial \log(\mu)}. \tag{1.20}$$

If the β function is positive the coupling constant will be weak at low energies and grow in strength as the energy scale is increased. If $\beta(g)$ is negative the opposite is true; at high energies the coupling is weak and strong at low energies. The complexity of many field theories has meant much of our understanding has come from a perturbative analysis that is only possible when a coupling constant is weak. This means that at low energy scales theories with a negative β function are notoriously hard to study. $SU(N)$ gauge theories, in general, fall into this category. There is however, another dimensionless parameter in such theories for which perturbation theory is possible in certain limits. By taking the integer N in $SU(N)$ gauge theories to infinity a perturbative analysis is possible in powers of $1/N$. Indeed in [29], t'Hooft demonstrates that in this limit, the interactions in such theories behave very much like interactions of closed loops in string theory when the string coupling, g_s, is small. This observation provides more support for the conjectured duality between string theories and gauge theories. It is important to note that when considering the large N limit of such theories, even if the gauge coupling is taken to zero, the infinite nature of the higher order corrections can lead to contributions. It is more useful in such situations to deal with the effective, or t'Hooft, coupling constant, λ

$$\lambda = g_{YM}^2 N. \tag{1.21}$$

On the other side of the correspondence we suggested that understanding string

theory on a curved background is very difficult. In order to be able to calculate, we would like to consider the regime in which the string theory can be described by supergravity. This will be the case if the string length is small in comparison to the radius of curvature of the spacetime i.e. $l_s \ll L$. From (1.18) and (1.19) we find

$$L^4 = 2g_{YM}^2 N l_s^4 = 2\lambda l_s^4, \tag{1.22}$$

and we see that a supergravity description is therefore valid in the limit of large t'Hooft coupling, $\lambda \gg 1$. This means our gauge field is strongly coupled. Keeping λ large, we can let $N \to \infty$ in such a way that the string coupling $2\pi g_s = g_{YM}^2 \to 0$ and string interactions can be ignored. In this way we have a duality between a weakly coupled supergravity theory, for which calculations are possible, and a strongly coupled gauge theory for which calculations are hard. This strong/weak duality is a key strength of the correspondence but also an obstacle to testing its validity.

1.2.3 The dictionary

So far we have seen briefly how the correspondence may be motivated by string theory but have not seen how it can be put to practical use. In [30], Witten provided a precise description of the correspondence by relating the physical observables in each of the dual theories. In this prescription the partition function of the QFT, $\mathcal{Z}_{QFT}$, is identified with the partition function of the string theory in the bulk spacetime, $\mathcal{Z}_{string}$

$$\langle e^{\int_{\partial\mathcal{M}} \phi_0(x)\mathcal{O}(x)} \rangle = \mathcal{Z}_{QFT}[\phi_0] \equiv \mathcal{Z}_{string}[\phi \to \phi_0], \tag{1.23}$$

where ϕ represents a field in the bulk spacetime and ϕ_0 its value at the boundary of that spacetime. A path integral expression of $\mathcal{Z}_{QFT}$ has been included on the left which shows that the boundary values of the fields are to be interpreted as sources that couple to the QFT operators, $\mathcal{O}$. This relation is non-perturbative and holds to all orders, however, since string theory on adS is poorly understood most practical

calculations are conducted in the low energy, large N limit where the string theory is well approximated by supergravity. In this limit (1.23) allows one to identify the supergravity action with the generating functional of connected paths in the QFT

$$S_{SUGRA}[\phi_0] = -W_{QFT}[\phi_0]. \tag{1.24}$$

Correlation functions of a boundary operator can then be computed by functional differentiation of S_{SUGRA} with respect to the source, ϕ_0,

$$\begin{aligned} \langle \mathcal{O}(x) \rangle &= \left. \frac{\delta S_{SUGRA}}{\delta \phi_0(x)} \right|_{\phi_0=0} \\ \langle \mathcal{O}(x_1)\mathcal{O}(x_2) \rangle &= \left. \frac{\delta^2 S_{SUGRA}}{\delta \phi_0(x_1)\delta\phi_0(x_2)} \right|_{\phi_0=0} \\ \langle \mathcal{O}(x_1)...\mathcal{O}(x_n) \rangle &= \left. \frac{\delta^n S_{SUGRA}}{\delta \phi_0(x_1)...\delta\phi_0(x_n)} \right|_{\phi_0=0}. \end{aligned} \tag{1.25}$$

This prescription allows one to relate scalar fields of the bulk to scalar operators of the QFT, gauge fields to current operators and even the metric in the bulk to an operator representing the QFTs energy momentum tensor.

There is however an added complication to performing calculations such as those in (1.25), namely that the gravitational action is in general divergent. This was to be expected since it is well known that QFT correlation functions suffer from UV, or high energy, divergences. It is a general feature of the gauge/gravity correspondence that these UV divergences of the QFT relate to divergence of the volume of the bulk spacetime as $r \to \infty$, [31]. These divergences must be removed by the addition of appropriate counter terms to the action in a process referred to as "holographic renormalization". This process is described in detail in [32] and [33] and an explicit example will be presented in section 3.6.

Avoiding a full derivation of the process here we shall demonstrate this field/-operator correspondence with an example. Consider a scalar field, ψ, in a $d+1$ dimensional asymptotically adS spacetime whose field equation is given by

$$\nabla_\mu \nabla^\mu \psi - m^2 \psi = 0, \tag{1.26}$$

where m is the scalar mass. The asymptotic falloff of ψ near the boundary is found to be

$$\psi(r) = \frac{\psi_0}{r^{\lambda_-}} + \frac{\psi_1}{r^{\lambda_+}} + ..., \tag{1.27}$$

where $\lambda_\pm = 1/2(d \pm \sqrt{d^2 + 4m^2L^2})$ and L is the adS lengthscale. If $m^2L^2 > -d^2/4+1$ then ψ_0 corresponds to a non-normalizable mode and must be interpreted as the source. After the addition of appropriate counter terms (1.25) gives

$$\langle \mathcal{O} \rangle \equiv \psi_1. \tag{1.28}$$

If $m^2L^2 \leq -d^2/4 + 1$ then both ψ_0 or ψ_1 are normalizable and either can be set as the source, leaving the other to be interpreted as the operator.

We can use the integral on the left hand side of (1.23) to calculate the scaling dimension of the operator. By insisting that the integral is invariant under the scaling symmetry of the boundary metric

$$t \to at, \qquad\qquad x^i \to ax^i, \tag{1.29}$$

it is straightforward to find that the scaling dimension of the dual operator is given by

$$\dim[\mathcal{O}_\pm] = \lambda_\pm. \tag{1.30}$$

This direct relation between the asymptotic boundary dynamics of the fields in the bulk spacetime to the operators of a QFT allows one to think of the QFT as "living" on the boundary of the bulk spacetime. In this way, the QFT is often referred to as "the boundary theory".

1.2.4 Adding Temperature

Finite temperature field theories are studied via the *imaginary time formalism* where the temporal coordinate is Wick rotated, $t \to i\tau$, thus rendering it "Euclidean".

Following [34] we can see how this works by looking at the QFT amplitude associated with propagating a system from a configuration ϕ_1 at time t_1 to ϕ_2 at t_2

$$\langle \phi_2, t_2 | \phi_1, t_1 \rangle = \int D[\phi] e^{iS[\phi]}. \tag{1.31}$$

In the Schrödinger picture, one can write this as

$$\langle \phi_2, t_2 | \phi_1, t_1 \rangle = \langle \phi_2 | e^{H(t_2 - t_1)} | \phi_1 \rangle, \tag{1.32}$$

where H is the Hamiltonian. We then Wick rotate the time coordinate and insist that this new imaginary coordinate is periodic. Then, by summing over a complete set of basis configurations one obtains the partition function of the field $\phi = \phi_1 = \phi_2$ at a temperature $T = 1/(k_B \beta)$, where β is the periodicity of τ

$$Z = \sum_i^n e^{-\beta E_i} = \sum_i^n e^{-E_i/(k_B T)} \tag{1.33}$$

where E_i is the energy of the state ϕ_i. From (1.31) we can express this partition function in the path integral representation

$$Z = \int D[\phi] e^{S_E[\phi]}, \tag{1.34}$$

where S_E is the Euclideanised action. This can then be used to calculate properties of the thermal QFT. For example by introducing a source, J, a Green's function can be obtained by functional differentiation of $Z[J]$ with respect to J at two different points. This will be the thermal two point propagator for a system at temperature $T = 1/(k_B \beta)$.

In 1976 Gibbons and Hawking, [35], applied these methods to gravitational systems in order to gain more understanding of the quantum nature of black holes. By treating the metric in a similar way to the field ϕ, above, they were able to re-derive the key formulae of black hole thermodynamics which show that, remarkably, black holes are thermal objects. In [36], Hawking had previously shown that black holes

emit radiation and have a temperature, T_H, given by

$$T_H = \frac{\kappa}{2\pi k_B}, \tag{1.35}$$

where κ is the surface gravity of the black hole. In [36–39] a consistent theory of black hole thermodynamics was presented showing that black holes have an entropy, S, given by

$$S = \frac{k_B \mathcal{A}}{4G_N}, \tag{1.36}$$

where $\mathcal{A}$ is the area of the black hole's event horizon and G_N is Newton's gravitational constant.

In [40] Witten used these findings to show how the gauge/gravity correspondence could apply to field theories at a finite temperature. The required string theory set up is similar to that described above but where the charges of the $D3$-branes are fixed such that the D-branes now correspond to *non*-extremal p-branes in supergravity. The metric of such a scenario is given by (1.17) but without the requirement that $r_0 \to 0$. We are still interested in the supergravity limit such that, $r \ll L$, so the metric becomes

$$ds^2 = \frac{r^2}{L^2}\left(\left(1 - \frac{r_0^4}{r^4}\right)dt^2 - d\overrightarrow{x}^2\right) - \frac{L^2}{r^2}\left(1 - \frac{r_0^4}{r^4}\right)^{-1} dr^2 - L^2 d\Omega_5^2. \tag{1.37}$$

This metric describes an asymptotically adS Schwarzschild black hole crossed with an S_5. The temperature of the black hole can be calculated by Wick rotating $t \to i\tau$ and ensuring that the horizon is regular. For this to be the case, τ must be periodic with $\Delta\tau = \beta = 4\pi/f'(r_0) = 1/(k_B T_H)$. Bulk theories such as this that possess a black hole are dual to thermal QFTs. This thermodynamic duality was further confirmed in [41], where the independently calculated entropies of each of the dual theories were shown to match[3].

It is important to note that the $\mathcal{N} = 4$ SYM gauge theory discussed in the canonical example of the correspondence is an example of a conformal field theory

[3]Technically they were shown to match up to a factor of 3/4.

(CFT). Such theories are invariant under a conformal symmetry group, which has complete scale invariance. By adding temperature to the system we break this scale invariance by introducing a temperature scale. However, in the absence of another scale, the absolute value of the temperature is meaningless and it is only by comparing the temperature to another scale that a meaningful value can be obtained. In the models of holographic superconductivity discussed in this thesis, this additional scale is provided by the charge density of the QFT.

1.2.5 Summary

At its heart the correspondence is a duality between a gravity theory in d dimensions and a lower dimensional field theory. In this way the gravity theory can be thought of as a *holographic* 'image' of the QFT. This concept of holography is not new to physics, but first emerged as a resolution to a paradox of black hole thermodynamics. The problem arose as a result of Bekenstein's assertion that the maximum entropy of a given volume scales with the area of that volume, as in (1.36). This contradicts the intuition that the complexity of a system grows with volume. The *holographic principle* was the solution, first proposed by 't Hooft, which states that a quantum gravity theory in some volume can be completely described by a field theory on the boundary of that volume with less than one degree of freedom per Planck area, [42, 43]. The gauge/gravity correspondence is a precise example of this principle. It is for this reason that approaches that use the gauge/gravity correspondence are often prefixed with the word *holographic*.

We have seen how a gauge/gravity correspondence can be motivated from one particular string theory set up. We have also seen how this can be deformed to include theories at finite temperature. In light of the holographic principle many now think that this correspondence may in fact be much more general, applying to many different string theories with different gravitational spacetimes with different duals. It is this view that has led some to assert that perhaps "*hidden within every non-Abelian gauge theory, even within the weak and strong nuclear interactions, is a theory of quantum gravity*", [44]. Of course, even the simplest manifestation of the correspondence has not been proven, let alone such a bold statement but it does

hint at the duality's potential power.

It is in this light that the correspondence is often put to use; with the dictionary being applied to arbitrary string and gravity theories to study a corresponding QFT. Without a proof, these approaches are obviously flawed but allow a possibility to find out new things about the world around us and the correspondence itself. With limited other means of studying strongly coupled theories it is certainly worth a try. The first applications of the correspondence were aimed at describing quantum chromodynamics - the strongly coupled Standard Model gauge theory describing quarks. However, with the existence of many open questions in condensed matter physics that involve strong coupling, attention soon turned in this direction. The work presented in this thesis is concerned with the application of the gauge/gravity correspondence to the problems of superconductivity.

Chapter 2

Holographic Superconductivity

We saw in the previous chapter that a theoretical understanding of high temperature superconductivity is still lacking. There are also indications that the underlying theory exhibits signs of strong coupling behaviour which would make the exploration of such a theory very difficult. Holographic superconductivity is an attempt to provide a strongly coupled description of superconducting behaviour via the gauge/gravity correspondence. The idea is to find a gravitational field theory in the bulk spacetime whose boundary theory exhibits superconducting behaviour. In 2008 such a theory was found by Gubser in [45] and developed by Hartnoll, Herzog and Horowitz in [46]. The remainder of this chapter will be concerned with outlining the key aspects of this model.

2.1 The Basic Model

The model presented in [45, 46] follows the traditional formulation of the gauge/-gravity duality where the bulk spacetime on the gravity side of the correspondence asymptotes to adS space. The theory of gravity in this spacetime is chosen to be classical general relativity which, in accordance with the correspondence, is to be thought of as a low energy effective theory to some unspecified overarching string theory. Such an approach is referred to as *bottom up*, as opposed to *top down* where one would start with a well defined string theory from which a specific low energy

theory can be derived[1].

The mechanism for superconductivity in this model is analogous to that of the Ginzburg Landau theory of superconductivity. As described in section 1.1.3, in GL theory the onset of superconductivity coincides with the condensation of the order parameter representing the number density of superconducting electrons. The order parameter at the boundary of the holographic model is an operator, $\langle\mathcal{O}\rangle$, that at high temperatures has a zero expectation value, but then condenses at some critical temperature, T_c. The gravitational dual to this operator is a complex scalar field, ψ, that propagates in the bulk. Since the notion of temperature is crucial to this model, the bulk spacetime must possess a black hole. The general idea is that at high temperatures of the black hole ψ has a trivially zero profile but condenses out of its vacuum as the temperature drops, corresponding to the condensation of $\langle\mathcal{O}\rangle$. In 2008 Gubser found these characteristics to be exhibited in the surprisingly simple model of a charged scalar field around a charged black hole in adS space.

Before we continue to describe this model in more detail it is interesting to note that a priori one might expect that such a model is destined to fail. The reason being that there exists a set of theorems, collectively known as the "no hair theorems", that prohibit matter fields of the type described above from having a non-trivial profile outside of the black hole radius, see [50] for a review and [51] for an explicit example. However, whilst these theorems are powerful there is no general no-hair theorem and counter examples do exist, [52]. Gubser's model is indeed one such example.

An interesting feature of fields propagating in an adS spacetime is that they can remain stable whilst having a tachyonic, or negative, mass squared, provided it is not below the Breitenlohner-Freedman (BF) bound, [53]

$$m^2L^2 \geq \frac{-d^2}{4}, \tag{2.1}$$

where L is the adS lengthscale. This bound can be found directly from (1.27) by

[1]Examples of top down theories of holographic superconductors have since been found, see [47–49] for examples.

ensuring that $\lambda_\pm$ are real. It turns out that in Gubser's model, if the mass of ψ lies in the vicinity of the BF bound[2] then the system can become unstable to the spontaneous formation of scalar hair at sufficiently low temperatures of the black hole. A rough argument is provided in [45] as to why this might be. The argument involves the effective mass of the scalar field, m_{eff}. In the model the effective mass is related to the actual scalar mass and the temporal component of the gauge field that gives the black hole its charge

$$m_{eff}^2 = m^2 - q^2 A_t g^{tt} A_t. \tag{2.2}$$

Gubser argues that at low temperatures of the black hole, the profile of g^{tt} and A_t can be such that m_{eff}^2 is large and negative enough over a sufficient range for an instability to set in.

The action that describes the bulk gravitational dynamics of this theory in $d+1$ dimensions is given by

$$\begin{aligned} S = \frac{1}{2\kappa^2}\int d^{d+1}x\sqrt{-g}\left[-R + \frac{d(d-1)}{L^2}\right] \\ + \int d^{d+1}x\sqrt{-g}\left[-\frac{1}{4}F^{ab}F_{ab} + |\nabla_a\psi - iqA_a\psi|^2 - V(|\psi|)\right], \end{aligned} \tag{2.3}$$

where $\kappa^2 = 8\pi G_{(d+1)}$ provides an explicit Planck scale in the system, g is the determinant of the metric and R is the Ricci scalar. The negative cosmological constant, $-d(d-1)/L^2$, has been written in terms of a length scale, L, $\mathbf{A}$ is the gauge field and ψ is a scalar field with charge q. As we are working with a bottom up approach to the correspondence there is no specific string theory that will fix our choice of potential, $V(|\psi|)$. Therefore the potential is simply chosen to be the simplest possible case consisting of a single term, quadratic in ψ

$$V(|\psi|) = m^2|\psi|^2, \tag{2.4}$$

[2]The problems associated with tachyonic masses, such as causality, *etc.* are not a problem here as the bulk theory is not attempting to describe the universe around us, but is simply a tool to describe the superconducting system on the boundary.

where m is the mass of the scalar field.

The early formulations of this model consider only what is known as the probe limit. This is the weakly gravitating limit in which the backreaction of the gauge and scalar fields on the metric can be neglected. This is an artificial limit but retains many of the key physical characteristics of the holographic superconductor.

In the probe limit the bulk spacetime is that of a planar Schwarzschild adS black hole in $d+1$ dimensions

$$ds^2 = f(r)dt^2 - \frac{dr^2}{f(r)} - r^2(dx_1^2 + ... + dx_{d-1}^2), \tag{2.5}$$

where

$$f(r) = \frac{r^2}{L^2}\left(1 - \frac{r_+^d}{r^d}\right). \tag{2.6}$$

It is straightforward to extremize the action (2.3) with respect to the gauge and scalar fields to obtain their respective field equations. Since a detailed analysis of very similar equations will be provided in the next chapter we shall not go through this here, but simply note that the fall off of the scalar field at the boundary is given by (1.27) and the expectation value of the boundary operator $\langle\mathcal{O}\rangle$ is identified with either ψ_0 or ψ_1, see section 1.2.3 for details. One can then find numerical solutions to the field equations for a range of temperatures in order to explore the variation of $\langle\mathcal{O}\rangle$. Figure 2.1 shows how $\langle\mathcal{O}_+\rangle$, where $\dim[\mathcal{O}_+] = 3$, varies with temperature in a theory where $d = 4$. The plot shows the sudden condensation of the operator out of its vacuum at a critical temperature T_c. It is straightforward to verify that in the vicinity of T_c

$$\langle\mathcal{O}\rangle \sim (T_c - T)^{1/2}, \tag{2.7}$$

precisely that prescribed by GL theory in (1.6).

In order to verify that the boundary theory is superconducting the electrical conductivity must be calculated. The conductivity is related to the linear response of the system to a time dependent perturbation of the gauge field of frequency ω.

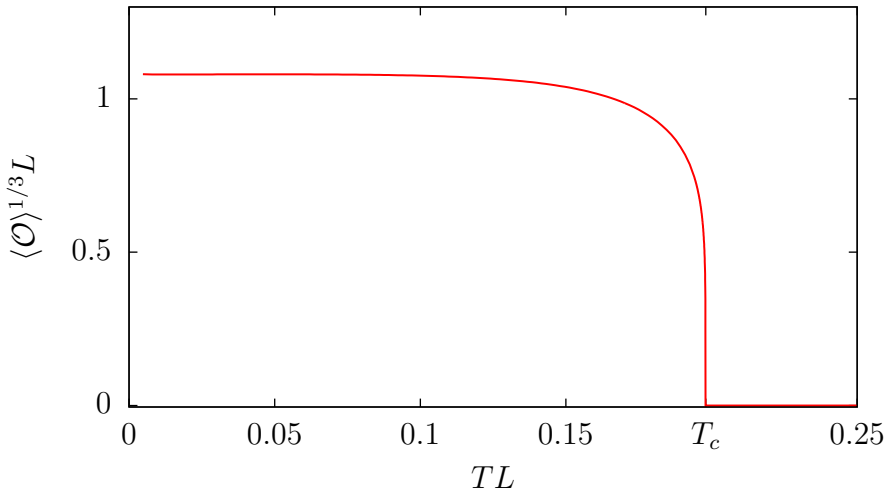

Figure 2.1: Plot depicting the condensation of a boundary operator.

The actual calculation involves computing a two point correlator via a process of holographic renormalization. This will be discussed in detail in section 3.6 and so will not be discussed here. The results of such a calculation are shown in figure 2.2. This plot shows the real, σ_r, and imaginary, σ_i, parts of the conductivity as a function of ω. The key feature of this plot is the presence of a step in σ_r which coincides with the minimum of σ_i. This step is interpreted as the frequency/energy gap of the system. The value, ω_g is determined by the minimum of σ_i. In BCS theory this would be the energy required to disassociate the electrons in a Cooper pair, above this frequency/energy normal conductivity resumes. At frequencies below the gap σ_r appears to be zero and σ_i diverges to infinity. These are precisely the desired characteristics since, by the Kramers-Kronig relations, (1.10), the pole in σ_i implies that σ_r must possess a δ function peak at $\omega = 0$ [3]. This profile of the conductivity for $\omega < \omega_g$ agrees precisely with what we expected from our Drude model calculations in section 1.1.4 and demonstrates that the boundary system does superconduct.

We have shown that the holographic superconductor shares a number of characteristics with GL theory but there are a number of distinctions that are worth mentioning, [54]. First of all GL theory is not a microscopic theory as the phase transition is put in by hand and it is only valid in the vicinity of T_c where the order

[3] Causality constraints guarantee that that our system is analytic in the upper half plane and that these relations apply, [15].

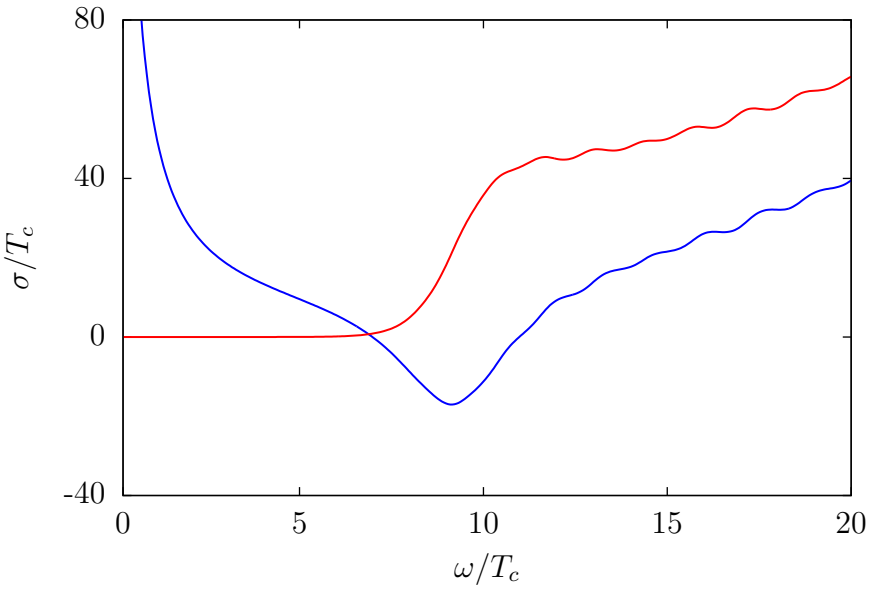

Figure 2.2: Plot showing the real (red) and imaginary (blue) parts of the DC electrical conductivity, σ, as a function of ω. The small oscillations at larger ω are a numerical artefact.

parameter is small. This is not the case with the holographic model as the dynamics are fully determined by the action and we can study the system at any temperature. Having said this, it is important to remember that as we are using a bottom up approach the potential in our action is arbitrary. The addition of higher powers of ψ to the action, for example, may have little effect near T_c but could dramatically alter the physics at lower temperatures. Thus, a truly microscopic description of holographic superconductivity can only be achieved from actions obtained from string theory.

This sums up our initial discussions of the holographic superconductor save for one important point. In the gauge/gravity correspondence local symmetries in the bulk correspond to global ones on the boundary. Since superconductivity is associated with the breaking of a local symmetry, and superfluidity, the breaking of a global one, it appears that we have superconductivity only in the bulk and superfluidity at the boundary. Whilst this is true it is still possible to view this boundary theory as superconducting in the limit that the $U(1)$ symmetry is *weakly gauged*, [55]. In this scenario we are saying that there is a gauge field on the boundary but that its charge is small and can be neglected. Such an approximation has the consequence

that photons on the boundary are non-dynamical. This does not pose much of a problem as in many models of condensed matter physics, including BCS theory, the dynamism of photons is neglected as their effects are small. For this reason we shall continue to refer to the boundary theory as a superconductor for the remainder of this thesis.

Chapter 3

The Gauss-Bonnet Holographic Superconductor

The research presented in this chapter is largely based on [1] and [2]. This chapter is concerned with the study of holographic superconductors in a model where the gravitational theory is given by Gauss-Bonnet (GB) gravity. GB gravity can be thought of as Einstein gravity with the addition of $\mathcal{O}(\alpha')$ corrections present in a perturbative expansion towards a full string theory. By including this GB term in the gravitational action, one can study the stability of the superconducting phenomena of these low energy models to the inclusion of higher order corrections. Such a set up was studied in the probe limit in [56], finding that the qualitative features of the model appeared stable to the inclusion of these GB terms but that the details were altered. Since that first paper a great many aspects of these models have been studied, see [57–62] for examples. This chapter is concerned with the findings of [1] and [2] in which the GB holographic superconductor was studied in the fully backreacting set up for a range of masses and different values of the GB coupling constant, α. We shall find that there are regions of parameter space where the inclusion of the GB term dramatically changes the nature of the system.

We begin with a brief overview of GB gravity followed by a discussion of the holographic model that we will use. We then solve the model numerically in order to study the consequences of the GB terms on the superconducting boundary theory. First, we focus on the critical temperature of the system, then we analytically inves-

tigate the zero temperature limit before finally studying the numerical conductivity of the system.

3.1 Gauss-Bonnet Gravity

GB gravity is Einstein gravity with the addition to the action of the GB term from Lovelock gravity [63]. Lovelock gravity is a generalization of Einstein theory to an arbitrary number of dimensions. The Lovelock lagrangian density is given by

$$\mathcal{L} = \sqrt{-g} \sum_{n=0}^{p} \alpha_n \mathcal{R}^n \tag{3.1}$$

where

$$\mathcal{R}^n = \frac{1}{2^n} R_{i_1 j_1 k_1 l_1} ... R_{i_n j_n k_n l_n} \epsilon^{i_1 j_1 ... i_n j_n} \epsilon^{k_1 l_1 ... k_n l_n} \tag{3.2}$$

is the Euler density of a $2n$ dimensional manifold. Here g is the determinant of the metric, R_{ijkl} is the Riemann tensor and α_n is an arbitrary coupling constant. The number of spacetime dimensions, d, is given by $d = 2p + 2$ if even, or $d = 2p + 1$ if odd. Like Einstein gravity, the field equations of Lovelock gravity are second order.

Expanding the sum in (3.1) we get

$$\mathcal{L} = \sqrt{-g} \left(\alpha_0 + \alpha_1 R + \alpha_2 \left(R^2 + R^{abcd} R_{abcd} - 4 R^{ab} R_{ab} \right) + ... \right) \tag{3.3}$$

where the term with the α_2 pre-factor is the GB term. This expansion shows that Einstein gravity can be thought of as a particular case of Lovelock gravity where $\alpha_1 = 1$, $\alpha_n = 0$ for $n \geq 2$ and α_0 may or may not be zero depending on whether a cosmological constant is required. For GB gravity one also allows $\alpha_2 \neq 0$ in addition to α_0 and α_1. In four dimensions the GB term is a topological invariant and will have only a trivial effect on the dynamics of the system. In order to observe the non-trivial effects of the GB term we must consider spacetimes with five or more dimensions.

In [64] GB gravity was found to be the low energy effective theory for $E_8 \times E_8$

heterotic string theory and in [65] it was shown to be ghost free. These findings, among others, have led many to think that the GB terms provide a suitable candidate for the $\mathcal{O}(\alpha')$ corrections of Einstein gravity in a perturbative expansion towards a full string theory. This is the key reason we are interested in studying the effect that these corrections have on the holographic superconductor. By studying these superconductors in GB gravity we are investigating the model's stability to the inclusion of higher order terms. In addition to this it is also interesting to study what effect these new terms could have on the superconductor away from a perturbative limit. For this reason we shall not restrict ourselves to the limit of small GB coupling.

3.2 The Model

We shall begin with the gravitational action of our GB holographic superconductor

$$S = \frac{1}{2\kappa^2}\int d^{d+1}x\sqrt{-g}\left[-R + \frac{d(d-1)}{L^2} + \frac{\alpha}{2}\left(R^{abcd}R_{abcd} - 4R^{ab}R_{ab} + R^2\right)\right] + \int d^{d+1}x\sqrt{-g}\left[-\frac{1}{4}F^{ab}F_{ab} + |\nabla_a\psi - iqA_a\psi|^2 - V(|\psi|)\right]. \tag{3.1}$$

This is simply the action in (2.3) with the addition of the GB term from (3.1). Here α is the GB coupling constant with dimensions of length squared. As before, we shall choose our potential, $V(|\psi|)$, to have the simple form of a single term, quadratic in ψ

$$V(|\psi|) = m^2|\psi|^2, \tag{3.2}$$

The gravitational field equations are obtained by extremizing this action with respect to the inverse metric, giving

$$R_{ab} - \frac{1}{2}Rg_{ab} + \frac{d(d-1)}{2L^2}g_{ab} - \alpha\left[H_{ab} - \frac{1}{4}Hg_{ab}\right] = 8\pi G T_{ab} \tag{3.3}$$

where

$$H_{ab} = R_a^{\ cde}R_{bcde} - 2R_{ac}R^c_b - 2R_{acbd}R^{cd} + RR_{ab}\ , \tag{3.4}$$

T_{ab} is the matter energy momentum tensor

$$T_{ab} = 2\mathcal{D}_{(a}\psi^{\dagger}\mathcal{D}_{b)}\psi - F_{ac}F_{b}{}^{c} - \left[|\mathcal{D}_{c}\psi|^{2} - \frac{1}{4}F_{cd}^{2} - m^{2}|\psi|^{2}\right] g_{ab} \ , \tag{3.5}$$

and $\mathcal{D}_a = \nabla_a - iqA_a$ is the gauge covariant derivative.

In the absence of any matter fields (3.3) admits a pure adS solution

$$ds^{2} = \frac{r^{2}}{L_{e}^{2}}\left[dt^{2} - (dx_{1}^{2} + ... + dx_{d-1})\right] - \frac{L_{e}^{2}}{r^{2}}dr^{2} \tag{3.6}$$

where

$$L_{\mathrm{e}}^{2} = \frac{L^{2}}{2}\left(1 + \sqrt{1 - \frac{4\alpha}{L^{2}}}\right) \rightarrow \begin{cases} \frac{1}{2}L^{2} \ , & \text{for } \alpha \rightarrow \frac{1}{4}L^{2} \\ L^{2} \ , & \text{for } \alpha \rightarrow 0 \\ \infty \ , & \text{for } \alpha \rightarrow -\infty, \end{cases} \tag{3.7}$$

is the effective adS lengthscale. This expression shows us that the presence of the GB term renormalizes the adS lengthscale away from the cosmological constant scale, L, as α becomes non-zero.

In order to study holographic superconductivity we look for plane-symmetric charged black hole solutions that may or may not have scalar hair. We choose our metric to have the following form

$$ds^{2} = f(r)e^{2\nu(r)}dt^{2} - \frac{dr^{2}}{f(r)} - h(r)\frac{r^{2}}{L_{e}^{2}}(dx_{1}^{2} + ... + dx_{d-1}^{2}), \tag{3.8}$$

where the function $e^{2\nu(r)}$ has been introduced to accommodate the backreaction of the matter fields on the metric. Since the Einstein-GB equations are invariant under coordinate rescalings we will use this gauge freedom to fix $h(r) = 1$.

We choose the matter fields to be static, given by

$$A_{a} = \phi(r)\delta_{a}^{0}, \qquad\qquad \psi = \psi(r), \tag{3.9}$$

where we can consistently take ψ to be real.

We shall restrict our analysis to a GB holographic superconductor with five bulk

spacetime dimensions. This is the minimum number of dimensions required for the GB term to have a dynamical effect and this choice also corresponds to a boundary theory with four spacetime dimensions. With our chosen Ansätze the fully coupled system of gravity, gauge and scalar equations take the simple form

$$\phi'' + \left(\frac{3}{r} - \nu'\right)\phi' - 2q^2\frac{\psi^2}{f}\phi = 0\,, \tag{3.10}$$

$$\psi'' + \left(\frac{3}{r} + \nu' + \frac{f'}{f}\right)\psi' + \left(\frac{q^2\phi^2}{f^2e^{2\nu}} - \frac{m^2}{f}\right)\psi = 0\,, \tag{3.11}$$

$$\left(1 - \frac{2\alpha f}{r^2}\right)\nu' = \frac{2\kappa^2}{3}r\left(\psi'^2 + \frac{q^2\phi^2\psi^2}{f^2e^{2\nu}}\right), \tag{3.12}$$

$$\left(1 - \frac{2\alpha f}{r^2}\right)f' + \frac{2}{r}f - \frac{4r}{L^2} = -\frac{2\kappa^2}{3}r\left[\frac{\phi'^2}{2e^{2\nu}} + m^2\psi^2 + f\psi'^2 + \frac{q^2\phi^2\psi^2}{fe^{2\nu}}\right], \tag{3.13}$$

$$\left(1 - \frac{2\alpha f}{r^2}\right)\left(\frac{1}{2}f'' + f\nu'' + f\nu'^2 + \frac{3}{2}f'\nu'\right) + \frac{f'}{r}\left(2 - \frac{\alpha f'}{r} - \frac{2\alpha f\nu'}{r}\right) + \frac{f'}{r}\left(\frac{1}{r} + 2\nu'\right) - \frac{6}{L^2} = -\kappa^2\left[\frac{-\phi^2\psi^2}{fe^{2\nu}} + f\psi'^2 - \frac{\phi'^2}{2e^{2\nu}} + m^2\psi\right], \tag{3.14}$$

where a prime denotes a derivative with respect to r. These five equations are not independent but related by a Bianchi identity which implies that one is redundant. We choose to drop (3.14) and use only (3.10) to (3.13) in our calculations.

If $\psi = \nu = 0$ there is an analytic solution to these equations describing a charged, black hole, [66, 67],

$$\phi = \frac{Q}{r_+^2}\left(1 - \frac{r_+^2}{r^2}\right) \tag{3.15}$$

$$f(r) = \frac{r^2}{2\alpha}\left[1 \pm \sqrt{1 - \frac{4\alpha}{L^2}\left(1 - \frac{r_+^4}{r^4}\right) + \frac{8\alpha\kappa^2Q^2}{3r^4r_+^2}\left(1 - \frac{r_+^2}{r^2}\right)}\right] \tag{3.16}$$

where r_+ is the event horizon, determining the "ADM" mass of the black hole, [68, 69], and Q is its charge. The lower sign choice in (3.16) must be taken if we wish to ensure that as $\alpha \to 0$ we retrieve the correct Einstein gravity description of a charged, Reissner-Nordström black hole:

$$f(r) = \frac{r_+^2}{L^2}\left(\frac{r^2}{r_+^2} - \frac{r_+^2}{r^2}\right) + \frac{2\kappa^2Q^2}{3r_+^4}\left(\frac{r_+^4}{r^4} - \frac{r_+^2}{r^2}\right). \tag{3.17}$$

From (3.16) one can see that the GB coupling constant must be restricted to $\alpha \leq$

$L^2/4$ in order to avoid a naked singularity. In a recent paper, [70], it was suggested that causality constraints from the hydrodynamic limit, [71], of the correspondence further limits the GB coupling to $\alpha \in [-0.711, 0.113]$. In this work, however, we shall permit the full range of $\alpha \in (-\infty, L^2/4]$ in our study for greater understanding of its effect.

We expect that (3.15) and (3.16) will describe the system at high temperatures and that below some critical temperature the scalar field will condense out of its vacuum and obtain some non-trivial profile. With the inclusion of back reaction a more rigorous argument than that presented in section 2.1 can be provided as to why this must be so.

As mentioned above, if $\psi = \nu = 0$, the system is described by a charged black hole given by (3.15) and (3.16). The temperature of this black hole is

$$T = \frac{1}{4\pi} f'(r)\Big|_{r=r_+} = \frac{r_+}{L^2\pi} - \frac{\kappa^2 Q^2}{3\pi r_+^5}. \tag{3.18}$$

If the mass and charge of the black hole balance such that

$$\frac{r_+^6}{L^2} = \frac{\kappa^2 Q^2}{3}, \tag{3.19}$$

the temperature will be zero and the horizon will become degenerate. Such black holes are called *extremal*. If we expand about the horizon of such an extremal black hole one sees that the topology of the metric becomes $adS_2 \times \mathbb{R}_3$

$$ds^2 = \frac{1}{2} f_+''(r - r_+)^2 dt^2 - \frac{2}{f_+''(r - r_+)^2} dr^2 - \frac{r_+^2}{L_e^2}\left(dx^2 + dy^2 + dz^2\right) \tag{3.20}$$

$$= \frac{12}{L^2}(r - r_+)^2 dt^2 - \frac{L^2}{12(r - r_+)^2} dr^2 - \frac{r_+^2}{L_e^2}\left(dx^2 + dy^2 + dz^2\right). \tag{3.21}$$

At large distances the spacetime asymptotes to adS_5 which places a BF bound on the scalar mass given by $m_{BF_5}^2 L_e^2 \geq -4$. In the near horizon limit the BF bound is that of an adS_2 geometry, $m_{BF_2}^2 L_{adS_2}^2 \geq -\frac{1}{4}$. Thus it is possible for the effective mass of the scalar to be above the BF bound from the adS_5 but below that of the

adS_2 leading to an instability in the near horizon region. Near extremality we have

$$\psi'' + \frac{2}{(r-r_+)}\psi' - \left(\frac{q^2Q^2L^4}{36r_+^6(r-r_+)^2} - \frac{m^2L^2}{12(r-r_+)^2}\right)\psi = 0 \tag{3.22}$$

$$\implies \qquad m_{eff}^2 = m^2 - \frac{q^2Q^2L^2}{3r_+^6}. \tag{3.23}$$

Therefore if the effective mass is more negative than the BF bound of the adS_2 there will be an instability

$$m_{eff}^2 L_{adS_2}^2 < -\frac{1}{4} \tag{3.24}$$

$$\implies \qquad 3 + m^2L^2 < \frac{q^2Q^2L^4}{r_+^6 3} = \frac{q^2L^2}{\kappa^2}. \tag{3.25}$$

This shows that in certain regions of parameter space, the system must become unstable at sufficiently low temperatures.

There are no known analytic solutions to these equations for the case of $\psi(r) \neq 0$, so we will obtain solutions numerically. The system that we wish to solve consists of two second order and two first order, coupled, non-linear, ordinary differential equations. In order to solve these we need to impose six boundary conditions, two at the horizon and four at the adS boundary. The position of the horizon, r_+, is defined by $f(r_+) = 0$. The horizon boundary conditions can be found by demanding that matter fields, metric and energy momentum tensor are regular there, which gives

$$\phi(r_+) = 0, \qquad \psi'(r_+) = \frac{m^2}{f'(r_+)}\psi(r_+)\ . \tag{3.26}$$

At the adS boundary we want the spacetime to asymptote to adS in standard coordinates so we shall look for a solution with

$$\nu \to 0\,, \qquad f(r) \sim \frac{r^2}{L_e^2} \qquad \text{as} \qquad r \to \infty\,, \tag{3.27}$$

where, in order to set $\nu(r \to \infty) = 0$ we have used a scaling symmetry of the metric

and equations of motion:

$$e^{\nu} \to a e^{\nu}, \qquad t \to t/a, \qquad \phi \to a\phi. \tag{3.28}$$

The asymptotic forms of ψ and ϕ are then determined by the field equations

$$\phi(r) \sim P - \frac{Q}{r^2}\,, \qquad \psi(r) \sim \frac{C_-}{r^{\Delta_-}} + \frac{C_+}{r^{\Delta_+}}\,, \tag{3.29}$$

where P, Q, C_- and C_+ are constants and $\Delta_\pm = 2 \pm \sqrt{4 + m^2 L_e^2}$. We choose to set $C_- = 0$, and interpret $\langle \mathcal{O}_{\Delta_+} \rangle \equiv C_+$, where $\mathcal{O}_{\Delta_+}$ is a boundary operator with conformal dimension Δ_+. If $\Delta_\pm > 3$, the opposite choice of $C_+ = 0$ and $\langle \mathcal{O}_{\Delta_-} \rangle \equiv C_-$ does give normalizable solutions but will not be considered in this work. An example of where such a choice is made for a system with Einstein gravity can be found in [72]. Q is proportional to the charge of the black hole and represents the charge density of the boundary theory, P is its chemical potential. We are now in a position to fix either P or Q for our boundary condition on ϕ. We choose to fix Q, keeping the charge density of the boundary field theory constant. Again see [72] for an example in which the opposite choice has been used.

One of the parameters of this system that we wish to investigate is m^2, the mass of the scalar field. We shall choose a sample of masses, greater or equal to that determined by the BF bound, $m^2 = -4/L_e^2$. Each choice of mass will be fixed with respect to the effective adS lengthscale, L_e, in order for the dimension of the boundary operator to remain constant with respect to variations in α.

In the next section we solve (3.10) to (3.13) numerically, reading this $1/r^{\Delta_+}$ fall-off of the scalar field to obtain $\langle \mathcal{O}_{\Delta_+} \rangle$ for a range of temperatures given by

$$T = \frac{1}{4\pi} f'(r) e^{\nu(r)} \bigg|_{r=r_+}\,. \tag{3.30}$$

Finally, the system of equations has a number of scaling symmetries in addition

to (3.28)

$$\begin{aligned}
&1. \quad r \to ar, \quad t \to at, \quad x^i \to ax^i, \qquad L \to aL, \quad q \to q/a, \quad \alpha \to a^2\alpha, \quad A \to aA \\
&2. \quad r \to br, \quad t \to t/b, \quad x^i \to x^i/b, \qquad f \to b^2 f, \qquad \phi \to b\phi \\
&3. \quad \phi \to c\phi, \quad \psi \to c\psi, \qquad q \to q/c, \quad \kappa^2 \to \kappa^2/c,
\end{aligned} \tag{3.31}$$

where the last symmetry involves a rescaling of the energy. For numerical convenience we will use these scaling symmetries to set $L = Q = q = 1$. With this rescaling κ^2 is the parameter used to vary the backreaction of the fields on the metric; if $\kappa^2 = 0$, referred to as the probe limit, the fields decouple from the metric entirely.

3.3 The boundary

Since we are interested in the asymptotic fall-off of the fields in our system it is convenient to compactify the radial distance by introducing a new coordinate

$$\rho = \frac{r_+}{r}. \tag{3.32}$$

In this new coordinate system the horizon is found at $\rho = 1$ and the adS boundary at $\rho = 0$. It also proves helpful to redefine the fields f and ψ according to

$$g(\rho) = \rho^2 f(\rho) \qquad\qquad X(\rho) = \frac{\psi(\rho) r_+^{\Delta-1}}{\rho^{\Delta-1}} \tag{3.33}$$

which provides us with a regular value of $g(0)$ and linear fall-off of $X(\rho \to 0)$. With these new definitions (3.10) to (3.13) become

$$X'' + X'\left(\frac{g'}{g} + \nu' + \frac{2\Delta - 5}{\rho}\right) \tag{3.34}$$

$$+ X\left((\Delta - 1)\left(\frac{g'}{g\rho} + \frac{\nu'}{\rho} + \frac{(\Delta - 5)}{\rho^2}\right) + r_+^2\left(\frac{q^2\phi^2}{g^2 e^{2\nu}} - \frac{m^2}{g\rho^2}\right)\right) = 0 \tag{3.35}$$

$$\phi'' - \phi'\left(\frac{1}{\rho} + \nu'\right) + \phi\left(\frac{\rho^{2\Delta-4}}{r_+^{2\Delta-4}}\frac{2q^2X^2}{g}\right) = 0, \tag{3.36}$$

$$g' = \frac{2g}{\rho} + \left(-g + \frac{1}{L^2}2r_+^2 - \frac{1}{3}\kappa^2 r_+^2 T_0^0\right)\frac{2r_+^2}{\rho(2\alpha g - r_+^2)} \tag{3.37}$$

$$\nu' = \frac{r_+^4\kappa^2}{3g\rho}\frac{(T_0^0 - T_\rho^\rho)}{(2\alpha g - r_+^2)} \tag{3.38}$$

where

$$T_0^0 = \frac{\phi'^2\rho^4}{2e^{2\nu}r_+^2} + \frac{\rho^{2(\Delta-1)}}{r_+^{2(\Delta-1)}}\left[\left(\frac{(\Delta-1)}{\rho}X + X'\right)^2\frac{g\rho^2}{r_+^2} + \frac{q^2\phi^2X^2\rho^2}{ge^{2\nu}} + m^2X^2\right],$$

$$T_0^0 - T_\rho^\rho = 2\frac{\rho^{2(\Delta-1)}}{r_+^{2(\Delta-1)}}\left[\left(\frac{(\Delta-1)}{\rho}X + X'\right)^2\frac{g\rho^2}{r_+^2} + \frac{q^2\phi^2X^2\rho^2}{ge^{2\nu}}\right].$$

These equations were solved using a numerical relaxation technique in which the profiles of each of the fields are guessed and then iteratively "relaxed" to profiles that solve the system of differential equations to the desired accuracy. Figure 3.1 shows an example of these solutions. The plot of $X(\rho)$ clearly shows that as the temperature drops below T_c the scalar field condenses out of its vacuum obtaining a non-trivial profile in the bulk, coinciding with a distortion of the profiles of ϕ, g and ν. Reading the linear fall-off of $X(\rho)$ allows $\langle\mathcal{O}\rangle$ to be plotted as a function of temperature, producing a plot very similar to figure 2.1. It is then straightforward to repeat this method for a variety of values of m^2, α and κ^2. Figure 3.2 shows the particular example of $m^2 = -3/L_e^2$ for three values of the GB coupling constant; $\alpha = 0$, 0.125 and 0.25 and two values of backreaction; $\kappa^2 = 0.0$ and 0.1. Each line in these plots shows the characteristic curve of the operator condensing out of its vacuum. The upper plot shows the un-normalized condensate, exhibiting how the inclusion of backreaction and higher curvature terms alter the hight and critical temperature of the condensate. In the lower plot the curves have been normalized

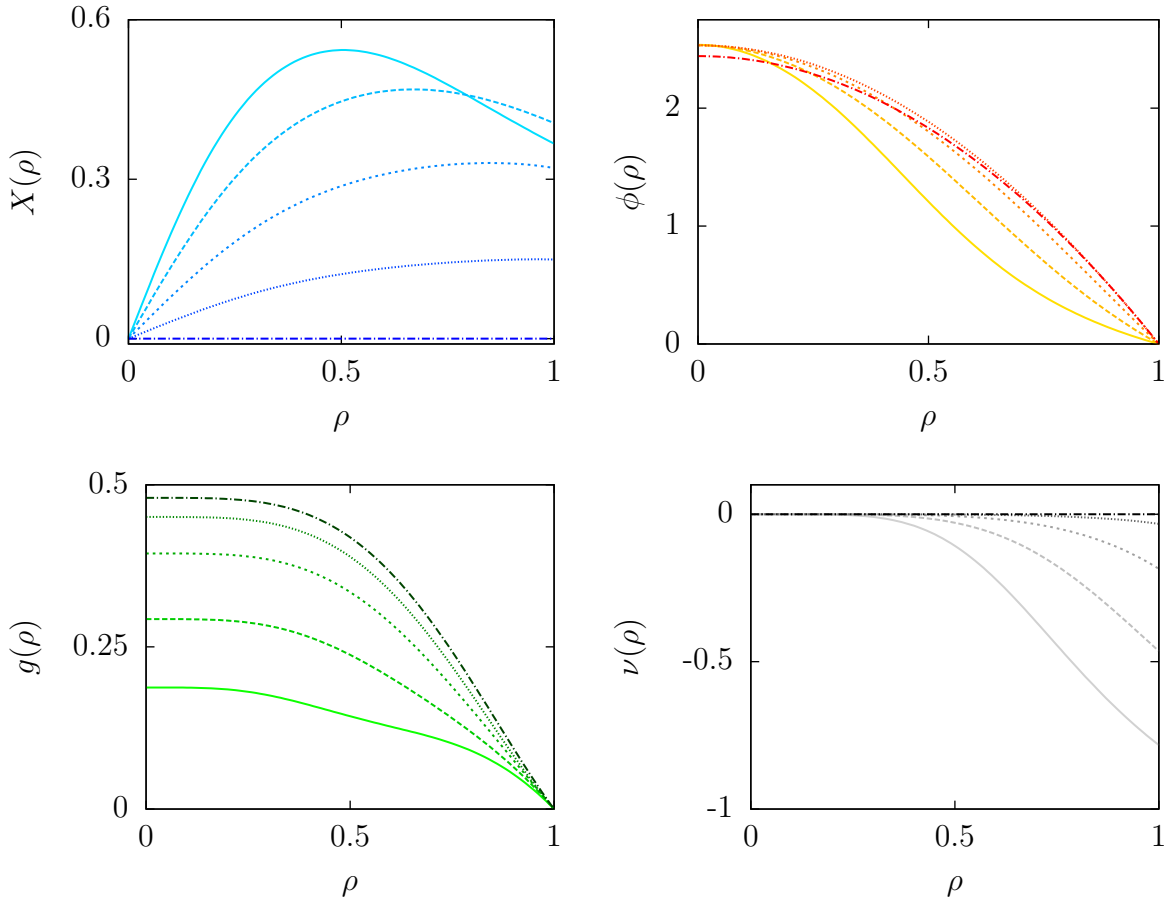

Figure 3.1: Plot showing the numerical solutions of (3.35) to (3.38) with $\alpha = 0.125$, $\kappa^2 = 0.1$ and $m^2 = -3/L_e^2$ for a variety of temperatures. The lines correspond to, from dark to light, $T/T_c \approx 1.14$, 0.98, 0.93, 0.70 and 0.63.

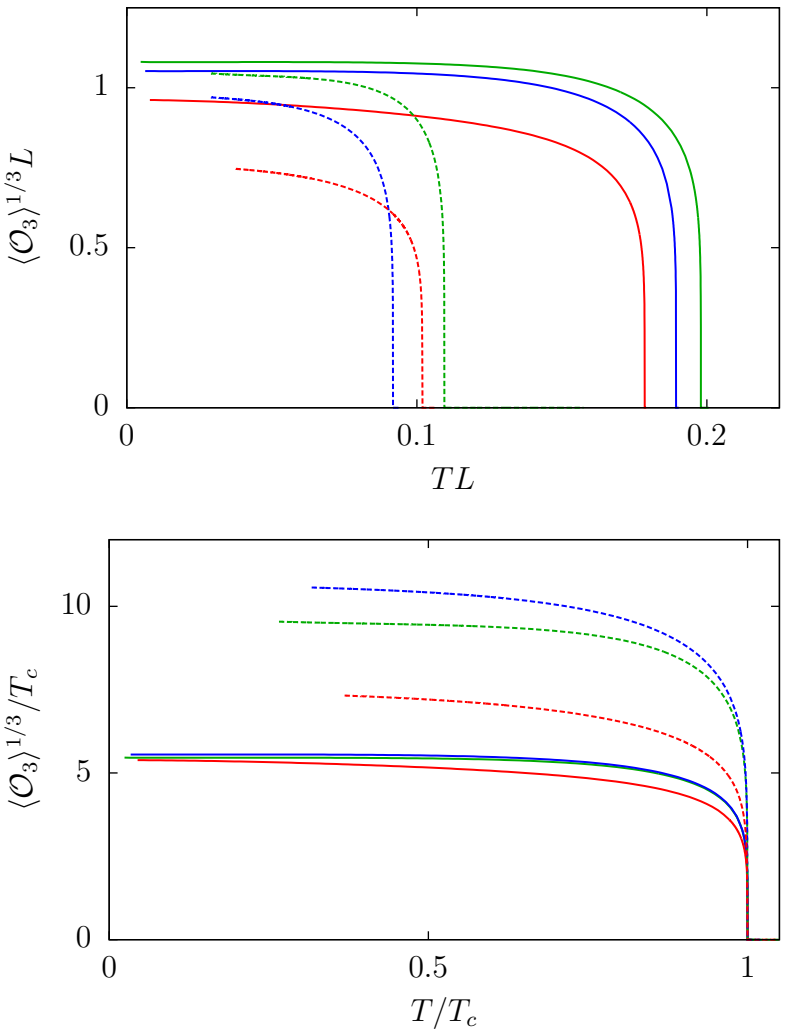

Figure 3.2: Two plots of the condensate as a function of temperature for $m^2 = -3/L_e^2$ and a selection of values of α and κ^2. In each case, solid lines correspond to $\kappa^2 = 0$ and dotted lines to $\kappa^2 = 0.1$. The green plot is $\alpha = 0$, blue is $\alpha = 0.125$ and red is $\alpha = 0.25$. The upper plot shows non-normalized data, which indicates the variation of critical temperature as both α and κ^2 vary. The lower plot shows the conventional plot of condensate against temperature, both rendered dimensionless by normalizing to T_c.

by T_c showing how alterations in α and κ^2 can change the shape of the condensate but that the near T_c fall-off remains the same.

3.4 The Critical Temperature

The curves in figure 3.2, as well as those from different regions of parameter space, are qualitatively similar so reproducing more of these plots provides little extra insight. The key information that we are interested in is the critical temperature of the system. As well as obtaining the exact value of T_c from plots such as those in figure 3.2, a rougher but quicker understanding can be obtained from an analytically generated lower bound introduced in [1]. This bound is found by looking at the scalar field equation near T_c. For temperatures just below T_c, the scalar is only marginally away from its vacuum and the metric and gauge field will be described by (3.16) and (3.15) up to corrections of order $\mathcal{O}(\psi^2)$. Thus, the scalar field satisfies a linear equation, (3.11), with f and ϕ taking their background values. Now letting $Y = r^3\psi$ and manipulating the equation of motion for Y implies that *if* a solution exists, then the integral

$$\int_{r_+}^{\infty} \frac{1}{r^3}\left[\frac{\phi_0^2}{f_0} + \frac{3}{L_e^2} + \frac{3f_0}{r^2} - \frac{3f_0'}{r}\right] = -\int_{r_+}^{\infty} \frac{f_0 Y'^2}{r^3 Y^2} \leq 0 \tag{3.39}$$

is negative. For much of parameter space this integral is negative at large T, and positive as $T \to 0$, thus observing where it changes sign provides a lower bound on T_c. It is important to note that negativity of this integral does not imply existence of a solution to the linearised equation near T_c as we have divided by $Y(r)$, but is simply a necessary condition on one if it exists.

Figures 3.3 to 3.5 show both the analytic lower bound (as lines) and numerical values (as points) of T_c for different values of α, κ^2 and m^2. Figure 3.3 demonstrates the dependence of T_c on m^2, focussing on $\alpha \geq 0$. It is possible to find superconducting solutions for $m^2 > 0$, indeed we found solutions up to a mass of $m^2 \approx 0.4$ for $\kappa^2 = 0$. We were able to find some solutions at non-zero backreaction but only for very small m^2 and κ^2 . The findings of [73] suggest that solutions exist at even larger values of m^2 but that numerical solutions become difficult to obtain due to an

intriguing "warping" of the space of permissible boundary conditions. The solutions that we did obtain for a small positive mass were only marginally different to those of $m^2 = 0$ and so these plots have not been included. In the plots that are shown we see that in the majority of the parameter space studied, the effect of increasing backreaction is to reduce the value of T_c. However, as $\alpha \to L^2/4$ and $m^2 \to -4/L_e^2$ the effect of backreaction is reversed and actually increases T_c. This can be explored in more detail by plotting T_c as a function of κ^2, as seen in figure 3.4. This plot clearly shows that in this very narrow region of parameter space the effect of backreaction can be to increase the critical temperature of the system substantially above its value in the probe limit. The ability to reach super-planckian values of backreaction has been verified numerically up to $\kappa^2 \approx 150$. It is also interesting to note that as one approaches this regime the lower bound on the critical temperature becomes significantly less accurate.

It is straightforward to extend this analysis to $\alpha < 0$, as shown in figure 3.5. In this regime the effect of altering the mass is less marked so one mass of $m^2 = -2/L_e^2$ has been chosen as a representative sample. These plots show that as α becomes more negative the critical temperature increases. Whilst this increase becomes more and more gradual as α is reduced it appears that an arbitrarily large T_c can be obtained by an appropriate choice of α. These plots also show that the effect of backreaction is, in all cases, to reduce T_c, but as α becomes large and negative its effect is diminished. This can be understood by looking at the action, (3.1). In the Einstein limit the curvature of the spacetime scales with κ. When $|\alpha|$ is large the higher order curvature terms dominate, meaning the curvature scales as $\sqrt{\kappa}$ and thus the effect of backreaction on the spacetime is reduced.

In an attempt to provide a clearer picture of the characteristics noted above we can use the analytically calculated lower bound and scan through the parameter space available to generate the lower bound on a surface of T_c, as seen in figure 3.6. Whilst these plots, at best, show only a lower bound to the true surface, they do exhibit some of the interesting characteristics of the system that have been supported by exact numerical results. We see immediately how altering the mass of the scalar field dramatically alters the nature of this superconducting system, particularly as

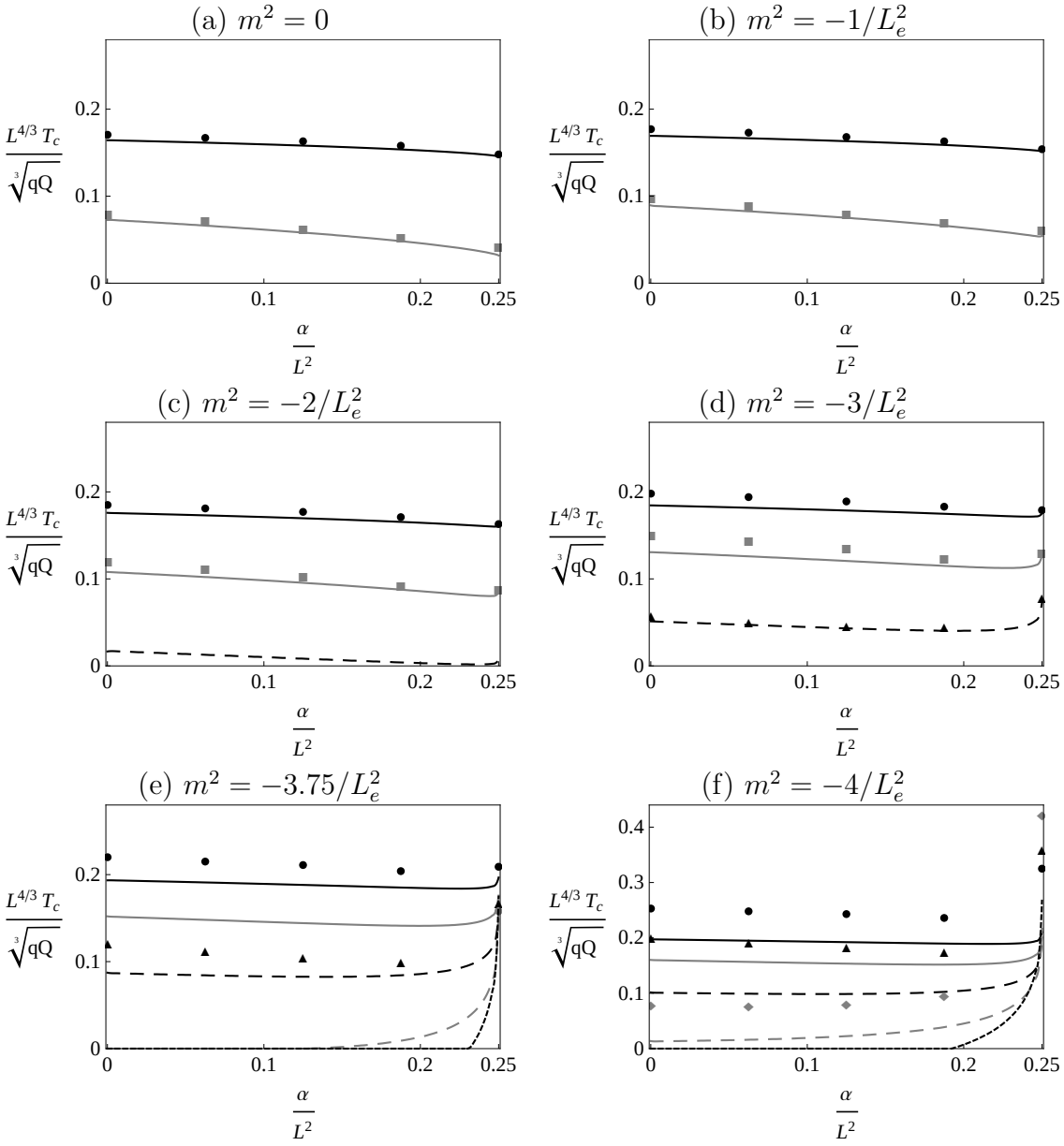

Figure 3.3: Plot of T_c as a function of α for a variety of κ^2; Lines represent the analytic lower bound, and the points represent numerically obtained values. The solid black lines and circular points corresponds to $\kappa^2 = 0.0$, solid grey lines and square points to $\kappa^2 = 0.05$, black (large) dashed with triangular points to $\kappa^2 = 0.2$, grey (large) dashed and diamond points to $\kappa^2 = 1$ and black (small) dashed to $\kappa^2 = 5$.

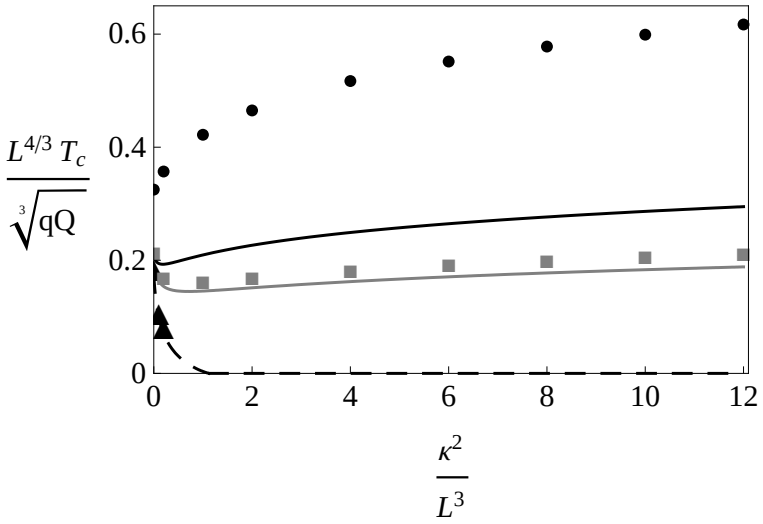

Figure 3.4: Plot of T_c as a function of κ^2 at $\alpha = 0.24999$ for different masses; For each mass the analytic lower bounds are represented as lines and numerical values as points. Black solid with circular points corresponds to $m^2 = -4/L_e^2$, grey with square points to $m^2 = -3.75/L_e^2$ and black dashed with triangular points to $m^2 = -3/L_e^2$.

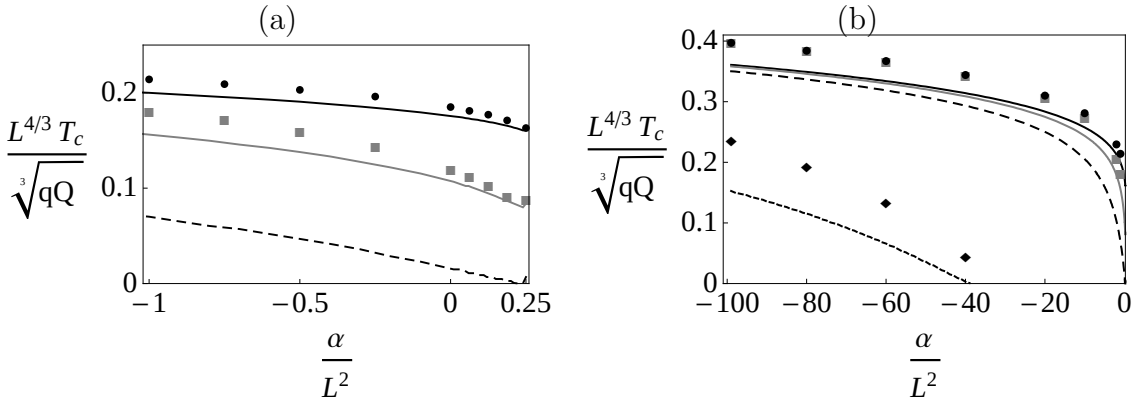

Figure 3.5: Plot of T_c with α for $m^2 = -2/L_e^2$. (a) shows the region $\alpha \in [-1, 0.25]$ and (b) shows the same plot but for $\alpha \in [-100, 0.25]$. The lines correspond to the lower bound, points to numerically obtained values of T_c. The black solid lines (and circular points) correspond to $\kappa^2 = 0$; solid grey (and square points) to $\kappa^2 = 0.05$; dashed black to $\kappa^2 = 0.2$ and (smaller) dashed black (with diamond points) to $\kappa^2 = 5$.

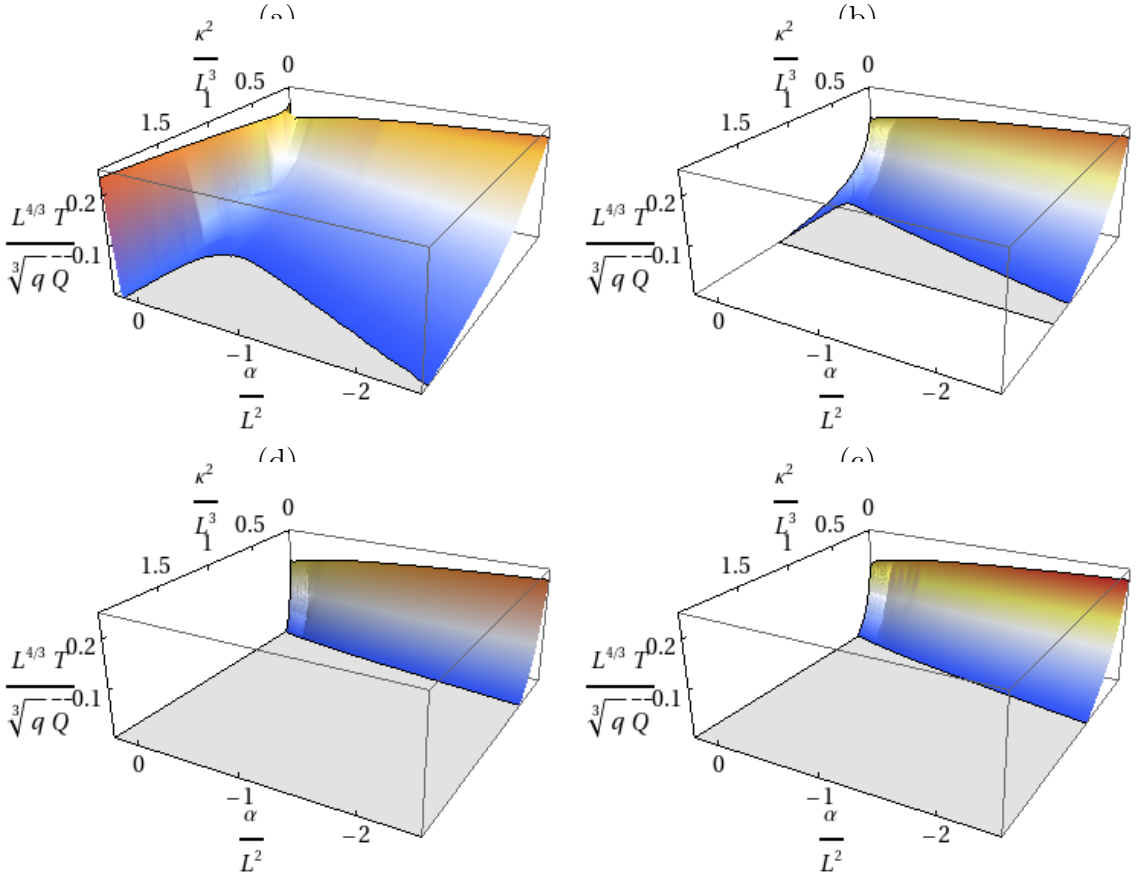

Figure 3.6: Plots (a), (b), (c) and (d) show the surface of a lower bound on T_c for $m^2 = -4/L_e^2$, $-3/L_e^2$, $-2/L_e^2$ and 0 respectively.

m^2 and α approach their lower and upper bounds respectively.

Having displayed these plots it is important to point out their limitations. We mentioned above that the negativity of the integral, (3.39), does not guarantee the existence of a solution to the field equations with $\psi \neq 0$ but is simply a bound on solutions if they exists. Thus, the strongest statement that we can make about these plots is that the true values of T_c must either be on or above these surfaces, or they must be zero.

3.5 Zero Temperature Superconductors

There is a great deal of interest in the zero temperature limit of these superconducting systems and in particular in the phase transitions that happen there. Most phase transitions are triggered by the thermal fluctuations of the system but at zero temperature, where there are no thermal fluctuations, phase transitions are triggered by the quantum fluctuations associated with Heisenberg's uncertainty principle. The critical points about which these zero temperature phase transitions occur are called quantum critical points (QCPs). It is thought that in certain regimes the effect of the QCP can extend to finite temperature giving rise to unusual physical phenomena. For real superconducting systems it is impossible to reach the absolute zero temperature required to study these QCPs. However, this is not necessarily the case with these theoretical models leading to a great deal of recent activity in this direction.

For holographic superconductors the temperature of the boundary theory is governed by the temperature of the black hole in the bulk spacetime. The temperature of a black hole in our system is given by

$$T = \frac{1}{4\pi} f'(r) e^{\nu(r)} \bigg|_{r=r_+} . \tag{3.40}$$

In general the temperature of a black hole can approach zero in a variety of ways depending on the type of black hole. For example, above the critical temperature of our system the black holes are simply Reissner-Nordström black holes in GB gravity. The temperature of such black holes is given by (3.18), which means that

the mass and charge can balance such that the temperature goes to zero at finite r_+. This is not the case for the uncharged Schwarzschild black hole that arises when $\kappa^2 = 0$. This has $f'(r_+) = 4r_+/L^2$ and the zero temperature limit is approached when $r_+ \to 0$. To study this limit of the holographic superconductor we must investigate the hairy black hole. A priori it is not immediately obvious how such black holes approach zero temperature; is it found at some finite r_+ or when $r_+ \to 0$? The numerical solutions indicate that the latter may be true since the temperature is reduced by reducing r_+ and within the range studied there have been no apparent zero temperature solutions at finite r_+. However, it is numerically very difficult to approach $r_+ = 0$ from some finite value and it is possible that a zero temperature-finite r_+ solution exists beyond the scope of the numerics. In [74] the authors calculated numerical results for holographic superconductors in a regime where r_+ is precisely zero and the results of which, reassuringly, seemed to correspond to the asymptote of their finite r_+ solutions. However the results that they obtain are singular, which as we shall see, raises some concerns.

We can attempt to find information about the true nature of the zero temperature superconductor with a little investigation of the field equations (3.10) to (3.13). In particular we will ask whether these equations permit the existence of zero temperature, regular solutions with a non-trivial scalar field. We will show that this is largely not the case. We extend the work of [75] by showing that there are no regular zero temperature solutions, including those with $r_+ = 0$ for scalars with tachyonic masses. We also address scalars with $m^2 \geq 0$.

We begin by imposing that our system be regular. This will be true if the energy momentum tensor, $T_{\mu\nu}$, is non-singular in coordinates that are locally regular at the horizon, or indeed, at $r = 0$ if there is no horizon. Using Eddington-Finkelstein coordinates defined by $v = t + r^*$ and $r = \rho$ where r^* is the *tortoise coordinate* defined by

$$dr^* = \frac{dr}{fe^{\nu}}, \tag{3.41}$$

the following combinations of the energy momentum tensor must be regular

$$T_{vv} = T_{tt} = fe^{\nu}T_t^t, \tag{3.42}$$

$$T_{v\rho} = \frac{-T_{tt}}{fe^{\nu}} = -e^{\nu}T_t^t, \tag{3.43}$$

$$T_{\rho\rho} = T_{rr} + \frac{T_{tt}}{f^2e^{2\nu}} = \frac{1}{f}(T_t^t - T_r^r). \tag{3.44}$$

(3.44) gives the most restrictive constraint, namely that

$$\frac{\phi^2\psi^2}{f^2e^{2\nu}} + \psi'^2 < \infty \tag{3.45}$$

must be finite and hence each of the individual terms must also be finite. We wish to assess whether the field equations permit these constraints to hold for a non-trivial solution at zero temperature. The field equations are unchanged by the coordinate transformation and we are free to use (3.10) to (3.13) in our analysis.

Note that (3.12), plus the regularity of $(T_0^0 - T_r^r)/f$ implies that $\nu'(r_+)$ is regular. If $\nu'(r_+)$ is regular then $\nu(r_+)$ is regular and $e^{\nu(r_+)} \neq 0$. Thus from the definition of the temperature of our black hole, (3.30), the requirement of zero temperature must imply that $f'(r_+) = 0$.

We shall now study what effect this constraint has on the scalar field equation

$$f\psi'' + \left(\frac{3}{r} + \nu' + \frac{f'}{f}\right)f\psi' + \left(\frac{q^2\phi^2}{fe^{2\nu}} - m^2\right)\psi = 0. \tag{3.46}$$

The terms containing ψ'' and ψ' go to zero at the horizon by the regularity of $\psi'(r_+)$ and the fact that $f'(r_+) = 0$, thus the last term must also go to zero. This implies that either $\psi(r_+) = 0$ or $m^2 = \frac{q^2\phi^2}{fe^{2\nu}}$. If $\psi(r_+) \neq 0$ then, by (3.44), $\frac{q^2\phi^2}{fe^{2\nu}} \to 0$ which implies that $m^2 = 0$. Our analysis does not rule out the existence of regular zero temperature solutions for this choice of mass. In fact, it seems likely that such solutions do exist in light of [74], where similar solutions were found for a system in four dimensional Einstein gravity. We leave the search for such solutions in this system to future research. To investigate non-zero masses we consider $\psi(r_+) = 0$. If $m^2 \leq 0$ then all the leading order terms of (3.46) have the same sign and cannot

balance irrespective of whether r_+ is finite or zero. Thus there can be no regular, superconducting solutions at zero temperature for scalar fields with tachyonic masses.

Turning to $m^2 > 0$, where $\psi(r_+) = 0$, it is possible to place strict constraints on these masses if solutions exist. Using the field equation for f:

$$\left(1 - \frac{2\alpha f}{r^2}\right) f' + \frac{2}{r} f - \frac{4r}{L^2} = -\frac{2\kappa^2}{3} r \left[\frac{\phi'^2}{2e^{2\nu}} + m^2\psi^2 + f\psi'^2 + \frac{q^2\phi^2\psi^2}{f e^{2\nu}}\right], \tag{3.47}$$

we see that if $\phi'(r_+) = 0$ then $r_+ = 0$ and $f(r) \sim r^2/L_e^2$ as $r \to 0$. From (3.46) we can then infer that $\phi(0) = 0$ as otherwise $q^2\phi^2\psi/fe^{2\nu}$ would be the only term at leading order. Then from the field equation for ϕ

$$\phi'' + \phi'\left(\frac{3}{r} - \nu'\right) - 2q^2\frac{\psi^2}{f}\phi = 0, \tag{3.48}$$

we see that the last term is sub-dominant and the remaining terms cannot cancel.

If $\phi'(r_+) \neq 0$, (3.48) implies that $r_+ \neq 0$. Then the leading and next to leading order terms of (3.47) give

$$\frac{\phi'^2}{e^{2\nu_+}} = \frac{12}{L^2\kappa^2}, \qquad\qquad f_+'' = \frac{24}{L^2}. \tag{3.49}$$

By using these expressions in (3.46) we obtain an equation for the allowed masses at zero temperature

$$m^2 = \frac{12}{L^2}(n^2 + n) + \frac{q^2}{\kappa^2}, \tag{3.50}$$

where $n \geq 1$ is the leading power of $(r - r_+)$ in an expansion of ψ about $r = r_+$.

This expression shows that there can be no regular solutions for $0 < m^2 < 24/L^2$. Thus if positive mass solutions do exist they can only be found at very large m^2 and/or backreaction; substantially above the values for which finite temperature solutions have been found. We also see that, unlike the finite temperature system, the "allowed" values of m^2 are directly related to κ^2. These observations suggest that this positive mass result may be spurious.

A key result of the above analysis is that the zero temperature limit of our superconducting systems with tachyonic scalars is not regular. We now wish to investigate this in a little more detail. In [74] a zero temperature solution was presented in which the spacetime, with no black hole, possessed logarithmic divergences as $r \to 0$. Such solutions can be found for our system in the Einstein limit but it becomes clear that they cannot be consistent with the idea of GB gravity as a perturbative expansion of Einstein gravity. The reason is that the logarithmic divergences of the metric cause the curvature invariants, such as the Riemann tensor and Ricci scalar, to diverge at $r = 0$. Since the GB terms involve higher order combinations of these invariants than Einstein gravity this singular behaviour will immediately be dominated by the GB terms as α becomes non-zero. If this is the case the concept of GB gravity being a perturbative correction to Einstein gravity is destroyed and the validity of such a solution must be questioned.

The manifestation of this problem on the fields themselves can be seen from a near horizon expansion. Following [74], for $\alpha = 0$, one can find a set of boundary conditions consistent with the field equations

$$\begin{aligned} \psi &= \sqrt{\frac{3}{\kappa^2}}(-\log r)^{1/2} + ..., & f &= \frac{m^2}{2} r^2 \log r + ..., \\ \phi &= \phi_0 r^\beta (-\log r)^{1/2} + ..., & e^{2\nu} &= K(\log r)^{-1} + ... \end{aligned} \tag{3.51}$$

where $\beta = -1 + \sqrt{1 - \frac{12q^2}{\kappa^2 m^2}}$ and ϕ_0/K is free parameter that can be used to tune the system. This Ansatz is consistent with the field equations provided $4q^2 > -m^2\kappa^2$ and after integrating the fields out from the horizon one finds the asymptotic profiles to be consistent with (3.29). Unlike in the four dimensional system we were unable to find an appropriate value of ϕ_0/K to remove the source of the boundary operator. As a result these solutions do not strictly describe a holographic superconductor. However, they are valid solutions of (3.10) to (3.13) and can be used to demonstrate our point.

The problem arises because α appears in the equations of motion, (3.10) to (3.13), like $(1 - \frac{2\alpha f}{r^2})$. From (3.13) it is possible to show that if $f(r) = f_s r^s (-\log r)^t$ then $s \leq 2$ which means that f/r^2 has at least a logarithmic singularity for $t > 0$.

Since for $\alpha = 0$, $t = 1 > 0$ this means turning on α immediately incorporates new, singular behaviour at $r = 0$ which destroys the perturbative relation between GB and Einstein gravity.

We have shown that there can be no regular solutions to our system at zero temperature, except possibly for massless or very massive scalars, and we have also given cause for caution when considering non-regular solutions. It is possible that consistent, non-regular, zero temperature solutions can be found that respect the relation between Einstein gravity and GB gravity but it seems unlikely. However, we can still find out information about the nature of this system in the zero temperature regime in the absence of such solutions. There are two analytic techniques which can provide bounds on the the critical values of the constants at the QCP. The first that we shall consider is precisely the bound in (3.25), found by studying the near horizon limit of an extremal Reissner Nordström black hole. This same bound can also be found in a very different way which I will briefly present here. The bound is found by studying the stability of the scalar vacuum solution to the formation of scalar hair. As described in [76, 77], we begin by perturbing the background solution, $\psi = 0$, by using the ansatz $\psi = \psi(r)e^{-i\omega t}$. Assuming $\psi(r) \ll 1$ the effects of back reaction can be ignored (since its effects occur at $\mathcal{O}(\psi^2)$) and the scalar field equation becomes

$$\psi'' + \left(\frac{3}{r} + \frac{f'}{f}\right)\psi' + \left(\frac{\omega^2}{f^2} + \frac{2q\phi\omega}{f^2} + \frac{q^2\phi^2}{f^2} - \frac{m^2}{f}\right)\psi = 0, \tag{3.52}$$

with ϕ and $f(r)$ taking their vacuum values (3.15) and (3.16)

The system is unstable if the field equation shows this small perturbation to diverge. This will be the case if there is a normalizable solution to (3.52) with ingoing boundary conditions at the horizon such that ω has a positive imaginary part. In general this equation can be solved numerically providing us with a bound on the critical values of the constants for general T. However, we are just interested in the $T = 0$ case for which an analytic expression can be obtained.

For zero temperature our (extremal) black hole has

$$\frac{r_+^6}{L^2} = \frac{\kappa^2 Q^2}{3} \tag{3.53}$$

and

$$f(r) = \frac{1}{2} f''_+ (r - r_+)^2 + ... \qquad \text{with} \qquad f''_+ = \frac{24}{L^2}. \tag{3.54}$$

It is then a simple exercise to expand (3.52) in the vicinity of r_+. It is suggested in [76, 77] that since we are concerned only with the onset of an instability it is sufficient to consider only the "threshold" case of $\omega = 0$. In this case we find the solution to the expanded field equation to be

$$\psi \to c_1 (r - r_+)^{\xi_+} + c_2 (r - r_+)^{\xi_-}, \tag{3.55}$$

$$\xi_\pm = \frac{1}{2} \left(-1 \pm \sqrt{1 - \frac{64 q^2 Q^2}{r^6 f''^2_+} + \frac{8 m^2}{f''_+}} \right). \tag{3.56}$$

If the expression inside the square root goes negative then ψ will turn imaginary and oscillate infinitely many times before reaching the horizon which, according to [77], indicates an instability. This provides us with a criterion determining the onset of an instability at extremality. Using (3.53) and (3.54) if

$$3 + m^2 L^2 < \frac{q^2 Q^2 L^4}{r_+^6 3} = \frac{q^2 L^2}{\kappa^2} \tag{3.57}$$

the blackhole is unstable to forming scalar hair, which is precisely the bound in (3.25).

Figure 3.7 shows both this bound (as red lines) and that taken from the zero temperature limit of the plots in figure 3.6 (blue lines). The regions below each of the curves are the regions of parameter space for which the system is unstable to forming scalar hair, as indicated by each bound. It was suggested in [76, 77] that the red lines are not simply a bound but actually indicate the location of the QCPs in the system. Assuming that the true surface of critical temperature is continuous these plots immediately show that this cannot be the case as in each plot the two

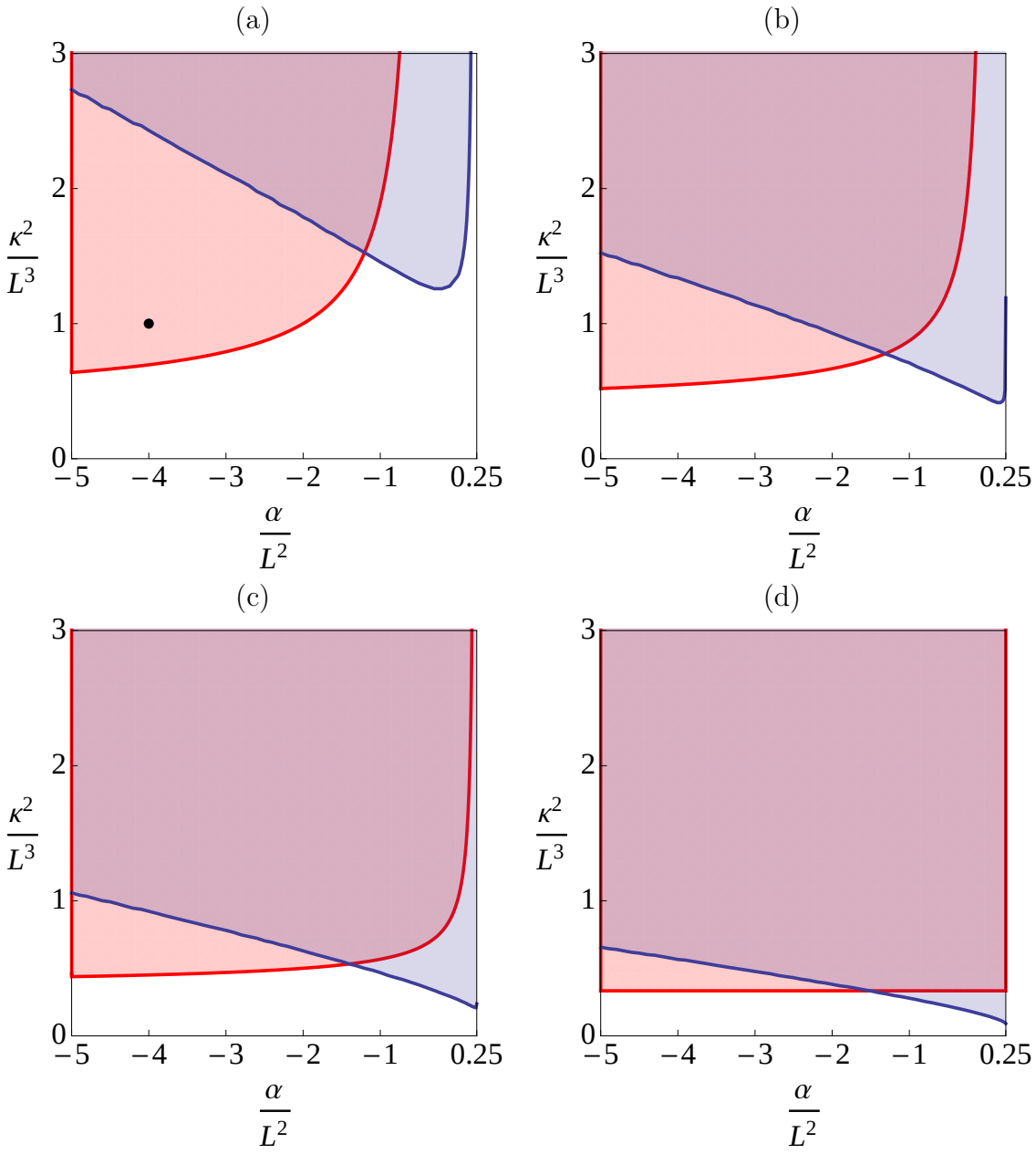

Figure 3.7: Plots (a), (b), (c) and (d) show two bounds, at $T = 0$, on the critical value of κ^2 as a function of α for $m^2 = -4/L_e^2$, $-3/L_e^2$, $-2/L_e^2$ and 0 respectively. The region below each of the lines is the region of instability. The blue lines were generated using (3.39) and the red, (3.57). The bounds continue to become less restrictive as m^2 increases above 0. The black point in (a) indicates a system with $m^2 = -4/L_e^2$, $\alpha = -4$ and $\kappa^2 = 1$ for which the critical temperature was found to be $T_c = 0.268$.

bounds cross. This has been further verified by the calculation of a non-zero critical temperature for a system with $m^2 = -4/L_e^2$, $\alpha = -4$ and $\kappa^2 = 1$ indicated by the black point in plot (a), which is outside the region of instability as indicated by bound (3.57). The correct way to see these curves is as complimenting lower bounds on the critical value of κ^2 as a function of α, being aware that the true critical values could be some way above these combined bounds.

The plots do however indicate that m^2 and α do have a significant effect on the zero temperature limit of the system with both bounds exhibiting the opening up of a region of superconductivity at large κ^2 as both α and m^2 approach their upper and lower bounds respectively. This observation fully supports that of figure 3.4 where numerically obtained values of T_c were found at large, super-planckian backreaction. From figure 3.7 (a) we see that this is unsurprising since in this region condensation must occur before the temperature drops to zero. What, however, still remains unclear is why the critical temperature increases with backreaction here. Another interesting observation that can be made from these plots is that there can be no QCPs in the absence of backreaction.

It is also interesting to see how these bounds relate to equation (3.50) which expresses the values that m^2 must take if regular, positive mass, superconducting solutions exist at zero temperature. Inserting (3.50) into (3.57) shows that that systems with these masses can never be in the unstable region as indicated by bound (3.57) and it is only for large and negative α that they can in the unstable region indicated by (3.39). This does not prove that these solutions do not exist but indicates that their existence may be unlikely.

3.6 Conductivity

In this section we investigate the electrical conductivity of the boundary theory. We begin with an explicit calculation of the conductivity which involves the process of holographic renormalization. We shall then numerically calculate the conductivity of our system and use it to analyse the nature of our superconducting boundary theory.

3.6.1 Holographic Renormalization

The conductivity, σ, is commonly expressed as the current density response to an applied electric field

$$\sigma = \frac{\mathcal{J}}{\mathcal{E}}, \tag{3.58}$$

where, $\mathcal{J}$ and $\mathcal{E}$ are the current density and electric field density respectively. According the the gauge/gravity correspondence, a bulk gauge field, A_μ, corresponds to a four-current density, J_μ, on the boundary

$$\langle J^\mu \rangle = \frac{\delta S}{L_e^{1/2} \delta A_\mu}, \tag{3.59}$$

where the factor of $L_e^{1/2}$ has been introduced to ensure the correct dimensionality of a four-current density. The conductivity can be calculated by perturbing A_μ in the bulk and studying its effect on the boundary four-current. As mentioned in section 1.2.3 there is a complication to this calculation relating to the fact that the action is, in general, divergent. Thus, before we can calculate $\langle J_\mu \rangle$ the divergences of the action must be removed by a process of holographic renormalization. Since this process is important to the correct derivation of an expression for the conductivity we shall look at this process in detail.

The method that we follow is presented in greater generality in [32]. The first step is to identify precisely how the action diverges. We shall consider the case of a general bulk gauge field A_μ. For simplicity, and due to its relevance to our problem, the only constraint that we shall place on the gauge field for now is $A_r = 0$. We are concerned with the behaviour of our action in the vicinity of the adS boundary, in this region the metric takes the form of (3.6). It is convenient to distinguish the radial part from the other parts of the metric

$$ds^2 = \gamma_{ab} d\xi^a d\xi^b - \frac{L_e^2}{r^2} dr^2 \tag{3.60}$$

and then write

$$\gamma_{ab} = \frac{r^2}{L_e^2}\left(\gamma_{ab}^{(0)} + \frac{\gamma_{ab}^{(1)}}{r} + ...\right), \tag{3.61}$$

such that $\gamma_{ab}^{(0)}$, $\gamma_{ab}^{(1)}$ *etc.* are independent of the radial coordinate.

In order to understand the behaviour of the action as $r \to \infty$ we need to know the form of the gauge field in this region; this is given by Maxwell's equations. In general Maxwell's equations involve source terms, which in our model are terms involving the scalar field, ψ. These terms are sub-dominant and can be neglected for the remainder of this calculation. Maxwell's equation are then given by

$$\nabla_\mu F^{\mu\nu} = 0 \tag{3.62}$$

$$\implies \frac{1}{r^3}(r^3 A_a')' + \frac{L_e^4}{r^4}\partial_{(0)}^2 A_a = 0, \tag{3.63}$$

where $\partial_{(0)}^2$ represents the wave operator with respect the boundary metric $\gamma_{ab}^{(0)}$. The general solution to this equation is a Bessel function whose large r behaviour can be shown to be

$$A_a = A_a^{(0)} + \frac{A_a^{(2)}}{r^2} + \frac{L_e^4 \partial_{(0)}^2 A_a^{(0)}}{2r^2}\log(r) + ..., \tag{3.64}$$

where $A_a^{(0)}$ and $A_a^{(2)}$ are integration constants. We are now in a position to assess the divergent nature of the action. Once again we only need consider the purely electromagnetic contribution

$$S = \int_{\mathcal{M}} -\frac{1}{4}F_{\mu\nu}F^{\mu\nu}\sqrt{-g}d^5x \tag{3.65}$$

$$= \int_{\mathcal{M}} \frac{1}{2}A_\mu \nabla_\nu F^{\mu\nu}\sqrt{-g}d^5x - \int_{\partial\mathcal{M}} \frac{1}{2}F^{\mu\nu}n_\mu A_\nu \sqrt{\gamma}d^4x \tag{3.66}$$

$$= \frac{1}{2}\int_{r=\Lambda} \frac{r^3}{L_e^3}\gamma^{(0)ab}A_a' A_b \sqrt{\gamma^{(0)}}d^4x, \tag{3.67}$$

where, from the second to third line, we have assumed the action to be on shell, such that $\nabla_\nu F^{\mu\nu} = 0$, and in the third line the boundary is defined to be at some large, but finite, value $r = \Lambda$. This is called the "regularized" action.

We can now insert (3.64) into (3.67) to isolate the divergent terms as $\Lambda \to \infty$

$$S = \frac{1}{2}\int_{r=\Lambda} A_a^{(0)}\gamma^{(0)ab}\left(-2A_b^{(2)} - L_e^4\partial_{(0)}^2 A_b^{(0)}\log\Lambda + \frac{1}{2}L_e^4\partial_{(0)}^2 A_b^{(0)}\right)\frac{\sqrt{\gamma^{(0)}}}{L_e^3}d^4x. \quad (3.68)$$

This expression clearly shows that the action possesses a logarithmic divergence as $\Lambda \to \infty$. This divergence must be removed by the addition of the correct counter term action. It is important that the action is expressed in terms of A_a and not $A_a^{(0)}$ as it is the former and not the latter that transforms under the gauge group of Einstein-GB gravity. Thus we must invert the expansion (3.64) to give $A_a^{(0)} = A_a + \mathcal{O}(1/r)$, and hence obtain:

$$S_{ct} = \frac{L_e\log\Lambda}{2}\int_{r=\Lambda} A_a\gamma^{(0)ab}\partial_{(0)}^2 A_b\sqrt{\gamma^{(0)}}d^4x \quad (3.69)$$

$$= \frac{L_e\log\Lambda}{2}\int_{r=\Lambda}\frac{1}{2}F_{ab}F^{ab}\sqrt{\gamma}d^4x \quad (3.70)$$

Adding this counter term action to our original action gives us our renormalized action, $S + S_{ct} = S_{ren}$, which is divergence free.

We are now in a position to compute the the boundary current, given by (3.59). Varying S_{ren} explicitly gives

$$\delta S_{ren} = \int_{\mathcal{M}} -F^{\mu\nu}\partial_\mu\delta A_\nu\sqrt{-g}d^5x - L_e\log\Lambda\int_{r=\Lambda}F^{ab}\partial_a\delta A_b\sqrt{\gamma}d^4x \quad (3.71)$$

$$= -\int_{r=\Lambda}\sqrt{\gamma}d^4x\delta A_a\gamma^{(0)ab}\left[\frac{r^3}{L_e^3}A_b' + L_e\log\Lambda\partial_{(0)}^2 A_b\right]. \quad (3.72)$$

Substituting for A_a from (3.64) gives

$$\frac{\delta S_{ren}}{L_e^{1/2}\delta A_a} = \left(2\frac{A_a^{(2)}}{L_e^{7/2}} + L_e^{1/2}\partial_{(0)}^2 A_a^{(0)}\log\Lambda - \frac{1}{2}\partial_{(0)}^2 A_a^{(0)}L_e^{1/2} - L_e^{1/2}\partial_{(0)}^2 A_a^{(0)}\log\Lambda\right)\gamma^{(0)aa} \quad (3.73)$$

$$= \left(\frac{2A_a^{(2)}}{L_e^{7/2}} - \frac{L_e^{1/2}}{2}\partial_{(0)}^2 A_a^{(0)}\right)\gamma^{(0)aa}. \quad (3.74)$$

Before we calculate the conductivity it helps to be a little more explicit about our gauge field. As mentioned before, the conductivity is the current density response

to an applied electric field. For our particular choice of gauge field, $A_a = \phi(r)\delta^0_a$, there is no electric field on the boundary. This must be added by introducing a perturbation to the gauge field of the form

$$\delta A_i = A_i(t, r, x^i) = A(r)e^{i\mathbf{k}\cdot\mathbf{x}-i\omega t}e_i, \tag{3.75}$$

where the perturbation lies only in the non-radial spatial directions. With this choice of field

$$\partial^2_{(0)}A_i = (k^2 - \omega^2)A_i, \tag{3.76}$$

$$E_i\big|_{r=\infty} = L_e^{1/2}F_{0i}\big|_{r=\infty} = L_e^{1/2}\dot{A}_i^{(0)}, \tag{3.77}$$

and it is straightforward to obtain an expression for the conductivity

$$\sigma = \frac{J_i}{E_i} = \frac{2A_i^{(2)}}{i\omega L_e^4 A_i^{(0)}} - \frac{i(\omega^2 - k^2)}{2\omega}. \tag{3.78}$$

It is important to note that the second piece in this expression is, to some extent, arbitrary. The reason for this is that there is an arbitrariness of scale associated with the removal of the logarithmic divergence in (3.68). This can be demonstrated by using $\log(c\Lambda)$ instead of $\log\Lambda$ in our counter term action. Such a choice still renormalizes the action but leaves a residual constant on the boundary. Indeed in [1] and [2] a different coordinate system was employed in the holographic renormalization process resulting in contribution to σ of the form $-i\omega\log(L_e/L)$.

In order to find the conductivity of our system all that remains to do is calculate the integration constants $A_a^{(0)}$ and $A_a^{(2)}$. This is achieved by solving the Maxwell equations that govern the dynamics of the perturbation. Since we are interested in including gravitational backreaction we must also accommodate the associated perturbation of the metric. The relevant Maxwell and Einstein-GB equation for this

perturbation are

$$\frac{e^{\nu}}{rf}[rfe^{\nu}A_i']' - \frac{\ddot{A}_i}{f^2e^{2\nu}} + \frac{L^2}{r^2f}\Delta A_i - \frac{2}{f}q^2\psi^2 A_i + \frac{\phi'}{fe^{2\nu}}\left(h_{ti}' - \frac{2}{r}h_{ti} - \dot{h}_{ri}\right) = 0 \quad (3.79)$$

$$\dot{h}_{ti}' - \frac{2}{r}\dot{h}_{ti} - \ddot{h}_{ri} + \frac{L^2fe^{\nu}}{r^2-2\alpha f}\left(1 - \frac{\alpha(2\nu'f+f')}{r}\right)\Delta h_{ri} + \frac{2\kappa^2r^2\dot{A}_i\phi'}{r^2-2\alpha f} = 0. \quad (3.80)$$

where h_{ab} is a perturbation to the metric tensor, A_i is the perturbation of the gauge field and Δ is the laplacian operator along the non-radial spatial directions.

These equations simplify greatly if we consider only the case of zero spatial momentum, $\mathbf{k} = \mathbf{0}$. In this case (3.80) can be integrated once with respect to t to give

$$h_{ti}' - \frac{2}{r}h_{ti} - \dot{h}_{ri} + \frac{2\kappa^2r^2A_i\phi'}{r^2-2\alpha f} \quad (3.81)$$

which can then be substituted directly into (3.79), removing the metric terms, resulting in

$$A'' + \left(\frac{f'}{f} + \nu' + \frac{1}{r}\right)A' + \left[\frac{\omega^2}{f^2e^{2\nu}} - \frac{2}{f}q^2\psi^2 - \frac{2\kappa^2r^2\phi'^2}{fe^{2\nu}\left(r^2-2\alpha f\right)}\right]A = 0\,. \quad (3.82)$$

We are only interested in solutions that obey the physically imposed constraint that there can be no outgoing radiation at the horizon. Therefore, the gauge field's near horizon behaviour must have the form

$$A(r) \sim f(r)^{-i\frac{\omega}{4\pi T_+}} \quad (3.83)$$

where T_+ is the Hawking temperature given by (3.30). The asymptotic form is, of course, given by (3.64). The solutions to this equation are in general, complex. This results in a complex conductivity which can be plotted as a function of ω as can be seen in the following section.

Before we actually calculate the conductivity it is worth noting that in [74] a very elegant interpretation of the holographic conductivity in a four bulk spacetime dimensional system was provided. It involved the recasting of their version of (3.82)

to the form of a one dimensional Schrödinger equation

$$-A,_{zz} + V(z)A = \omega^2 A, \tag{3.84}$$

where z is a new radial parameter. σ was then interpreted as a combination of the reflection and transmission coefficients of a wave passing through the potential barrier, $V(z)$. Viewing it in this way allowed intuition from quantum mechanics to be used to understand many key aspects of the conductivity of their system. Unfortunately, due to the higher dimensionality of the system discussed in this paper, such a treatment has proven less straightforward. Transforming (3.82) in to the form of (3.84) requires a change of radial coordinate to $dz = \frac{dr}{fe^{\nu}}$ followed by a change of variable of $A = r^{-\frac{1}{2}}\tilde{A}$. Proper treatment of this system via the Schrödinger equation requires $\tilde{A}$ to be normalizable. Since $A(r \to \infty)$ is finite, $\tilde{A}(r \to \infty)$ is infinite and hence non-normalizable.

3.6.2 Numerical Conductivity

In this section we shall study the numerical conductivity by looking at plots of the real and imaginary parts as a function of ω for a variety of values of m^2, α and κ^2 at different temperatures. The first plot that we shall consider is figure 3.8, showing the conductivity for a boundary theory at $m^2 = -2/L_e^2$, $\alpha = 0.125$ and $\kappa^2 = 0$ at temperatures of 110%, 50%, 35% and 25% of T_c. The first thing to note is that below T_c the curves look very similar to those of figure 2.2, with the presence of a step in $\mathrm{Re}(\sigma)$ and a pole at the origin of $\mathrm{Im}(\sigma)$ which indicates the infinite conductivity of the system. Since the lines in this plot have been generated for $\alpha \neq 0$ we see that the superconducting nature of the system is preserved despite the presence of these higher order terms. Indeed, this was verified in [56] where is was shown that the inclusion of GB terms in the probe limit had a largely quantitative and not qualitative effect on the system, at least in the region of parameter space that they studied. This plot also shows the conductivity of the system above the critical temperature, showing clearly that the step and pole disappear with $\mathrm{Re}(\sigma)$ approaching some finite, non-zero value.

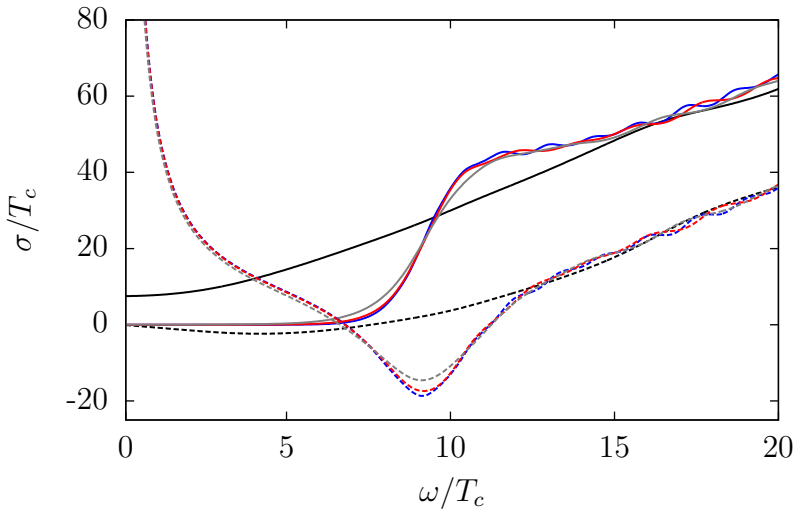

Figure 3.8: Conductivity: A plot showing the real (solid lines) and imaginary (dashed lines) parts of the conductivity, σ/T_c, as a function of ω/T_c for $m^2 = -2/L_e^2$, $\alpha = 0.125$, $\kappa^2 = 0$ at a variety of temperatures. The black, grey, red and blue lines correspond to temperatures of 110%, 50%, 35% and 25% of the critical temperature respectively. The small oscillations at larger ω are a numerical artefact.

It is important to add here though, that the idea that the presence of a pole in $\mathrm{Im}(\sigma)$ guarantees the superconductivity of the system is not quite true. Indeed, as backreaction is switched on ($\kappa^2 > 0$) $\mathrm{Im}(\sigma)$ develops a pole, even at temperatures above T_c, as seen in figure 3.9. This is somewhat alarming as it implies that the system is infinitely conducting in its normal phase. As is explained in [54] however, this infinite conductivity is not superconductivity but results instead from the translational invariance of the system. A charged system that has translational invariance cannot have finite DC conductivity as the application of an electric field will cause uniform acceleration of the charge. Whilst this translational invariance can persist below T_c there are additions to the pole in $\mathrm{Im}(\sigma)$, that persist when translational invariance is broken. It is these additional contributions that correspond to the superconductivity of the system. Indeed, this is the case in the probe limit. By decoupling the matter and gravitational fields we are formally breaking translational invariance which results in the pole for $T > T_c$ disappearing and means that the presence of a pole below T_c must have another cause.

Returning to figure 3.8, the plot shows the effect of reducing the temperature below T_c. For this choice of mass we see that reducing the temperature alters the

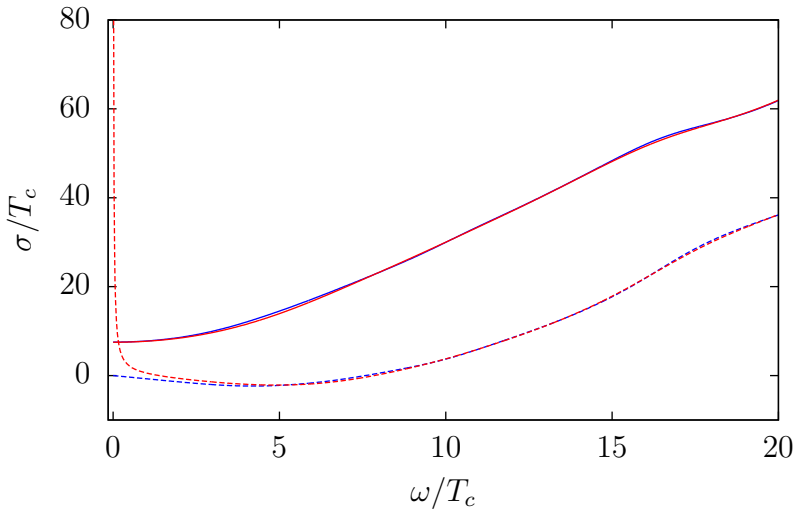

Figure 3.9: The real (solid) and imaginary (dashed) parts of the conductivity at $T = 1.1T_c$. The blue and red lines correspond to $\kappa^2 = 0$ and $\kappa^2 = 0.001$ respectively. Otherwise $m^2 = -2/L_e^2$ and $\alpha = 0.125$.

plot only slightly; making the step and dip sharper and more pronounced, but does not change the value of ω_g. Accessing lower temperatures has proved numerically very difficult. The absence of a reliable zero temperature solution means we can cast no light on what happens at as $T \to 0$.

As we approach the BF bound the plot behaves quite differently, as can been seen in figure 3.10. Now we see that lowering the temperature does dramatically alter the plot. At $T = 0.5T_c$ the plots looks very similar to that of figure 3.8, but as the temperature drops the step and dip shift to higher ω, developing distinct peaks which turn into poles. These poles are interpreted as quasi-normal modes, [78,79] that have moved to the real axis from elsewhere in the complex plane [72, 74]. Quasinormal modes arise in perturbations of black holes of the form $e^{-i\omega t}$, exactly as we have done in perturbing the gauge field A_μ. If ω develops a negative imaginary part the perturbation will have an exponential decay. As a result of imposing boundary conditions at the horizon and infinity there are only a discrete set of these modes which are referred to as quasinormal modes. These modes appear as poles in the retarded Green's function, [80], and therefore will appear in the conductivity of our system. If the modes cross the real axis the exponential decay will turn into exponential growth indicating the presence of an instability. The presence of these

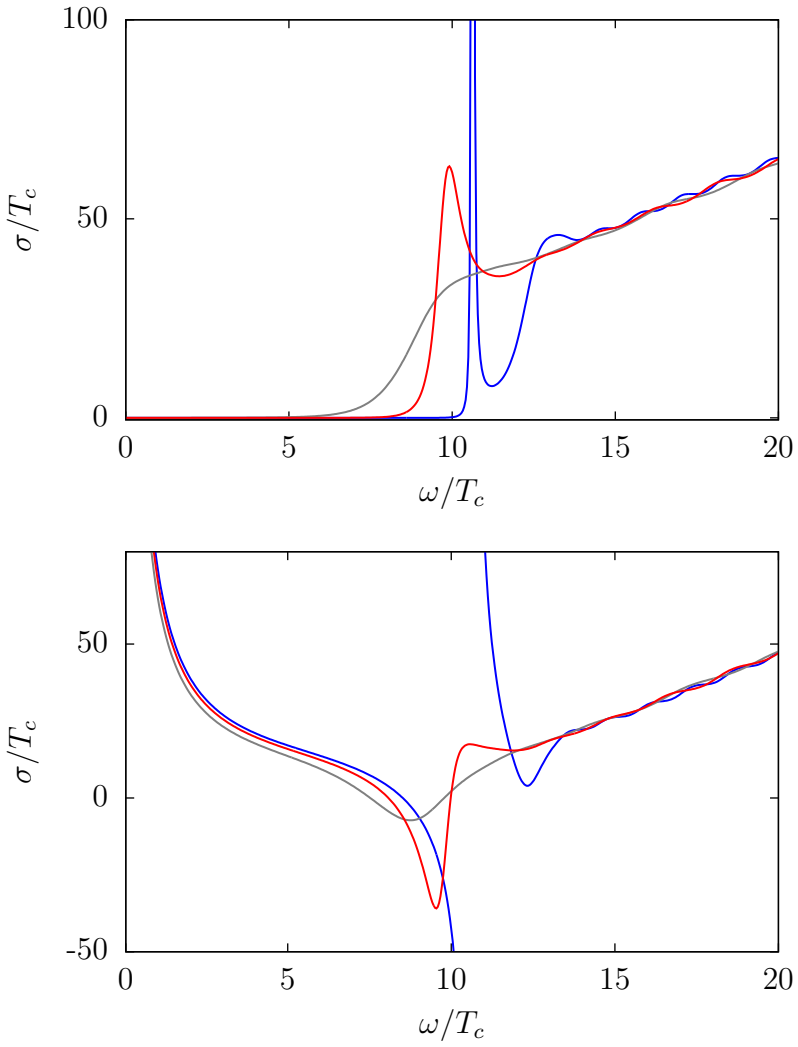

Figure 3.10: Conductivity: Plots showing the real (left) and imaginary (right) parts of the conductivity, σ, as a function of ω/T_c for $m^2 = -4/L_e^2$, $\alpha = 0.125$, $\kappa^2 = 0$ at a variety of temperatures. The grey, red and blue lines correspond to temperatures of 50%, 35% and 25% of the critical temperature respectively.

modes at the real axis of the plot in figure 3.10 is therefore consistent with the system being at the threshold of an instability associated with the scalar mass saturating the BF bound. As the temperature drops further more poles appear at higher values of ω/T_c (not shown). It is suggested in [81] that in the probe limit of Einstein gravity, as $T \to 0$ the number of these poles diverges. Since such low temperature analysis is outside the scope of this paper, we can shed no light on whether or not this occurs away from the Einstein limit.

We are interested in observing the effect that varying α, κ^2 and m^2 has on these phenomena. We will begin by looking at the first case; away from the BF bound where temperature dependent effects are less prominent. In [1] the authors studied the effect of α, κ^2 for $m^2 = -3/L_e^2$. They found that increasing α above the Einstein limit increased the value of ω_g and made the step and dip more pronounced. The effect of increasing κ^2 was to smooth out the features of the plot but not affecting the value of ω_g, that is until the smoothing removes the presence of the hard gap[1], at least within the temperature range studied. Studying the conductivity for larger masses we see very similar results with quantitative differences rather than qualitative. The key information has been captured on a plot of ω_g against T_c as seen in figure 3.11.

The grey points in the left plot in figure 3.11 correspond to the probe, Einstein limit of the superconductor. One can see that for the range of masses presented, the points all fall close to the line $\omega_g = 8T_c$. This observation contributed ammunition to the speculation, [72], that this may be a universal relation. This plot shows that such a relation is unstable to higher curvature corrections as found in [1].

The plot shows that increasing α increases ω_g and largely reduces T_c, except for very close to $\alpha = L^2/4$. This has the effect of moving the point decidedly off the line. Decreasing the mass from $m^2 = 0$ increases ω_g and T_c with the greatest differences occurring towards the upper bound of α where variations in T_c are more pronounced. The right hand plot shows the effect of backreaction. Increasing κ^2 has very little effect on ω_g with the majority of the effect coming from the reduction in T_c. As α gets large and negative the points converge corresponding to the diminished effect of

[1] i.e Re(σ) no longer is zero for small ω.

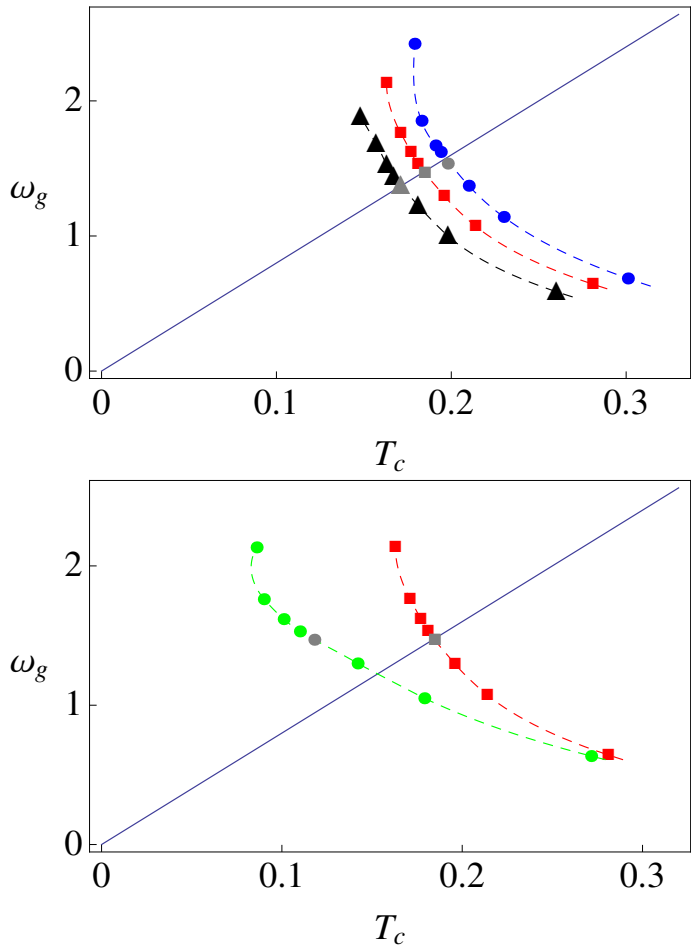

Figure 3.11: The upper plot shows ω_g against T_c for $\kappa^2 = 0$ and $m^2 = 0$, black (triangular) points; $m^2 = -2/L_e^2$, red (square) points and $m^2 = -3/L_e^2$, blue (circular) points. The lower plot shows ω_g against T_c for $m^2 = -2/L_e^2$ for $\kappa^2 = 0$ red (square) points and $\kappa^2 = 0.05$ green (circular) points. In both plots from top to bottom the points correspond to $\alpha = 0.24999$, 0.1875, 0.125, 0.0625, 0, -0.25, -1, -10, with the grey points corresponding to Einstein gravity. The dashed lines have been added to guide the eye. The straight line corresponds to $\omega_g = 8T_c$.

backreaction in this regime that was noted above. We were unable to extend these plots to much larger negative coupling as numerical artefacts began to obscure the key features of the plot, though since calculation of the condensate seems possible for arbitrarily large, negative α one might expect these curves to continue towards the axis without ever reaching it.

We now turn our attention to systems at the BF bound, and in particular what effect α and κ^2 have on the development of the quasi-normal modes. Figure 3.12 shows $\mathrm{Re}(\sigma)$, measured at $T = T_c/4$, for $m^2 = -4/L_e^2$, $\kappa^2 = 0$ for a variety of values of α.

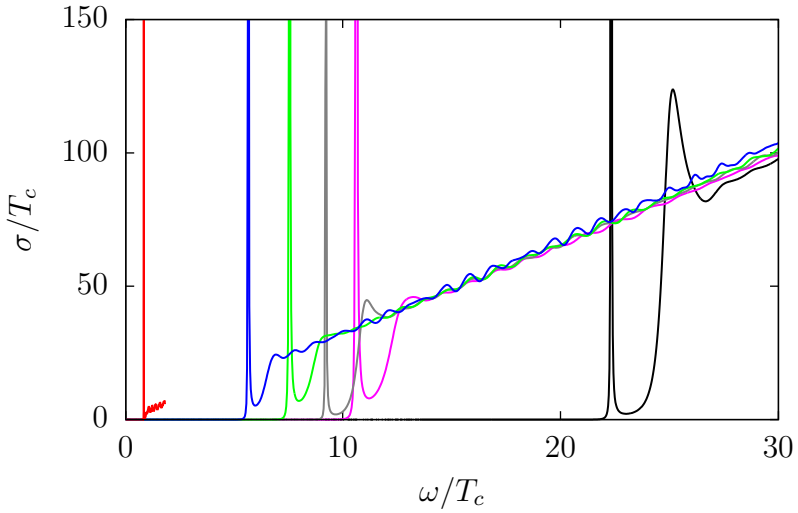

Figure 3.12: Plot showing $\mathrm{Re}(\sigma)$ measured at $T = T_c/4$, $m^2 = -4/L_e^2$ and $\kappa^2 = 0$ for a range of values of α. From left to right: red, $\alpha = -100$; blue, $\alpha = -1.0$; green, $\alpha = -0.25$; grey, $\alpha = 0$; purple, $\alpha = 0.125$ and black, $\alpha = 0.24999$. The small oscillations are a numerical artefact.

This plot shows that increasing or decreasing α does not seem to hinder the development of these quasi-normal modes. The dominant effect of, say, increasing the GB coupling constant is to shift the poles to higher ω/T_c. This increase with α is particularly marked as you approach the upper limit of the coupling constant.

Figure 3.13 shows the effect that backreaction has on the development of the quasi-normal modes with a plot of $\mathrm{Re}(\sigma)$, measured at $T = T_c/4$, for $m^2 = -4/L_e^2$, $\alpha = 0.24999$ for a variety of κ^2. We see that turning on backreaction very quickly removes the appearance of the poles, at least at this temperature; it is still quite conceivable that they may appear as the temperature is dropped. Analysis of this

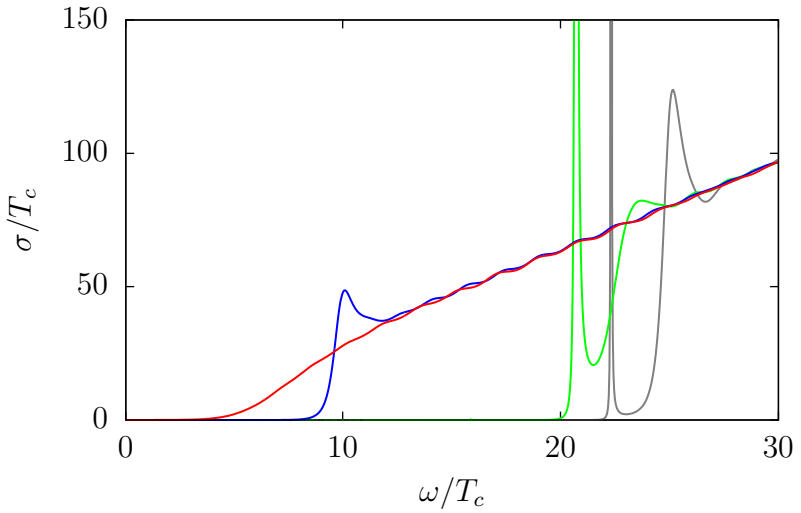

Figure 3.13: Plot showing Re(σ) measured at $T = T_c/4$ at $m^2 = -4/L_e^2$ and $\alpha = 0.24999$ for a range of values of κ^2. From left to right: red $\kappa^2 = 0.1$; blue $\kappa^2 = 0.01$; green, $\kappa^2 = 0.001$ and grey, $\kappa^2 = 0.0001$.

phenomenon at much lower values of α show the existence of quasi-normal modes up to much higher values of κ^2, supporting the observation that the effect of back-reaction diminishes as α is reduced.

3.7 Summary

The aim of this research was to explore how the superconductor is effected by the inclusion of higher order curvature terms. It was shown in [56] that in the probe limit for a particular choice of mass the effect of the GB terms was quantitative and not qualitative. Our results largely support this claim but identify a number of regions where the effect can be quite pronounced. We found that in the majority of parameter space increasing backreaction reduces T_c but that in a narrow region where $m^2 \to -4/L_e^2$ and $\alpha \to L^2/4$ its effect is reversed and actually increases T_c. In this regime large, super-planckian values of backreaction are numerically attainable. We also found that as α becomes large and negative T_c increases and the effect of backreaction is diminished as the gravitational action is dominated by the higher curvature terms. Again, this provides a regime where large critical temperatures and large values of backreaction are attainable.

The bounds on the critical values of α and κ^2, studied in section 3.5, show that

the curvature terms can have a considerable effect in the zero temperature limit. We also found that the concept of GB gravity being a perturbative correction to Einstein gravity can be important when considering spacetimes in this limit. We found that mildly singular solutions were incompatible with this interpretation and thus their validity must be questioned.

We studied general solutions in this zero temperature limit finding that there can be no regular, tachyonic solutions to our system and placed constraints on the masses of non-tachyonic solutions if they exits. These findings applied to both GB and Einstein gravity.

We also studied the conductivity of the system. We found that in the region away from the BF bound α and κ^2 changed the value of the frequency gap, ω_g, ruling out a universal relation between it and the critical temperature. In the vicinity of the BF bound the effect of α was to shift the location of the quasi-normal modes that appear there but otherwise did not effect their development. The effect of backreaction was more notable: increasing backreaction away from the probe limit quickly prevented the appearance of these quasi-normal modes, at least within the temperature range that we were able to study.

Chapter 4

Towards A Holographic Superconductor with Lifshitz Scaling

The holographic systems that we have so far considered asymptote to an adS spacetime at radial infinity. The boundary theories of such systems exhibit a scale invariance of the form

$$t \to \lambda t, \qquad x^i \to \lambda x^i. \tag{4.1}$$

There is, however, no reason why this scaling symmetry must act in the same way on space and time. Assuming spatial isotropy, the scaling can be generalized to

$$t \to \lambda^z t, \qquad x^i \to \lambda x^i, \qquad \text{with} \quad z \neq 1 \tag{4.2}$$

where z is called the *dynamical exponent*, [82] . There are many condensed matter systems that exhibit this scaling with different values of z, see [82] and [76] for examples. Field theories that have this scaling symmetry, but no boost symmetry, have become known as *Lifshitz field theories*.

There has been a great deal of recent work in developing a holographic description of these theories. Such a duality was first proposed in [83] in which the bulk

spacetime metric was presented as

$$ds^2 = L^2 \left(r^{2z} dt^2 - \frac{dr^2}{r^2} - r^2 dx_i dx^i \right), \tag{4.3}$$

where L represents an overall curvature scale. A spacetime with this metric is referred to as a *Lifshitz spacetime*. There are now a number of phenomenological, [83,84] and string theoretic models, [85–89], for which (4.3) is a solution and work has been done in developing a holographic dictionary for these theories that allows the fields in the bulk to be interpreted as operators of a dual boundary theory, [83,90,91].

As in the adS case, the presence of a black hole in the bulk introduces temperature to the boundary theory and a number of asymptotically Lifshitz black holes have now been found, [92–95]. However, at the time of writing there are no asymptotically Lifhshitz black hole solutions to a top down model for an arbitrary dynamical exponent. The aim of the research in this chapter is to address this by finding black hole solutions to a particular top down model, [96], that permits an arbitrary dynamical exponent, $z \geq 1$. These solutions form a crucial first step towards developing a top down model of holographic superconductivity in this theory.

4.1 The Model

The theory that we shall consider in this chapter is a six-dimensional $\mathcal{N} = 4$ gauged supergravity, first presented in [97]. It was shown in [98] that this theory can be obtained from a consistent truncation of massive Type IIA supergravity which means that the solutions of the six dimensional theory can be uplifted to solutions in string theory. In [96] this theory was shown to permit Lifshitz solutions.

In general, the metric (4.3) is not a solution to the vacuum Einstein equations and appropriate matter content must be found to generate a spacetime of this form. The bosonic field content presented in [96] consists of the metric, $g_{\mu\nu}$, a dilaton, ϕ, an anti-symmetric two-form gauge field, $B_{\mu\nu}$, and a set of gauge vectors, $(A^{(i)}_{\mu}, A_{\mu})$

for the gauge group $SU(2) \times U(1)$. The bosonic part of the action for this theory is

$$S = \int d^6x\sqrt{-g}\left[-\frac{1}{4}R + \frac{1}{2}\partial^\mu\phi\partial_\mu\phi - \frac{e^{-\sqrt{2}\phi}}{4}\left(H^{\mu\nu}H_{\mu\nu} + F^{(i)\mu\nu}F^{(i)}_{\mu\nu}\right)\right.$$
$$\left. + \frac{e^{2\sqrt{2}\phi}}{12}G_{\mu\nu\rho}G^{\mu\nu\rho} + \frac{1}{8}\left(\lambda^2 e^{\sqrt{2}\phi} + 4\lambda m e^{-2\sqrt{2}\phi} - m^2 e^{-3\sqrt{2}\phi}\right)\right]$$
$$- \frac{1}{8}\int d^6x\sqrt{-g}\epsilon^{\mu\nu\rho\theta\sigma\tau}B_{\mu\nu}\left(\mathcal{F}_{\rho\theta}\mathcal{F}_{\sigma\tau} + mB_{\rho\theta}\mathcal{F}_{\sigma\tau} + F^{(i)}_{\rho\theta}F^{(i)}_{\sigma\tau}\right) \tag{4.4}$$

where λ is the gauge coupling, m is the mass of the dilaton, the spacetime indices, $\mu, \nu, ...$ run from 0 to 5, and the gauge indices, (i) run from 1 to 3. The last term is a "topological" term where ϵ^{abcdef} is the Levi-Civita tensor. The field strengths are given by

$$\mathcal{F}_{\mu\nu} = \partial_\mu\mathcal{A}_\nu - \partial_\nu\mathcal{A}_\mu \tag{4.5}$$
$$F^{(i)}_{\mu\nu} = \partial_\mu A^{(i)}_\nu - \partial_\nu A^{(i)}_\mu \tag{4.6}$$
$$G_{\mu\nu\rho} = 3\partial_{[\mu}B_{\nu\rho]}, \tag{4.7}$$

and to simplify the expression we follow [96] in defining a new field strength

$$H_{\mu\nu} = \mathcal{F}_{\mu\nu} + mB_{\mu\nu}. \tag{4.8}$$

Varying the action with respect to each field in turn gives the following equations of motion:

$$R_{\mu\nu} = 2\partial_\mu\phi\partial_\nu\phi + g_{\mu\nu}P(\phi) + e^{2\sqrt{2}\phi}\left(G_\mu{}^{\rho\lambda}G_{\nu\rho\lambda} - \frac{1}{6}g_{\mu\nu}G^{\rho\lambda\sigma}G_{\rho\lambda\sigma}\right)$$
$$- e^{-\sqrt{2}\phi}\left(2H_\mu{}^\rho H_{\nu\rho} + 2F_\mu{}^{\rho\,(i)}F^{(i)}_{\nu\rho} - \frac{1}{4}g_{\mu\nu}\left(H^{\rho\lambda}H_{\rho\lambda} + F^{\rho\lambda\,(i)}F^{(i)}_{\rho\lambda}\right)\right) \tag{4.9}$$
$$\Box\phi = \frac{\partial P}{\partial\phi} + \frac{1}{3}\sqrt{\frac{1}{2}}e^{2\sqrt{2}\phi}G^{\mu\nu\rho}G_{\mu\nu\rho} + \frac{1}{2}\sqrt{\frac{1}{2}}e^{-\sqrt{2}\phi}\left(H^{\mu\nu}H_{\mu\nu} + F^{\mu\nu\,(i)}F^{(i)}_{\mu\nu}\right) \tag{4.10}$$
$$\nabla_\nu\left(e^{-\sqrt{2}\phi}H^{\nu\mu}\right) = \frac{1}{6}\,\epsilon^{\mu\nu\rho\lambda\sigma\tau}H_{\nu\rho}G_{\lambda\sigma\tau} \tag{4.11}$$
$$\nabla_\nu\left(e^{-\sqrt{2}\phi}F^{\nu\mu\,(i)}\right) = \frac{1}{6}\,\epsilon^{\mu\nu\rho\lambda\sigma\tau}F^{(i)}_{\nu\rho}G_{\lambda\sigma\tau} \tag{4.12}$$
$$\nabla_\rho\left(e^{2\sqrt{2}\phi}G^{\rho\mu\nu}\right) = -me^{-\sqrt{2}\phi}H^{\mu\nu} - \frac{1}{4}\mathrm{e}\,\epsilon^{\mu\nu\rho\lambda\sigma\tau}\left(H_{\rho\lambda}H_{\sigma\tau} + F^{(i)}_{\rho\lambda}F^{(i)}_{\sigma\tau}\right), \tag{4.13}$$

where the scalar potential, $P(\phi)$, is defined to be

$$P(\phi) = \frac{1}{8}\left(\lambda^2 e^{\sqrt{2}\phi} + 4\lambda m e^{-\sqrt{2}\phi} - m^2 e^{-3\sqrt{2}\phi}\right) . \tag{4.14}$$

It is shown in [96] that there are solutions to this system of equations whose metric is that of a four dimensional Lifhshitz space time crossed with a two dimensional hyperbolic space, $(Li_4 \times H_2)$,

$$ds^2 = L^2\left(r^{2z}dt^2 - r^2dx_1^2 - r^2dx_2^2 - \frac{dr^2}{r^2}\right) - \frac{a^2}{y_2^2}(dy_1^2 + dy_2^2), \tag{4.15}$$

where a is the radius of curvature of the hyperboloid, which can be taken to be compact, see [99] for details. The specific field configurations that generate this spacetime were found to be

$$\begin{aligned} F^{(3)}_{tr} &= \alpha L^2 r^{z-1}, & F^{(3)}_{y_1y_2} &= \gamma\,\frac{a^2}{y_2^2} \\ G_{x_1x_2r} &= \beta L^3 r \qquad \Rightarrow & B_{x_1x_2} &= \frac{\beta}{2}L^3r^2\,, \end{aligned} \tag{4.16}$$

where the dilaton is a constant, ϕ_∞. The equations are somewhat simplified by the following rescalings

$$\begin{aligned} &\hat{\alpha} = L\alpha e^{-\phi_\infty/\sqrt{2}} && \hat{\beta} = L\beta e^{\sqrt{2}\phi_\infty} && \hat{\gamma} = L\gamma e^{-\phi_\infty/\sqrt{2}} \\ &\hat{\lambda} = L\lambda e^{\phi_\infty/\sqrt{2}} && \hat{a} = a/L && \hat{m} = L\,m\,e^{-3\phi_\infty/\sqrt{2}}\,, \end{aligned} \tag{4.17}$$

Equations (4.9) to (4.13) then reduce to a simple set of algebraic equations with the following solutions

$$\begin{aligned} &\hat{\beta}^2 = z-1 && \hat{\alpha}^2 = \hat{\gamma}^2(z-1) \\ &\hat{\gamma}^2 = \frac{(2+z)(z-3) \pm 2\sqrt{2(z+4)}}{2z} && \hat{\lambda}^2 = 2z(4+z) \\ &\frac{\hat{m}^2}{2} = \frac{6+z \mp 2\sqrt{2(z+4)}}{z} && \frac{1}{\hat{a}^2} = 6 + 3z \mp 2\sqrt{2(z+4)}\,. \end{aligned} \tag{4.18}$$

These define two Lifshitz spacetimes, one for each of the sign choices in (4.18). The

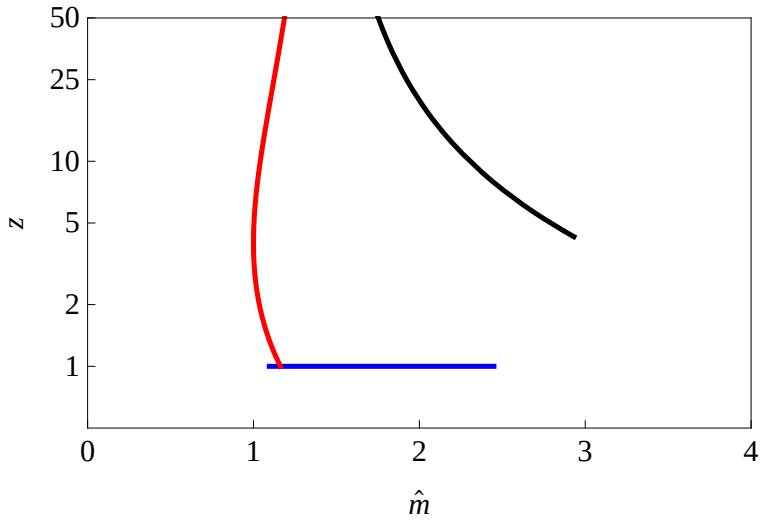

Figure 4.1: Plot showing the values of z and $\hat{m}$ that the Lifshitz and adS solutions can take. The blue line indicates the adS solutions, the red line corresponds to the Lifshitz solutions with the upper sign choice in (4.18) and the black to the lower sign choice.

requirement that $\hat{\beta}$ is real restricts z to $z \geq 1$ and for the lower sign choice, for $\hat{\gamma}$ to be real we find that z must be greater than approximately 4.29.

In addition to these Lifshitz solutions the system permits a 1 parameter family of adS solutions defined by $z = 1$ and $\hat{\beta} = \hat{\alpha} = 0$. With these constraints the field equations give

$$\begin{aligned} \hat{\lambda} &= \frac{\hat{m}}{2} + \frac{3}{\hat{m}}, \\ \frac{1}{\hat{a}^2} &= \frac{5\hat{m}^2}{8} - \frac{3}{2} + \frac{9}{2\hat{m}^2}, \\ \gamma^2 &= -\frac{5\hat{m}^2}{16} + \frac{9}{4} - \frac{9}{4\hat{m}^2}, \end{aligned} \tag{4.19}$$

where $\hat{m}$ is a free parameter. In this case the requirement that $\hat{\gamma}$ is real implies that $\hat{m} \in [\sqrt{\frac{6}{5}}, \sqrt{6}]$. Figure 4.1 shows the values of z and $\hat{m}$ that these Lifshitz and adS solutions can take.

4.2 Finite Temperature Solutions

We wish to find black hole solutions to this system of equations that asymptote to the Lifshitz solutions described above. In order to gain a fuller understanding of the

system it is also useful to investigate black hole solutions in the asymptotically adS spacetimes as well. In order to do this we must introduce new terms into the metric and field strength Ansätze to accommodate deviations from the pure Lifshitz and adS spacetimes.

For simplicity we shall look for black hole solutions that respect the planar symmetry and static nature of (4.3). Thus the alterations to the metric need only have radial dependence

$$ds^2 = L^2\left(f(r)r^{2z}dt^2 - \frac{dr^2}{g(r)r^2} - h(r)r^2dx_idx^i\right) - \frac{k(r)a^2}{y_2^2}(dy_1^2 + dy_2^2). \tag{4.20}$$

Since Einstein's equations are invariant under coordinate rescalings we shall use this gauge freedom to fix r such that $h(r) = 1$. We also need to insert functions into the field strengths, (4.16), as follows

$$F^{(3)}_{tr} = \alpha L^2 r^{z-1} p(r) \qquad F^{(3)}_{y_1y_2} = \gamma\,\frac{a^2}{y_2^2} \tag{4.21}$$

$$B_{x_1x_2} = \frac{1}{2}\beta L^3 r^2 s(r) \qquad G_{rx_1x_2} = \frac{1}{2}\beta L^3 (r^2 s(r))' \tag{4.22}$$

and in addition we allow the dilaton to vary, $\phi = \phi(r)$. Here, a prime denotes differentiation with respect to r. Note that no additional function has been added to $F^{(3)}_{y_1y_2}$, the reason being that a non-trivial function here is forbidden by closure, $dF^{(3)} = 0$, of this field strength.

The system can be simplified further by observing that the equation of motion for $F^{(3)}$, (4.12), relates p and s via

$$\left(\frac{e^{-\sqrt{2}\phi}r^2 k\sqrt{g}\alpha p}{\sqrt{f}}\right)' = \gamma\beta L(r^2 s)'. \tag{4.23}$$

At radial infinity the constant of integration is zero, whether in a Lifshitz or adS spacetime, and therefore must be zero everywhere. Integrating both sides we find

$$F^{(3)}_{tr} = \alpha L^2 r^{z-1} p = \frac{\sqrt{f}\gamma\beta L^3 r^{z-1} s e^{\sqrt{2}\phi}}{k\sqrt{g}}. \tag{4.24}$$

Once again, the equations can be simplified by applying the rescalings (4.17).

We shall also scale out the asymptotic value of the dilaton by letting $\varphi = \phi - \phi_\infty$. The remaining field equations now become

$$\begin{aligned} rg' = -g\left(4 + 2z + \frac{rf'}{f} + 2\frac{rk'}{k}\right) \\ + 2\left(\hat{P}(\varphi) - (s^2 + rs's + \frac{r^2 s'^2}{4})\hat{\beta}^2 g e^{2\sqrt{2}\varphi} - \frac{3}{8}\hat{m}^2\hat{\beta}^2 s^2 e^{-\sqrt{2}\varphi}\right. \\ \left. -\frac{1}{2}\frac{\hat{\beta}^2\hat{\gamma}^2 s^2 e^{\sqrt{2}\varphi}}{k^2} + \frac{1}{2}\frac{\hat{\gamma}^2 e^{-\sqrt{2}\varphi}}{k^2}\right) \end{aligned} \tag{4.25}$$

$$\begin{aligned} r^2 f'' = -2f\left(2z + z^2 + z\frac{rk'}{k} + z\frac{rg'}{2g}\right) - rf'\left(3 + 2z + \frac{rk'}{k} + \frac{rg'}{2g} - \frac{rf'}{2f}\right) \\ + \frac{2f}{g}\left(\hat{P}(\varphi) + (s^2 + rs's + \frac{r^2 s'^2}{4})\hat{\beta}^2 g e^{2\sqrt{2}\varphi} + \frac{1}{8}\hat{m}^2\hat{\beta}^2 s^2 e^{-\sqrt{2}\varphi}\right. \\ \left. +\frac{3}{2}\frac{\hat{\beta}^2\hat{\gamma}^2 s^2 e^{\sqrt{2}\varphi}}{k^2} + \frac{1}{2}\frac{\hat{\gamma}^2 e^{-\sqrt{2}\varphi}}{k^2}\right) \end{aligned} \tag{4.26}$$

$$\begin{aligned} r^2 k'' = -\frac{2}{\hat{a}^2 g} - rk'\left(3 + z + \frac{rf'}{2f} + \frac{rg'}{2g}\right) \\ + \frac{2k}{g}\left(\hat{P}(\varphi) + (s^2 + rs's + \frac{r^2 s'^2}{4})\hat{\beta}^2 g e^{2\sqrt{2}\varphi} + \frac{1}{8}\hat{m}^2\hat{\beta}^2 s^2 e^{-\sqrt{2}\varphi}\right. \\ \left. -\frac{1}{2}\frac{\hat{\beta}^2\hat{\gamma}^2 s^2 e^{\sqrt{2}\varphi}}{k^2} - \frac{3}{2}\frac{\hat{\gamma}^2 e^{-\sqrt{2}\varphi}}{k^2}\right) \end{aligned} \tag{4.27}$$

$$\begin{aligned} r^2\varphi'' = -r\varphi'\left(3 + z + \frac{rf'}{2f} + \frac{rg'}{2g} + \frac{rk'}{k}\right) \\ + \frac{1}{g}\left(-\frac{\partial\hat{P}(\varphi)}{\partial\varphi} + \sqrt{2}(s^2 + rs's + \frac{r^2 s'^2}{4})\hat{\beta}^2 g e^{2\sqrt{2}\varphi}\right) \\ + \frac{1}{g}\left(-\frac{\sqrt{2}}{8}\hat{m}^2\hat{\beta}^2 s^2 e^{-\sqrt{2}\varphi} + \frac{\sqrt{2}}{2}\frac{\hat{\beta}^2\hat{\gamma}^2 s^2 e^{\sqrt{2}\varphi}}{k^2} - \frac{\sqrt{2}}{2}\frac{\hat{\gamma}^2 e^{-\sqrt{2}\varphi}}{k^2}\right) \end{aligned} \tag{4.28}$$

$$r^2 s'' = -s\left(2z + \frac{rf'}{f} + 2\frac{rk'}{k} + \frac{rg'}{g} + 4\sqrt{2}r\varphi' - \frac{\hat{m}^2 e^{-3\sqrt{2}\varphi}}{g} - \frac{4\hat{\gamma}^2 e^{-\sqrt{2}\varphi}}{gk^2}\right) - rs'\left(3 + z + \frac{rf'}{2f} + \frac{rg'}{2g} + \frac{rk'}{k} + 2\sqrt{2}r\varphi'\right) \tag{4.29}$$

And the G^r_r component of the Einstein tensor gives

$$\frac{1}{\hat{a}^2 k} + g\left(1 + \frac{r^2 k'^2}{4k^2} + z\frac{rk'}{k} + \frac{r^2 k' f'}{2kf} + 2z + \frac{rf'}{f} + 2\frac{rk'}{k}\right) = r^2\varphi'^2 g + 2\hat{P}(\varphi) + (s^2 + rs's + \frac{r^2 s'^2}{4})\hat{\beta}^2 g e^{2\sqrt{2}\varphi} - \frac{1}{4}\hat{m}^2\hat{\beta}^2 s^2 e^{-\sqrt{2}\varphi} - \frac{\hat{\beta}^2\hat{\gamma}^2 s^2 e^{\sqrt{2}\varphi}}{k^2} - \frac{\hat{\gamma}^2 e^{-\sqrt{2}\varphi}}{k^2}. \tag{4.30}$$

The scalar potential now takes the form

$$\hat{P}(\varphi) = \frac{1}{8}(\hat{\lambda}^2 e^{\sqrt{2}\varphi} + 4\hat{\lambda}\hat{m}e^{-\sqrt{2}\varphi} - \hat{m}^2 e^{-3\sqrt{2}\varphi}). \tag{4.31}$$

Whilst we have six equations with only five unknowns it can be shown that a combination of (4.25) to (4.29) is equal to the derivative of (4.30) via a Bianchi identity and the system is well defined. It is possible to use (4.30) to completely remove g from the system of equations leaving only four unknown variables.

The metric and field equations are invariant under the following rescaling

$$r \to br, \qquad t \to \frac{t}{b^z}, \qquad x^i \to \frac{x^i}{b}, \tag{4.32}$$

which means we are free to set the Schwarzschild radius of the black hole, r_+, to 1. We will choose, however, to keep r_+ explicitly in our calculations for clarity.

4.2.1 Boundary Conditions

Before attempting to find black hole solutions to this system it is important to investigate the system at its boundaries. We shall begin with the boundary at radial infinity. We defined our fields such that they all tend to 1, except for φ which

tends to zero, in the asymptotically Lifshitz spacetime:

$$f = g = k = s = 1, \qquad \varphi = 0 \qquad \text{and} \quad f' = g' = k' = s' = \varphi' = 0. \tag{4.33}$$

Our choice of coordinates is not quite so convenient for in the asymptotically adS case since s now goes to zero which means that the factoring out of $\hat{\beta}$ is unnecessary. We propose that for the adS solutions that are disconnected from the Lifshitz solutions we shall set $\hat{\beta} = 1$ and the fields shall tend to the following:

$$f = g = k = 1, \qquad s = \varphi = 0 \qquad \text{and} \quad f' = g' = k' = s' = \varphi' = 0, \tag{4.34}$$

In each case the gradients of the fields go to zero meaning these asymptotic regions define fixed points of the system. In order to find black hole solutions it is useful to investigate the stability of each of these fixed points. We do this by adding a small perturbation to each field, $f = 1 + \delta f$, $g = 1 + \delta g$, *etc.* and observing how the field equations effect these perturbations at linear order.

The adS Fixed Point

Following [100] we observe that the system at the adS fixed point is greatly simplified by the fact that equation (4.29) fully decouples from the others at linear order, giving

$$r^2 \delta s'' + 4r\delta s' + \delta s(2 - \hat{m}^2 - 4\hat{\gamma}^2) = 0. \tag{4.35}$$

From this isolated equation we obtain the asymptotic form of s:

$$\delta s \sim s_+ r^{\theta_+} + s_- r^{\theta_-}, \qquad \theta_\pm = \frac{1}{2}\left(-3 \pm \sqrt{37 - \hat{m}^2 - \frac{36}{\hat{m}^2}}\right). \tag{4.36}$$

From a combination of the linearised versions of (4.25) and (4.26) one finds that $r^2\delta f'' + 4r\delta f'(r) = 0$ which implies

$$\delta f \sim f_0 + f_1 r^{-3}. \tag{4.37}$$

Finally, linearising (4.27) and (4.28) show that the equations for k and φ form a coupled system given by

$$\mathcal{L}_I \begin{pmatrix} \delta\varphi \\ \delta k \end{pmatrix} = \begin{bmatrix} (3\hat{m}^2 - \hat{\lambda}^2)/2 & \sqrt{2}\hat{\gamma}^2 \\ 2\sqrt{2}\hat{\gamma}^2 & 2(\hat{\gamma}^2 + 3) \end{bmatrix} \begin{pmatrix} \delta\varphi \\ \delta k \end{pmatrix}, \tag{4.38}$$

where $\mathcal{L}_I X = r^2 \frac{d^2}{dr^2} X + 4r \frac{d}{dr} X$ is a linear operator. The eigenvalues and eigenvectors of this system are:

$$\xi_\pm = \frac{1}{8\hat{m}^2} \left(3\hat{m}^4 + 36\hat{m}^2 - 36 \pm \left(\hat{m}^2 - 6\right) \sqrt{36 - 60\hat{m}^2 + 89\hat{m}^4} \right) \tag{4.39}$$

$$\mathbf{v}_\pm = (v_{1\pm}, v_{2\pm})^T = \left(\frac{-8\hat{m}^2 \pm \sqrt{36 - 60\hat{m}^2 + 89\hat{m}^4}}{\sqrt{2}(5\hat{m}^2 - 6)}, 1 \right)^T. \tag{4.40}$$

We can now solve the eigenvalue equation to find

$$X_1 \sim x_{1+} r^{\left(-3+\sqrt{9+4\xi_+}\right)/2} + x_{1-} r^{\left(-3-\sqrt{9+4\xi_+}\right)/2}, \tag{4.41}$$

$$X_2 \sim x_{2+} r^{\left(-3+\sqrt{9+4\xi_-}\right)/2} + x_{2-} r^{\left(-3-\sqrt{9+4\xi_-}\right)/2}, \tag{4.42}$$

were X_1 and X_2 are the coefficients of X corresponding to ξ_+ and ξ_- in the eigenvalue equation respectively. The fall-offs of $\delta\varphi$ and δk are then given by

$$\delta\varphi \sim v_{1+} X_1 + v_{1-} X_2, \tag{4.43}$$

$$\delta k \sim v_{2+} X_1 + v_{2-} X_2. \tag{4.44}$$

Figure 4.2 shows a plot of these exponents as a function of $\hat{m}$. Each field has a pair of exponents which are symmetric about $-3/2$ and whose coefficients can be interpreted, in precisely the same way as described in section 1.2.3, as a source and operator in the boundary field theory. As is noted in [100] the straight part of the red curve, where $\sqrt{6/5} < \hat{m} < 1.254$, indicates that this exponent has turned imaginary. This occurs when $\xi_- < -9/4$ in (4.43) and (4.44) which is equivalent to a mass violating the BF bound of adS_4, see (2.1). With these complex exponents

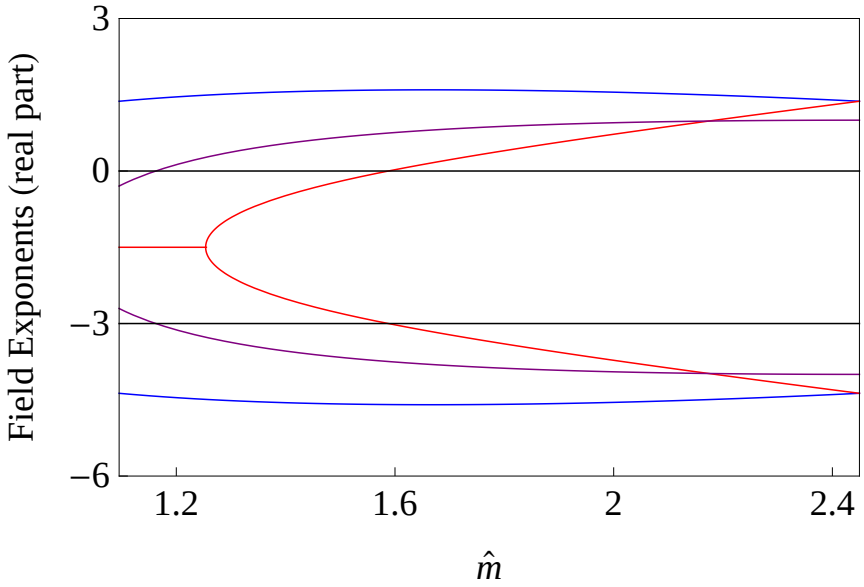

Figure 4.2: Plot showing the real part of the field exponents as they approach an adS spacetime as $r \to \infty$. A combination of the blue and red lines correspond to the exponents of k and φ, the black lines correspond to the exponents of f and the purple to s. Each pair of exponents sum to $-3/2$. The joining of the red lines for small $\hat{m}$ indicate that the exponents turn complex.

the analogy with operators and sources of the boundary theory cannot be made.

Figure 4.2 shows that for all $\hat{m} \in [\sqrt{6/5}, \sqrt{6}]$ there is at least one positive eigenvalue. Exciting these particular modes will lead a solution to diverge from the fixed point as $r \to \infty$.

The Lifshitz Fixed Point

At the Lifshitz fixed point, (4.29) no longer decouples from the others and we must make do with a numerical understanding of the stability. We do this by decomposing our system of equations into nine first order differential equations by the introduction of four new variables for each of the second order differential equations: $\tilde{f} = rf'$, $\tilde{k} = rk'$, *etc.* The linearised system of equations can then be written in the following form

$$\mathcal{L}_{II} F^i = A^{ij} F^j, \tag{4.45}$$

where $\mathcal{L}_{II}$ is a new linear operator defined by $\mathcal{L}_{II}X = r\frac{d}{dr}X$, F^i is a vector of all the field perturbations, $F^i = (\delta f, \delta\tilde{f}, \delta g, \delta k, \delta\tilde{k}, \delta s, \delta\tilde{s}, \delta\varphi, \delta\tilde{\varphi})^T$ and A^{ij} is a 9 by 9 matrix. This equation is equivalent to

$$\mathcal{L}_{II}X^i = J^{ij}X^j, \qquad\qquad X^k = (S^{-1})^{km}F^m, \tag{4.46}$$

where J^{ij} is the Jordan normal form of A^{ij} and is independent of r. S^{km} is an invertible matrix such that $A^{ij} = S^{ik}J^{kl}(S^{-1})^{lj}$. Once in this form it is straightforward to solve the system of equations. We numerically calculate J^{ij} and S^{ij} and find A^{ij} to be diagonalizable with eigenvalues, Δ_i, giving

$$F^i = \sum_j S^{ij}r^{\Delta_j}. \tag{4.47}$$

Figure 4.3 shows the real part of the numerically obtained eigenvalues as a function of z for both the upper and lower sign choices in (4.18). Note that only eight eigenvalues have been plotted in these graphs since the eigenvalue corresponding to g can be removed by the use of (4.30). Each pair of eigenvalues is symmetric about $-(z+2)/2$ which is consistent with the fall-off of a general field in an asymptotically Lifshitz spacetime. This can be demonstrated with the example of a generic scalar field, ψ, propagating in a $d+1$ dimensional spacetime defined by (4.3), with an equation of motion given by

$$\nabla_a\nabla^a\psi - M^2\psi = 0, \tag{4.48}$$

where M is the mass of the scalar field. The solution to this equation will be valid in the vicinity of radial infinity and is given by

$$\psi = \psi_+ r^{\Lambda_+} + \psi_- r^{\Lambda_-}, \tag{4.49}$$

where

$$\Lambda_\pm = \frac{-(d+z-1)}{2} \pm \sqrt{\frac{(d+z-1)^2}{4} + M^2L^2}. \tag{4.50}$$

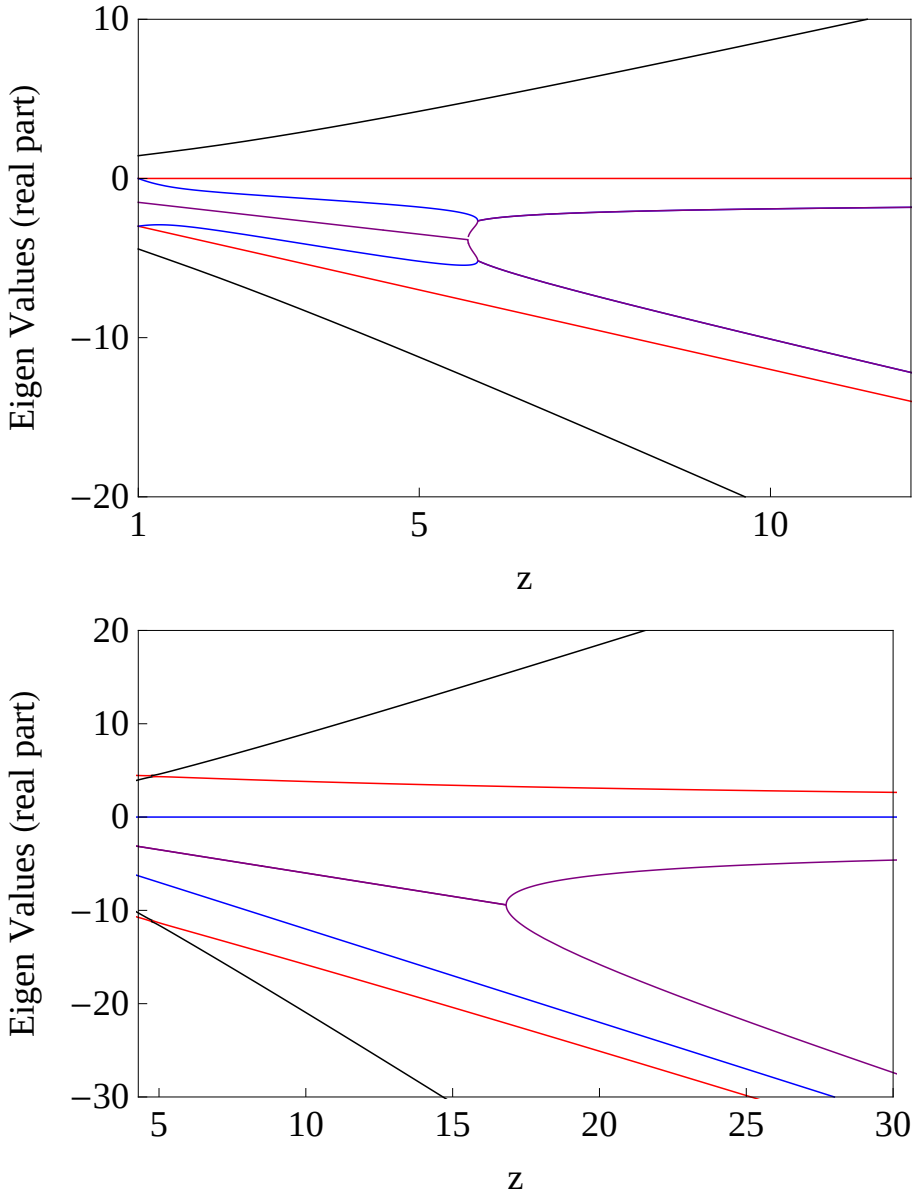

Figure 4.3: Plots of the real parts of the eigenvalues of A_{ij} in (4.45) as a function of z. The upper and lower plots correspond to the upper and lower sign choices in (4.18) respectively.

Here we see that the exponents of each of the fall-offs lie either side of $-(d+z-1)/2$, which in our four dimensional Lifshitz spacetime is $-(z+2)/2$. In a similar way to the adS case we can interpret these pairs as an operator and source term in the dual theory.

Once again, as is noted in [100], there are regions of each plot for which some of the eigenvalues are complex. For the lower sign choice one finds complex eigenvalues for $z < 16.82$, which, using intuition from the adS case, may be associated with a violation of the Lifshitz equivalent of the BF bound. One can see from (4.50) that in order for the $\Lambda_\pm$ to be real the following bound on the scalar mass must be satisfied

$$M^2L^2 \geq -\frac{(d+z-1)^2}{4}, \tag{4.51}$$

where in our case $d = 3$. Whilst this is reminiscent of the BF bound in adS space, a proper analysis of whether this does indicate an instability has yet to be done.

The upper sign choice is more complicated with a second region of complex eigenvalues appearing at larger z. In fact there is only a small window, $5.69 < z < 5.83$, in which all the eigenvalues are real. At present we do not have a clear understanding of why this is so.

Each plot shows the presence of irrelevant operators for the full range of z.

The Horizon

To obtain black hole solutions for this system we must ensure that our boundary conditions are consistent with the nature of the near horizon region of a black hole spacetime. These conditions will be the same irrespective of whether we are interested in asymptotically Lifshitz or adS black holes. Assuming that the horizon in non-degenerate, we wish the g_{tt} component of the metric to have a simple zero and the g_{rr} to have a simple pole at $r = r_+$. Checking that the matter and metric fields and the energy momentum tensor are regular at the horizon imposes no further

constraints and we find the near horizon expansion of the fields to be

$$\begin{aligned} f(r) &= f_1(r-r_+) + f_2(r-r_+)^2 + ... \\ g(r) &= g_1(r-r_+) + g_2(r-r_+)^2 + ... \\ k(r) &= k_0 + k_1(r-r_+) + k_2(r-r_+)^2 + ... \\ \varphi(r) &= \varphi_0 + \varphi_1(r-r_+) + \varphi_2(r-r_+)^2 + ... \\ s(r) &= s_0 + s_1(r-r_+) + s_2(r-r_+)^2 + ... \end{aligned} \tag{4.52}$$

By inserting these into the field equations and expanding order by order, appropriate boundary conditions can be found. This procedure leaves us with four independent field variables at the horizon, f_1, k_0, s_0 and φ_0 for each choice of z or $\hat{m}$. Recall from (4.32) that r_+ can be set to 1 without loss of generality.

4.3 AdS Black Holes

We begin our search for black hole solutions in the more familiar asymptotically adS spacetimes. Due to the slightly simpler nature of systems in this case it is possible to gain some analytic understanding of the black hole spacetimes, which we shall discuss first.

4.3.1 Analytic Black Holes

We start with the simplest possible case of a system with $s(r) = 0$ and a constant dilaton and k field. Recall that for asymptotically adS solutions the parameters of the system are defined by (4.19) with $\hat{\beta} = 1$. In this case the field equations admit the planar adS Schwarzschild solution:

$$f(r) = g(r) = 1 - \frac{r_+^3}{r^3}. \tag{4.53}$$

Whilst we are unable to find more complicated analytic solutions to the fully non-linear set of equations we are able to study 'probe' solutions of the linearised equations. We use the word probe here in a slightly different sense to its use in chapters

2 and 3 since we no longer have a free parameter to tune the backreaction to zero. The solutions that we shall study now are perturbations to φ, k and s that are consistent with (4.53).

We begin by allowing s to vary but keeping φ and k constant. Once again (4.29) decouples from the other equations at linear order giving

$$\left[\left(1-\frac{r_+^3}{r^3}\right)(r^2 s)'\right]' = (12-\hat{\lambda}^2)s. \tag{4.54}$$

By writing $x = (r_+/r)^3$ and

$$s(x) = x^{-\theta_\pm/3}P(x), \tag{4.55}$$

where $\theta_\pm$ is given by (4.36), this equation becomes a hypergeometric equation:

$$x(1-x)P_{xx} + [(1-x)2\theta_\pm/3]P_x + (2+\theta_\pm)(2-\theta_\pm)P/9 = 0. \tag{4.56}$$

This has solutions

$$s(x) = x^{-\theta_\pm/3}\,{}_2F_1[-(\theta_\pm+2)/3, (2-\theta_\pm)/3; -2\theta_\pm/3, x] \tag{4.57}$$

where ${}_2F_1[a,b;c,x]$ is a hypergeometric function. Since $a+b=c$ each ${}_2F_1[a,b;c,x]$ has a logarithmic singularity at $x=1$, however a non-singular combination of the two functions can be found, giving

$$\begin{aligned} s(x) \propto & \frac{\Gamma[-2\theta_-/3]x^{-\theta_+/3}}{\Gamma[(2-\theta_-)/3]\Gamma[-(\theta_-+2)/3]}\,{}_2F_1[-(\theta_++2)/3,(2-\theta_+)/3;-2\theta_+/3,x] \\ & - \frac{\Gamma[-2\theta_+/3]x^{-\theta_-/3}}{\Gamma[(2-\theta_+)/3]\Gamma[-(\theta_++2)/3]}\,{}_2F_1[-(\theta_-+2)/3,(2-\theta_-)/3;-2\theta_-/3,x]. \end{aligned} \tag{4.58}$$

The large r fall-off of this expression agrees precisely with (4.36). To ensure non-singular solutions in this limit we wish $\theta_+ < 0$ which is true for $\hat{\lambda}^2 > 10$ ($\hat{m} < \sqrt{10}-2$). For an example we shall take $\hat{\lambda}^2 = 52/5$ which gives $\theta_\pm = (-3\pm\sqrt{37/5})/2$. Figure 4.4 shows a plot of s as a function $\log r$.

We can also consider black hole solutions with non-trivial φ and k. Fixing $s = 0$ we once again find that the equations (4.27) and (4.28) form an isolated coupled system similar to (4.38)

$$\mathcal{L}_{III}\begin{pmatrix}\delta\varphi\\ \delta k\end{pmatrix} = \begin{bmatrix}(3\hat{m}^2 - \hat{\lambda}^2)/2 & \sqrt{2}\hat{\gamma}^2\\ 2\sqrt{2}\hat{\gamma}^2 & 2(\hat{\gamma}^2+3)\end{bmatrix}\begin{pmatrix}\delta\varphi\\ \delta k\end{pmatrix}, \tag{4.59}$$

but where

$$\mathcal{L}_{III}X = \frac{1}{r^2}\frac{d}{dr}\left[r^4\left(1-\frac{r_+^3}{r^3}\right)\frac{dX}{dr}\right]. \tag{4.60}$$

The eigenvalues and eigenvectors are once again given by (4.39) and (4.40). As above we can recast the eigenvalue equation, $\mathcal{L}_{III}X = \xi_\pm X$, into hypergeometric form by writing $X = x^\mu Y$ where

$$\mu_\pm(\xi_\pm) = (1 \pm \sqrt{1 + 4\xi_\pm/9})/2, \tag{4.61}$$

giving

$$x(1-x)Y_{xx} + (2\mu_\pm - (1+2\mu_\pm)x)Y_x - \mu_\pm^2 Y = 0. \tag{4.62}$$

This has solutions

$$X = x^{\mu_\pm}\,{}_2F_1[\mu_\pm, \mu_\pm; 2\mu_\pm; x], \tag{4.63}$$

where each of the elements in X correspond to a different choice of $\xi_\pm$. Once again the solutions are singular at $x = 1$ but a non-singular combination can be found

$$\begin{aligned} X \propto & \frac{\Gamma[2\mu_-]}{\Gamma[\mu_-]\Gamma[\mu_-]}x^{\mu_+}\,{}_2F_1[\mu_+, \mu_+; 2\mu_+; x] \\ - & \frac{\Gamma[2\mu_+]}{\Gamma[\mu_+]\Gamma[\mu_+]}x^{\mu_-}\,{}_2F_1[\mu_-, \mu_-; 2\mu_-; x]. \end{aligned} \tag{4.64}$$

In order to have a non-singular solution at $x = 0$ we require $\mu_\pm(\xi_\pm) > 0$. Plotting $\mu_-(\xi_+)$ as a function of $\hat{m}$ shows $\mu_-(\xi_+) < 0$ for all $\hat{m} \in [\sqrt{6/5}, \sqrt{6}]$, which means

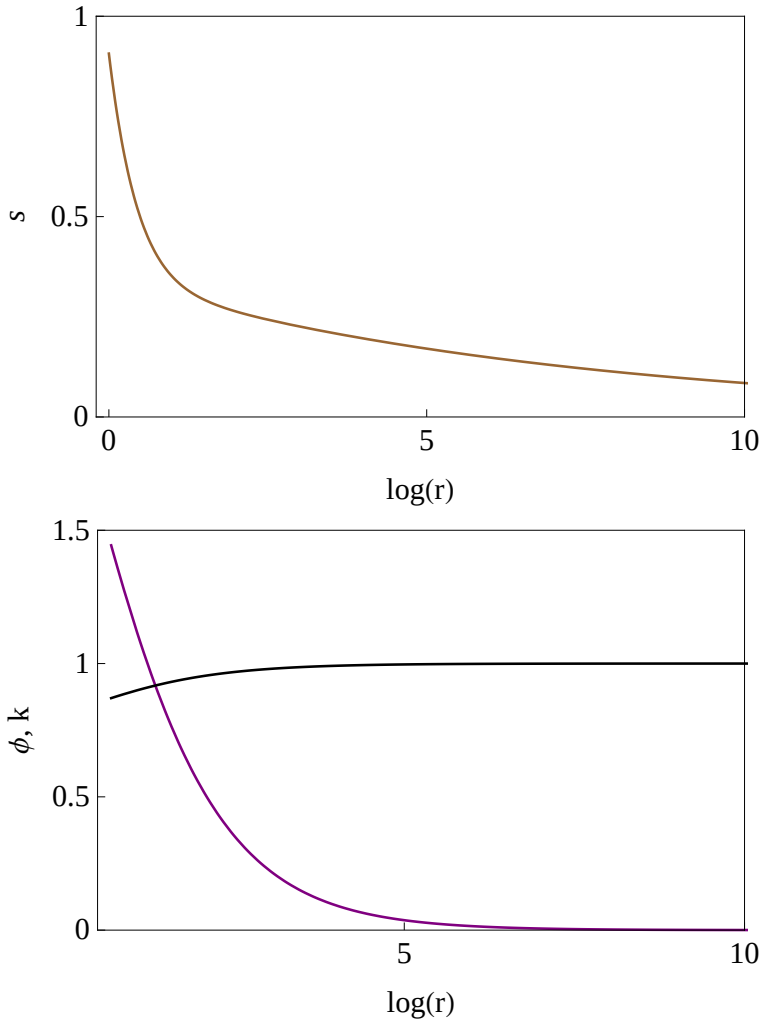

Figure 4.4: The upper plot shows a perturbation of s that is consistent with (4.53) for $\hat{m} = \sqrt{10} - 2$. The lower plot shows consistent perturbations of φ and k for $\hat{m} = 3/2$.

that the element of X corresponding to this eigenvalue must be set to zero. We also find that we must restrict our solutions to the range $1.254 < \hat{m} < 1.588$ as above this range $\mu_-(\xi_-) < 0$ and below this range both $\mu_+(\xi_-)$ and $\mu_+(\xi_-)$ are complex.

From (4.64) it is straightforward to find the expressions for $\delta\varphi$ and δk

$$\delta\varphi = v_{1-} X_2 \tag{4.65}$$

$$\delta k = v_{2-} X_2, \tag{4.66}$$

where X_2 corresponds to the eigenvalue ξ_-. Figure 4.4 shows an example of $\varphi = \delta\varphi$ and $k = 1 + \delta k$ as a function of $\log r$ for $\hat{m} = 3/2$.

Whilst these findings are not true solutions to the full system of equations they provide a strong indication that similar solutions to the full system may be found.

4.3.2 Numerical Solutions

We now wish to find numerical solutions to the full coupled set of differential equations. These can be found by fixing $\hat{m}$ and using a "shooting method" in which the initial data are guessed and each equation is integrated from the horizon out to some large radial distance. The initial data can then be tuned to give the desired asymptotic fall-off.

Due to the presence of an irrelevant operator at the fixed point our numerical solutions will diverge from the fixed point. It is however possible to tune the initial data to reach a solution that is arbitrarily close to the fixed point solution. This process is simplest in systems that have only one positive eigenvalue as any general solution must necessarily converge to a line in parameter space upon which the fixed point solution must lie. Tuning the initial data then moves the solution along this line and the location of the fixed point is indicated by a sign flip in the divergences of the fields.

As we desire the fixed point to have at most one irrelevant operator we shall only consider asymptotically adS black holes with $\hat{m} \in [\sqrt{6/5}, 1.162]$. Note that in this range the exponents of φ and k are complex.

Via this process we find a two parameter family of asymptotically adS black hole solutions for a fixed value of $\hat{m}$. A priori we are free to choose any two of f_1, k_0, φ_0 and s_0 as our two free parameters and we shall choose them to be φ_0 and s_0.

Figures 4.5 to 4.7 show examples of the asymptotically adS black hole solutions with $\hat{m} = 1.105$. Figure 4.5 shows two solutions where $s_0 = 0$, which implies that $s(r) = 0$ for all r meaning these solutions correspond to uncharged black holes. The upper plot shows the effect of a small perturbation to the dilaton. It leads to a smaller perturbation in k and largely leaves f and g unchanged which is consistent with the approximations made in finding the analytic solution (4.64). Since the range of $\hat{m}$, for which we have numerical solutions, does not overlap with the range of $\hat{m}$ for which (4.65) and (4.66) are valid we are unable to compare the two solutions directly.

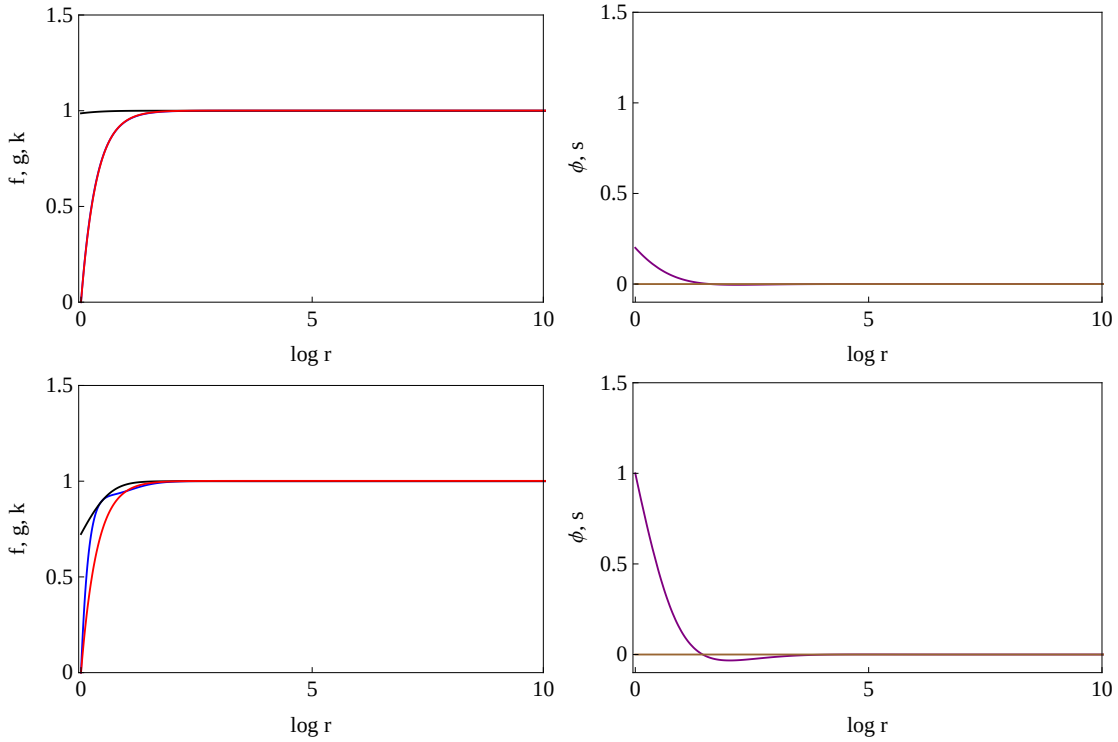

Figure 4.5: Field profiles for asymptotically adS black holes with $\hat{m} = 1.105$. In each plot the red line corresponds to f, the blue to g, black to k, purple to φ and brown to s. The upper plot corresponds to $\varphi_0 = 0.2$, $s_0 = 0$ and the lower to $\varphi_0 = 1$, $s_0 = 0$.

The lower plot shows the effect of turning φ_0 up to one. Now the perturbation in k grows and f and g are no longer equal.

Figure 4.6 shows solutions with $\varphi = 0$ and $s_0 \neq 0$. Again, the upper plot shows the effect of a small perturbation in s which leaves the other fields largely unchanged. This is consistent with the approximations made in finding (4.58). In this case it is possible to overlay the analytic and numerically generated profiles of s for the same value of $\hat{m}$, in doing so one finds that the two appear identical to the naked eye until the numerical solution begins to diverge from the fixed point. Increasing s_0 alters all the other fields as seen in the lower plot. Figure 4.7 shows an example of a solutions for $\varphi_0 \neq 0$ and $s_0 \neq 0$.

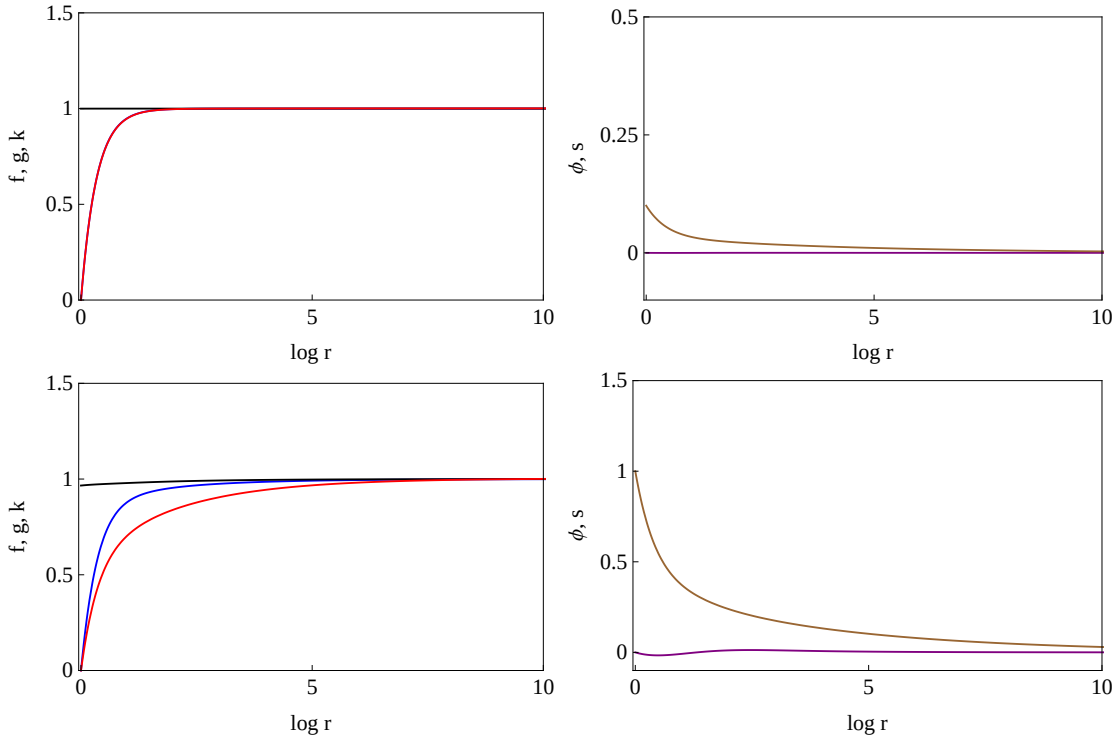

Figure 4.6: Field profiles for asymptotically adS black holes with $\hat{m} = 1.105$. In each plot the red line corresponds to f, the blue to g, black to k, purple to φ and brown to s. The upper plot corresponds to $\varphi_0 = 0$, $s_0 = 0.1$ and the lower to $\varphi_0 = 0$, $s_0 = 1$.

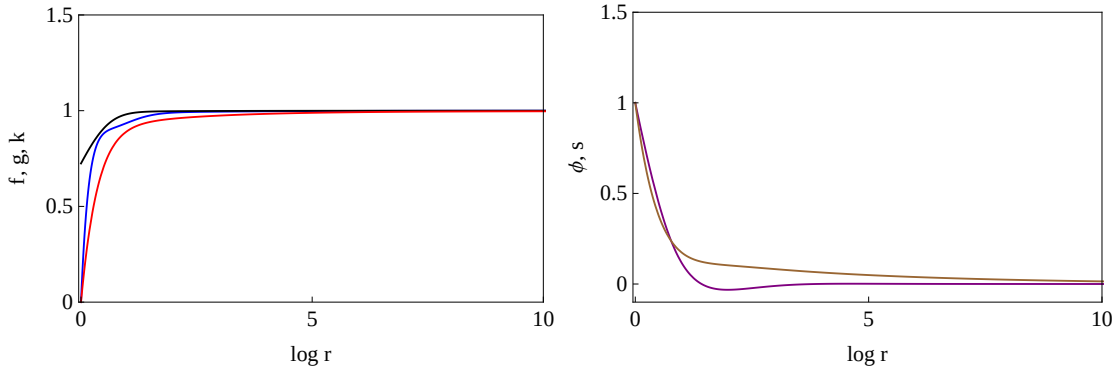

Figure 4.7: Field profiles for asymptotically adS black holes with $\hat{m} = 1.105$, $\varphi_0 = 1$ and $s_0 = 1$. The red line corresponds to f, the blue to g, black to k, purple to φ and brown to s.

4.4 Lifshitz Black holes

We are now interested in finding black hole solutions that asymptote to the Lifshitz spacetime defined by (4.18). A crucial difference between this case and the asymptotically adS case is that it is necessary that $s \neq 0$ in order to generate the Lifshitz spacetime. As a result it is less straightforward to obtain an analytic expression for the black hole similar to (4.53) and we must rely solely on numerical results. The numerical solutions are found in precisely the same way as in the adS case with the only difference being that the parameters of the theory are now defined by (4.18) where the dynamical exponent $z \geq 1$ is used to fix the theory as opposed to $\hat{m}$. For simplicity we only consider the solutions corresponding to the upper sign choice in (4.18) since, in this case, the fixed point has only one irrelevant operator. By integrating the equations of motion (4.25) to (4.29) we once again find a two parameter family of asymptotically Lifshitz black hole solutions for each value of z to which we assign the free parameters φ_0 and s_0.

Figures 4.8 and 4.9 show examples of the field profiles for these asymptotically Lifshitz black holes. The upper plots in figure 4.8 depict the case of $z = 2$, $\varphi_0 = 0$ and $s_0 = 1$. These plots show a dramatic discrepancy between the profiles of f and g and also show that φ and k are perturbed. In fact, it is possible to show that for $z \neq 1$ there is no value of s_0 for which φ and k have trivial profiles. This can be seen from the boundary conditions governing φ_1 and k_1 that appear in (4.52). Setting $\varphi_0 = 0$ and $k_0 = 1$ for a system defined by (4.18), the boundary conditions become:

$$\sqrt{2}\varphi_1 = \frac{\hat{\beta}^2}{g_1}\left(s_0^2\left(\hat{\gamma}^2 - \frac{\hat{m}^2}{4}\right) - 2 - \left(\hat{\gamma}^2 - \frac{\hat{m}^2}{4}\right)\right) \tag{4.67}$$

$$k_1 = \frac{\hat{\beta}^2}{g_1}\left(-s_0^2\left(\hat{\gamma}^2 - \frac{\hat{m}^2}{4}\right) - 2 + \left(\hat{\gamma}^2 - \frac{\hat{m}^2}{4}\right)\right). \tag{4.68}$$

If the field profiles are to be trivial then φ_1 and k_1 must both be zero. From (4.67) and (4.68) we can see that this is only possible when $\hat{\beta}^2 = 0$ which only occurs at $z = 1$. Thus, for $z \neq 1$ there can be no solutions where both φ and k have trivial profiles.

Another possibility is that s may be trivially equal to one, with φ and k having

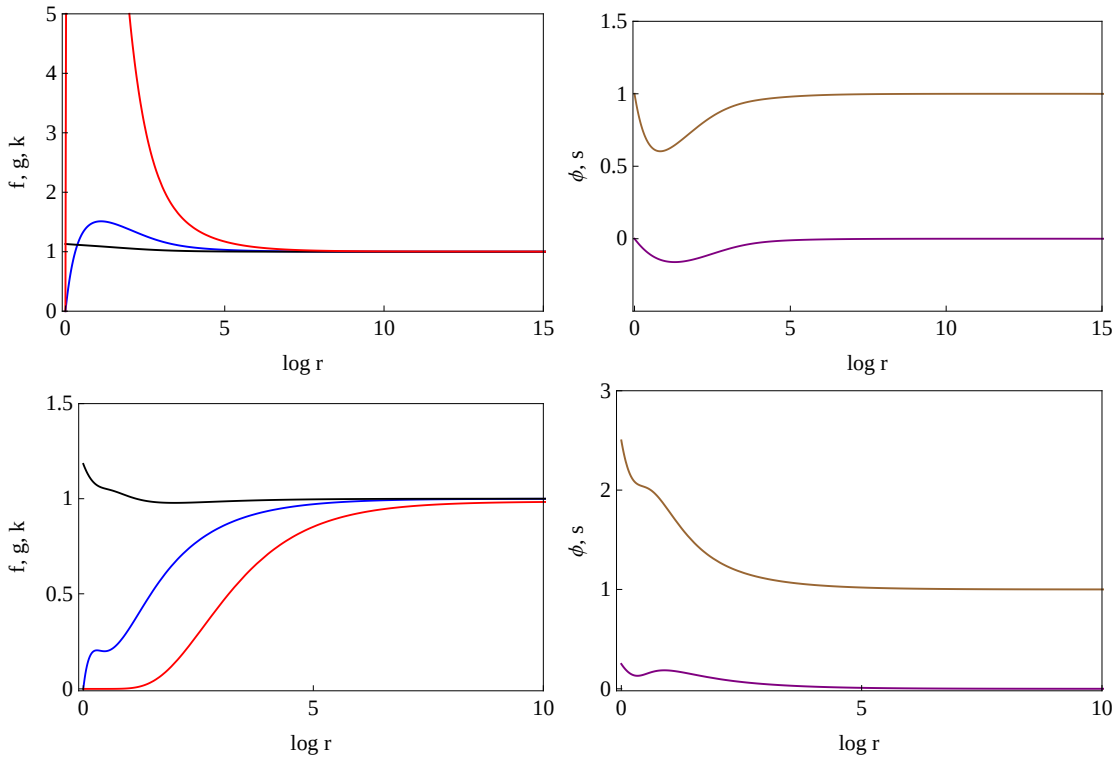

Figure 4.8: Plots showing the field profiles for asymptotically Lifshitz black holes for $z = 2$. The red, blue, black, brown and purple lines correspond to f, g, k, s and φ respectively. The upper plots show the fields for $\varphi_0 = 0$, $s_0 = 1$ and the lower plot shows $\varphi_0 = 0.25$, $s_0 = 2.5$.

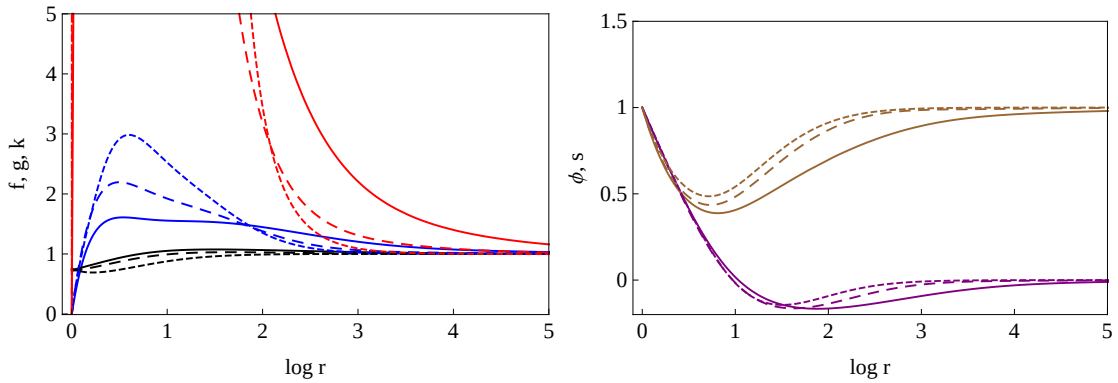

Figure 4.9: Plots showing the field profiles for asymptotically Lifshitz black holes for $\varphi_0 = s = 1$. The red, blue, black, brown and purple lines correspond to f, g, k, s and φ respectively. The solid lines correspond to $z = 2$ the larger dashed lines to $z = 3$ and the smaller dashed lines to $z = 5.75$.

non-trivial profiles. We have no analytic arguments to say whether or not this is possible, but we have seen no indication of this in our numerical solutions.

In the lower plots of figure 4.8 two different values of φ_0 and s_0 have been chosen which show how the values of these parameters can dramatically alter the profiles of the fields.

The plots in figure 4.9 show the effect of altering the dynamical exponent for a system with $\varphi_0 = s = 1$. The plots show the field profiles for $z = 2$, $z = 3$ and $z = 5.75$, where the last value was chosen to be within the range for which all the eigenvalues of figure 4.3 are real. These plots show how z can alter the field profiles, particularly f and g, and that increasing z quickens the convergence to the Lifshitz solution. This was to be expected as, as can be seen in figure 4.3, increasing z largely reduces the eigenvalues governing each fields approach to the Lifshitz fixed point.

4.5 Temperature

Having found these black hole solutions it is interesting to investigate some of the characteristics other than their field profiles. In this section we make the first few steps of this exploration by studying the dependence of the temperature of these black holes on the initial parameters φ_0 and s_0.

An expression for the temperature is found by Wick rotating the metric and ensuring that the horizon is non singular, giving

$$T = \frac{1}{\beta_\tau} = \frac{r_+^{z+1}}{4\pi} \left(f' g'\right)^{\frac{1}{2}} \Big|_{r=r_+}, \tag{4.69}$$

where β_τ is the periodicity of the Wick rotated time coordinate, $t \to i\tau$. Note that β_τ scales as b^{-z} under the rescaling (4.32) which is consistent with the invariance of $\frac{2\pi}{\beta_\tau} d\tau$ that appears in the metric.

Figures 4.10 to 4.12 show the temperatures of both the asymptotically adS and Lifshitz black holes as a function of our initial parameter s_0, for a variety of values of φ_0. Figure 4.10 shows the asymptotically adS black hole for $\hat{m} = 1.105$ and figure 4.11 shows the Lifshitz black hole for $z = 2$. Both plots show that increasing s_0 reduces the temperature. A key difference between the adS and Lifshitz black holes

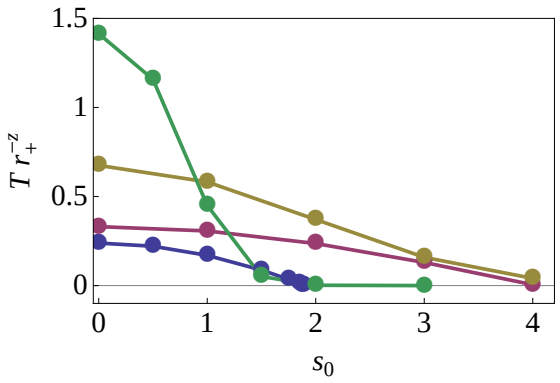

Figure 4.10: Plot of the temperature of an asymptotically adS black hole with $\hat{m} = 1.105$ as a function of s_0. Each line corresponds to different values of φ_0: the blue to $\varphi_0 = 0$, red to $\varphi_0 = 1$, yellow to $\varphi_0 = 2$ and green to $\varphi_0 = 3$.

is their behaviour as $s_0 \to 0$. This is a valid regime of adS black holes for which their temperature is finite. Lifshitz black holes however, do not exist at $s_0 = 0$ and it appears that the temperature diverges as this limit is approached.

The plots also show how the temperature is altered as φ_0 is changed. In the adS case we see that increasing φ_0 dramatically increases the temperature of the uncharged black hole, and quickens its decent as s_0 is increased. In the Lifshitz case increasing φ_0 initially increases the temperature before reducing it. Unfortunately we were unable to verify whether, like the adS case, these curves cross as s_0 is reduced further.

We can also investigate the effect of altering z on the temperature, as seen in figure 4.12. The left plot shows that increasing z raises the temperature for small s_0 but then quickens its decent as s_0 is increased. The curves appear to intersect at one point which may suggest that this point is invariant under changes in z. The plot on the right shows that this is not the case. It shows that while the three curves do intersect within a very small region of parameter space, the intersection point for curves corresponding to lower values of z moves away from this point, as seen by the square and triangular points corresponding to $z = 1.5$ and 1.3 respectively.

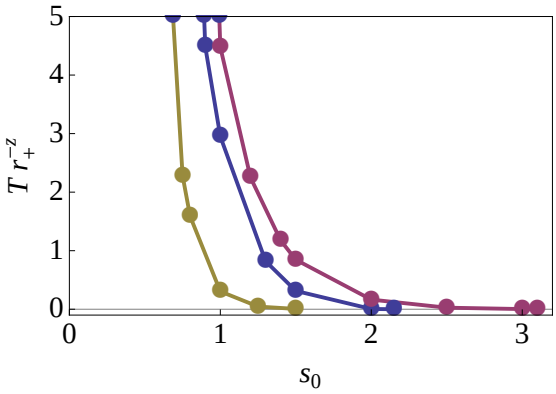

Figure 4.11: Plot of the temperature of an asymptotically Lifshitz black hole with $z = 2$ as a function of s_0. Each line corresponds to different values of φ_0: the blue to $\varphi_0 = 0$, red to $\varphi_0 = 1$ and yellow to $\varphi_0 = 2$.

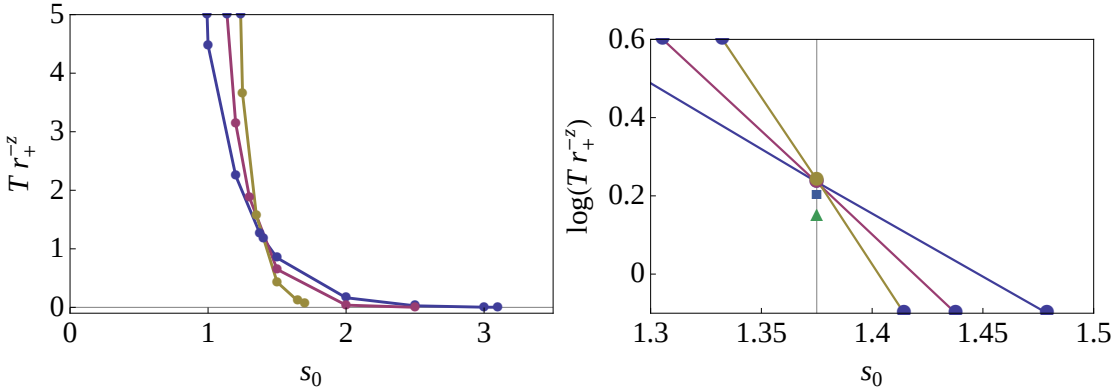

Figure 4.12: Plot of the temperature of an asymptotically Lifshitz black hole with $\varphi_0 = 1$ as a function of s_0. Each curve corresponds to a different value of z: blue to $z = 2$, red to $z = 3$, and yellow to $z = 5$. The three curves presented in the left plot all appear to intersect at a single point. The plot on the right shows that this common intersection point does not hold as z is reduced below 2 since the square and triangular points, corresponding to $z = 1.3$ and $z = 1.5$ respectively, do not lie on this point.

4.6 Summary

The aim of this research was to find asymptotically Lifshitz black holes solutions to the model presented in [96]. The motivation was to introduce temperature into the theory as a crucial step towards developing a model of holographic superconductivity in this top down model that permits an arbitrary dynamical exponent, $z \geq 1$. We succeeded in finding these black hole solutions and made a few steps towards investigating their characteristics.

We began by studying the asymptotically adS solutions that this theory permits in addition to the Lifshitz ones. We numerically found a two parameter family of asymptotically adS black hole solutions. These numerical solutions are supported by the finding of analytic black hole solutions that are valid in the regime where there is no backreaction of the matter fields upon the metric at linear order.

We then moved on to numerically find a two parameter family of asymptotically Lifshitz black hole solutions. By altering these two parameters it was possible to dramatically alter the field profiles of these Lifshitz black holes. We also investigated the effect that z had on the field profiles. Increasing z changed the profiles slightly and quickened the convergence towards the Lifshitz fixed point.

We then made some initial investigations into the temperature of these black holes. We found that for both types of black hole the temperature reduced as s_0 increased. Unfortunately it was outside the scope of our horizon Ansatzë to ascertain whether or not the temperature ever reached precisely zero.

In the Lifshitz case, and unlike the adS case, we saw that the temperature diverged as s_0 was reduced. We also studied the effect that z has on temperature finding that it seems to raise the temperature at small values of s_0 but quicken its decent as s_0 is increased.

Chapter 5

Outlook

This thesis considers two different aspects of holographic superconductivity which we shall now discuss in turn.

In chapter 3 we study the stability of a fully backreacting model of holographic superconductivity to the inclusion of higher order corrections to Einstein gravity. We found that while the key features of the superconductor persist, the details can be dramatically altered. When studying the zero temperature limit of the system, we found that the perturbative corrections can have a significant effect that must lead one to question the validity of some of the solutions in this regime. By considering the conductivity we have also been able to rule out a universal relation between the frequency gap and the critical temperature.

The findings of this research suggest a number of interesting avenues for future work, most notably in relation to the zero temperature limit. The first thing to do might be to either find, or disprove the existence of zero mass solutions of the sort presented in [74]. If they exist one could see what effect the GB terms have on these solutions and the quantum phase transitions that happen there.

Having shown that this system does not permit regular, superconducting, zero temperature, tachyonic solutions a possible next step might be to find out whether there exist non-regular solutions that are compatible with the perturbative relation between Einstein and GB gravity. If so, it would be interesting to find out how this non-regularity can be interpreted. It would also be interesting to study the conductivity of this system in such a case, particularly in light of [81] which suggests

that an infinite tower of quasi-normal modes may appear on the real axis as the temperature goes to zero.

Another line of enquiry might be to further investigate the regime of positive scalar masses at finite temperature. In this work we were only able to find solutions for very small positive m^2 which proved to be only marginally different to those of $m^2 = 0$. In [73], which studied the $m^2 > 0$ case in the probe limit, the authors found solutions at larger masses but found that solutions become difficult to attain due to an observed warping of the solution space which was dramatically enhanced by increasing m^2. By investigating this regime in more detail we may be able to see how the inclusion of higher curvature terms and backreaction affect this phenomenon.

One key limitation of the model that we have considered is that our choice of potential was completely arbitrary. This, of course, is a consequence of the bottom up approach and is useful in understanding some of the basic phenomena at play. However, at temperatures below T_c and particularly in the zero temperature limit the effect of different choices of potential are likely to be significant. Therefore, studying the effect of GB terms in top down models might be a useful next step.

In chapter 4 we studied black hole solutions to a gravitational model rooted in string theory in which the spacetime exhibits Lifshitz scaling with an arbitrary dynamical exponent, z. We studied the black hole solutions as a crucial first step towards developing a top down model of a Lifshitz holographic superconductor with an arbitrary $z \geq 1$. Using numerical techniques we were able to find a two parameter family of asymptotically Lifshitz black hole solutions.

The next step towards building a holographic superconductor is to add a complex scalar field to the system in the hope that it may act as a condensate in the boundary theory as we saw in adS superconductors of chapters 2 and 3. Ideally the complex scalar field should be added in such a way that is consistent with a string theory embedding and the top down approach of this model. However, a simpler first step may be to add a phenomenological scalar and gauge field of the sort used in the model of chapter 3 in order to see if superconductivity is at least possible.

Aside from developing a holographic superconductor the research presented in chapter 4 shows that this system has a very rich structure within which a great deal

more research can be done. Our investigation into the black holes of this system has highlighted some interesting characteristics which we have yet to find an explanation for. One example is the divergence of the temperature of the asymptotically Lifshitz black hole as the initial parameter s_0 is reduced. This could be investigated further by seeing how this diverging temperature affects the other physical characteristics of the black hole.

One might also wish to study the zero temperature limit of these black holes, which unfortunately was outside the scope of our horizon Ansatz. Having ascertained whether or not a regular zero temperature limit exists it would would be interesting to study the topology of the near horizon region as this may may be of significance to holographic superconductivity.

One limitation of this research is that we only considered regions of parameter space for which the fixed points of the theory have at most one irrelevant operator. In the adS case this meant restricting our analysis to values of $\hat{m}$ for which the fall-offs of some of the fields were complex which raises concerns when considering a holographic interpretation of these results. We were also only able to study one of the two Lifshitz solutions that this system permits. This research could be developed further by widening the study to include these regions that were not included in this initial investigation.

Due to the complexity of the system we had to rely solely on numerics to obtain our asymptotically Lifshitz black hole solutions. Another avenue of future research might be to try and gain a greater analytic understanding of these Lifshitz black holes. This is particularly important for holographic systems since without a full understanding of the bulk theory at the boundary we cannot fully understand its dual. One region where a perturbative analytic understanding may be possible is in the limit in which $z \to 1$, where one might expect the Lifshitz solutions to be similar to the adS solutions found at $z = 1$.

The work in this thesis forms part of a wider effort of applying the gauge/gravity correspondence to a range of open problems in physics from condensed matter systems to quantum chromodynamics. Its use in this way is interesting for two reasons; firstly, it provides a means of investigating physics at strong coupling which

is otherwise very difficult and secondly, by using the correspondence in regimes in which experimental testability is possible we may, in future, be able to test the validity of the conjectured correspondence itself. The use of the correspondence in condensed matter physics is still very much in its infancy but it is possible that some experimentally testable result may be lurking just around the corner.

Bibliography

[1] L. Barclay, R. Gregory, S. Kanno and P. Sutcliffe, *Gauss-Bonnet Holographic Superconductors*, *JHEP* **1012** (2010) 029 [1009.1991].

[2] L. Barclay, *The Rich Structure of Gauss-Bonnet Holographic Superconductors*, *JHEP* **1110** (2011) 044 [1012.3074].

[3] J. G. Bednorz and K. A. Muller, *Possible high tc superconductivity in the balacuo system*, *Zeitschrift fr Physik B Condensed Matter* **64** (1986) 189–193. 10.1007/BF01303701.

[4] J. M. Maldacena, *The large N limit of superconformal field theories and supergravity*, *Adv. Theor. Math. Phys.* **2** (1998) 231–252 [hep-th/9711200].

[5] H. K. Onnes, *The dissapearance of the resistivity of mercury*, *Comm. Leiden* **119b, 120b, 122b, 124c** (1911).

[6] F. London and H. London, *The electromagnetic equations of the supraconductor*, *Proceedings of the Royal Society of London. Series A, Mathematical and Physical Sciences* **149** (1935), no. 866 pp. 71–88.

[7] M. Tinkham, *Introduction to superconductivity*. Dover books on physics and chemistry. Dover Publications, 2004.

[8] J. Bardeen, L. N. Cooper and J. R. Schrieffer, *Microscopic theory of superconductivity*, *Phys. Rev.* **106** (1957) 162.

[9] L. N. Cooper, *Bound electron pairs in a degenerate fermi gas*, *Phys. Rev.* **104** (Nov, 1956) 1189–1190.

[10] J. Hubbard, *Electron correlations in narrow energy bands*, *Proceedings of the Royal Society of London. Series A. Mathematical and Physical Sciences* **276** (1963), no. 1365 238–257.

[11] P. W. ANDERSON, *The resonating valence bond state in la2cuo4 and superconductivity*, *Science* **235** (1987), no. 4793 1196–1198.

[12] V. L. Ginzburg and L. D. Landau, *On the Theory of superconductivity*, *Zh. Eksp. Teor. Fiz.* **20** (1950) 1064–1082.

[13] P. Drude, *Zur Elektronentheorie der Metalle*, *Annalen der Physik* **306** (1900) 566–613.

[14] R. D. L. KRONIG, *On the theory of dispersion of x-rays*, *J. Opt. Soc. Am.* **12** (Jun, 1926) 547–556.

[15] J. Jackson, *Classical electrodynamics*. Wiley, 1999.

[16] G. Veneziano, *Construction of a crossing - symmetric, Regge behaved amplitude for linearly rising trajectories*, *Nuovo. Cim.* **A57** (1968) 190–197.

[17] A. Einstein, *Die Grundlage der allgemeinen Relativittstheorie*, *Annalen der Physik* **354** (1916) 769–822.

[18] A.M. and Polyakov, *Quantum geometry of bosonic strings*, *Physics Letters B* **103** (1981), no. 3 207 – 210.

[19] A.M. and Polyakov, *Quantum geometry of fermionic strings*, *Physics Letters B* **103** (1981), no. 3 211 – 213.

[20] R. Haag, J. T. Lopuszaski and M. Sohnius, *All possible generators of supersymmetries of the s-matrix*, *Nuclear Physics B* **88** (1975), no. 2 257 – 274.

[21] M. B. Green and J. H. Schwarz, *Supersymmetric dual string theory: (iii). loops and renormalization*, *Nuclear Physics B* **198** (1982), no. 3 441 – 460.

[22] J. Polchinski, *Lectures on D-branes*, `hep-th/9611050`.

[23] C. Johnson, *D-branes*. Cambridge Monographs on Mathematical Physics. Cambridge University Press, 2006.

[24] D. Z. Freedman, P. van Nieuwenhuizen and S. Ferrara, *Progress toward a theory of supergravity*, *Phys. Rev. D* **13** (Jun, 1976) 3214–3218.

[25] J. Polchinski, *Dirichlet-Branes and Ramond-Ramond Charges*, *Phys. Rev. Lett.* **75** (1995) 4724–4727 [hep-th/9510017].

[26] G. T. Horowitz and A. Strominger, *Black strings and p-branes*, *Nuclear Physics B* **360** (1991), no. 1 197 – 209.

[27] M. J. Duff, H. Lu and C. N. Pope, *The black branes of M-theory*, *Phys. Lett.* **B382** (1996) 73–80 [hep-th/9604052].

[28] O. Aharony, S. S. Gubser, J. M. Maldacena, H. Ooguri and Y. Oz, *Large N field theories, string theory and gravity*, *Phys. Rept.* **323** (2000) 183–386 [hep-th/9905111].

[29] G. t Hooft, *A planar diagram theory for strong interactions*, *Nuclear Physics B* **72** (1974), no. 3 461 – 473.

[30] E. Witten, *Anti-de Sitter space and holography*, *Adv. Theor. Math. Phys.* **2** (1998) 253–291 [hep-th/9802150].

[31] L. Susskind and E. Witten, *The holographic bound in anti-de Sitter space*, hep-th/9805114.

[32] K. Skenderis, *Lecture notes on holographic renormalization*, *Class. Quant. Grav.* **19** (2002) 5849–5876 [hep-th/0209067].

[33] D. Marolf and S. F. Ross, *Boundary conditions and new dualities: Vector fields in AdS/CFT*, *JHEP* **11** (2006) 085 [hep-th/0606113].

[34] G. Gibbons and S. Hawking, *Euclidean quantum gravity*. World Scientific, 1993.

[35] G. W. Gibbons and S. W. Hawking, *Action Integrals and Partition Functions in Quantum Gravity*, *Phys. Rev.* **D15** (1977) 2752–2756.

[36] S. W. Hawking, *Particle Creation by Black Holes*, *Commun. Math. Phys.* **43** (1975) 199–220.

[37] J. D. Bekenstein, *Black holes and entropy*, *Phys. Rev.* **D7** (1973) 2333–2346.

[38] S. W. Hawking, *Black Holes and Thermodynamics*, *Phys. Rev.* **D13** (1976) 191–197.

[39] J. B. Hartle and S. W. Hawking, *Path Integral Derivation of Black Hole Radiance*, *Phys. Rev.* **D13** (1976) 2188–2203.

[40] E. Witten, *Anti-de Sitter space, thermal phase transition, and confinement in gauge theories*, *Adv. Theor. Math. Phys.* **2** (1998) 505–532 [hep-th/9803131].

[41] S. S. Gubser, I. R. Klebanov and A. W. Peet, *Entropy and Temperature of Black 3-Branes*, *Phys. Rev.* **D54** (1996) 3915–3919 [hep-th/9602135].

[42] G. 't Hooft, *Dimensional reduction in quantum gravity*, gr-qc/9310026.

[43] L. Susskind, *The World as a hologram*, *J. Math. Phys.* **36** (1995) 6377–6396 [hep-th/9409089].

[44] G. T. Horowitz and J. Polchinski, *Gauge / gravity duality*, gr-qc/0602037.

[45] S. S. Gubser, *Breaking an Abelian gauge symmetry near a black hole horizon*, *Phys. Rev.* **D78** (2008) 065034 [0801.2977].

[46] S. A. Hartnoll, C. P. Herzog and G. T. Horowitz, *Building a Holographic Superconductor*, *Phys. Rev. Lett.* **101** (2008) 031601 [0803.3295].

[47] S. S. Gubser, C. P. Herzog, S. S. Pufu and T. Tesileanu, *Superconductors from Superstrings*, *Phys. Rev. Lett.* **103** (2009) 141601 [0907.3510].

[48] J. P. Gauntlett, J. Sonner and T. Wiseman, *Holographic superconductivity in M-Theory*, *Phys. Rev. Lett.* **103** (2009) 151601 [0907.3796].

[49] J. P. Gauntlett, J. Sonner and T. Wiseman, *Quantum Criticality and Holographic Superconductors in M- theory*, *JHEP* **02** (2010) 060 [0912.0512].

[50] J. D. Bekenstein, *Black hole hair: Twenty-five years after*, gr-qc/9605059.

[51] S. L. Adler and R. B. Pearson, *"no-hair" theorems for the abelian higgs and goldstone models*, *Phys. Rev. D* **18** (Oct, 1978) 2798–2803.

[52] M. S. Volkov and D. V. Galtsov, *NonAbelian Einstein Yang-Mills black holes*, *JETP Lett.* **50** (1989) 346–350.

[53] P. Breitenlohner and D. Z. Freedman, *Stability in Gauged Extended Supergravity*, *Ann. Phys.* **144** (1982) 249.

[54] S. A. Hartnoll, C. P. Herzog and G. T. Horowitz, *Holographic Superconductors*, *JHEP* **12** (2008) 015 [0810.1563].

[55] C. P. Herzog, *Lectures on Holographic Superfluidity and Superconductivity*, *J. Phys.* **A42** (2009) 343001 [0904.1975].

[56] R. Gregory, S. Kanno and J. Soda, *Holographic Superconductors with Higher Curvature Corrections*, *JHEP* **10** (2009) 010 [0907.3203].

[57] Q. Pan, B. Wang, E. Papantonopoulos, J. Oliveira and A. B. Pavan, *Holographic Superconductors with various condensates in Einstein-Gauss-Bonnet gravity*, *Phys. Rev.* **D81** (2010) 106007 [0912.2475].

[58] Q. Pan and B. Wang, *General holographic superconductor models with Gauss- Bonnet corrections*, *Phys. Lett.* **B693** (2010) 159–165 [1005.4743].

[59] R.-G. Cai, Z.-Y. Nie and H.-Q. Zhang, *Holographic p-wave superconductors from Gauss-Bonnet gravity*, *Phys. Rev.* **D82** (2010) 066007 [1007.3321].

[60] Y. Brihaye and B. Hartmann, *Holographic Superconductors in 3+1 dimensions away from the probe limit*, 1003.5130.

[61] M. Siani, *Holographic Superconductors and Higher Curvature Corrections*, 1010.0700.

[62] J. Jing, L. Wang, Q. Pan and S. Chen, *Holographic Superconductors in Gauss-Bonnet gravity with Born-Infeld electrodynamics*, *Phys. Rev.* **D83** (2011) 066010 [1012.0644].

[63] D. Lovelock, *The einstein tensor and its generalizations*, *Journal of Mathematical Physics* **12** (1971), no. 3 498–501.

[64] P. Candelas, G. T. Horowitz, A. Strominger and E. Witten, *Vacuum configurations for superstrings*, *Nuclear Physics B* **258** (1985) 46 – 74.

[65] B. Zwiebach, *Curvature squared terms and string theories*, *Physics Letters B* **156** (1985), no. 5-6 315 – 317.

[66] D. G. Boulware and S. Deser, *String Generated Gravity Models*, *Phys. Rev. Lett.* **55** (1985) 2656.

[67] R.-G. Cai, *Gauss-Bonnet black holes in AdS spaces*, *Phys. Rev.* **D65** (2002) 084014 [hep-th/0109133].

[68] S. Deser and B. Tekin, *Energy in generic higher curvature gravity theories*, *Phys. Rev.* **D67** (2003) 084009 [hep-th/0212292].

[69] L. F. Abbott and S. Deser, *Stability of Gravity with a Cosmological Constant*, *Nucl. Phys.* **B195** (1982) 76.

[70] A. Buchel *et. al.*, *Holographic GB gravity in arbitrary dimensions*, *JHEP* **03** (2010) 111 [0911.4257].

[71] L. Landau and E. Lifshits, *Fluid mechanics*. Course of theoretical physics. Pergamon Press, 1959.

[72] G. T. Horowitz and M. M. Roberts, *Holographic Superconductors with Various Condensates*, *Phys. Rev.* **D78** (2008) 126008 [0810.1077].

[73] Y. Kim, Y. Ko and S.-J. Sin, *Density driven symmetry breaking and Butterfly effect in holographic superconductors*, *Phys. Rev.* **D80** (2009) 126017 [0904.4567].

[74] G. T. Horowitz and M. M. Roberts, *Zero Temperature Limit of Holographic Superconductors*, *JHEP* **11** (2009) 015 [0908.3677].

[75] J. Fernandez-Gracia and B. Fiol, *A no-hair theorem for extremal black branes*, *JHEP* **11** (2009) 054 [0906.2353].

[76] S. A. Hartnoll, *Lectures on holographic methods for condensed matter physics*, *Class. Quant. Grav.* **26** (2009) 224002 [0903.3246].

[77] F. Denef and S. A. Hartnoll, *Landscape of superconducting membranes*, *Phys. Rev.* **D79** (2009) 126008 [0901.1160].

[78] G. T. Horowitz and V. E. Hubeny, *Quasinormal modes of AdS black holes and the approach to thermal equilibrium*, *Phys.Rev.* **D62** (2000) 024027 [hep-th/9909056].

[79] D. K. Brattan and S. A. Gentle, *Shear channel correlators from hot charged black holes*, 1012.1280.

[80] D. Birmingham, I. Sachs and S. N. Solodukhin, *Conformal field theory interpretation of black hole quasi- normal modes*, *Phys. Rev. Lett.* **88** (2002) 151301 [hep-th/0112055].

[81] G. Siopsis, J. Therrien and S. Musiri, *Holographic conductors near the Breitenlohner-Freedman bound*, 1011.2938.

[82] J. A. Hertz, *Quantum critical phenomena*, *Phys. Rev. B* **14** (Aug, 1976) 1165–1184.

[83] S. Kachru, X. Liu and M. Mulligan, *Gravity Duals of Lifshitz-like Fixed Points*, *Phys. Rev.* **D78** (2008) 106005 [0808.1725].

[84] M. Taylor, *Non-relativistic holography*, 0812.0530.

[85] K. Balasubramanian and K. Narayan, *Lifshitz spacetimes from AdS null and cosmological solutions*, *JHEP* **08** (2010) 014 [1005.3291].

[86] A. Donos and J. P. Gauntlett, *Lifshitz Solutions of D=10 and D=11 supergravity*, *JHEP* **12** (2010) 002 [1008.2062].

[87] A. Donos, J. P. Gauntlett, N. Kim and O. Varela, *Wrapped M5-branes, consistent truncations and AdS/CMT*, *JHEP* **12** (2010) 003 [1009.3805].

[88] D. Cassani and A. F. Faedo, *Constructing Lifshitz solutions from AdS*, *JHEP* **05** (2011) 013 [1102.5344].

[89] J. Blaback, U. H. Danielsson and T. Van Riet, *Lifshitz backgrounds from 10d supergravity*, *JHEP* **02** (2010) 095 [1001.4945].

[90] S. F. Ross and O. Saremi, *Holographic stress tensor for non-relativistic theories*, *JHEP* **0909** (2009) 009 [0907.1846].

[91] S. F. Ross, *Holography for asymptotically locally Lifshitz spacetimes*, *Class.Quant.Grav.* **28** (2011) 215019 [1107.4451].

[92] U. H. Danielsson and L. Thorlacius, *Black holes in asymptotically Lifshitz spacetime*, *JHEP* **03** (2009) 070 [0812.5088].

[93] I. Amado and A. F. Faedo, *Lifshitz black holes in string theory*, *JHEP* **07** (2011) 004 [1105.4862].

[94] M. H. Dehghani, R. B. Mann and R. Pourhasan, *Charged Lifshitz Black Holes*, *Phys. Rev.* **D84** (2011) 046002 [1102.0578].

[95] K. Balasubramanian and J. McGreevy, *An analytic Lifshitz black hole*, *Phys. Rev.* **D80** (2009) 104039 [0909.0263].

[96] R. Gregory, S. L. Parameswaran, G. Tasinato and I. Zavala, *Lifshitz solutions in supergravity and string theory*, *JHEP* **12** (2010) 047 [1009.3445].

[97] L. Romans, *THE F(4) GAUGED SUPERGRAVITY IN SIX-DIMENSIONS*, *Nucl.Phys.* **B269** (1986) 691.

[98] M. Cvetic, H. Lu and C. Pope, *Gauged six-dimensional supergravity from massive type IIA*, *Phys.Rev.Lett.* **83** (1999) 5226–5229 [hep-th/9906221].

[99] J. M. Maldacena and C. Nunez, *Supergravity description of field theories on curved manifolds and a no go theorem*, *Int. J. Mod. Phys.* **A16** (2001) 822–855 [hep-th/0007018].

[100] H. Braviner, R. Gregory and S. F. Ross, *Flows involving Lifshitz solutions*, *Class.Quant.Grav.* **28** (2011) 225028 [1108.3067].